Recent Progresses and Ongoing Developments on Satellite Data Assimilation in GRAPES

Ruoying Yin[1,2], Hao Wang[1,2], Jincheng Wang[1,2], Hongyi Xiao[1,2], Yan Liu[1,2], Di Di[3], Hao Chen[4],Lei Bi[5], Hejun Xie[5] ,Ke Chen[6] and Wei Han[1,2]

[1]NWPC/CMA [2]NMC/CMA [3]NUIST [4]JMO [5]ZJU [6]HUST

ITSC-23, June 29, 2021

Outline

- **Progresses on Satellite data assimilation in GRAPES**

  FY-4A GIIRS,AGRI

  FY-2H VISSR, FY-3D MWRI, HIRAS

  HY-2B HSCAT-B Wind

- **Ongoing developments on Satellite data assimilation**

  Assimilation of surface sensitive microwave channels

  Actual spectral response of FY-3D MWTS in radiance assimilation

  Fast non-spherical scattering calculation for all-sky FY-3D radiance assimilation

  OSSE for future GEO microwave sounder

Fengyun Satellite Series

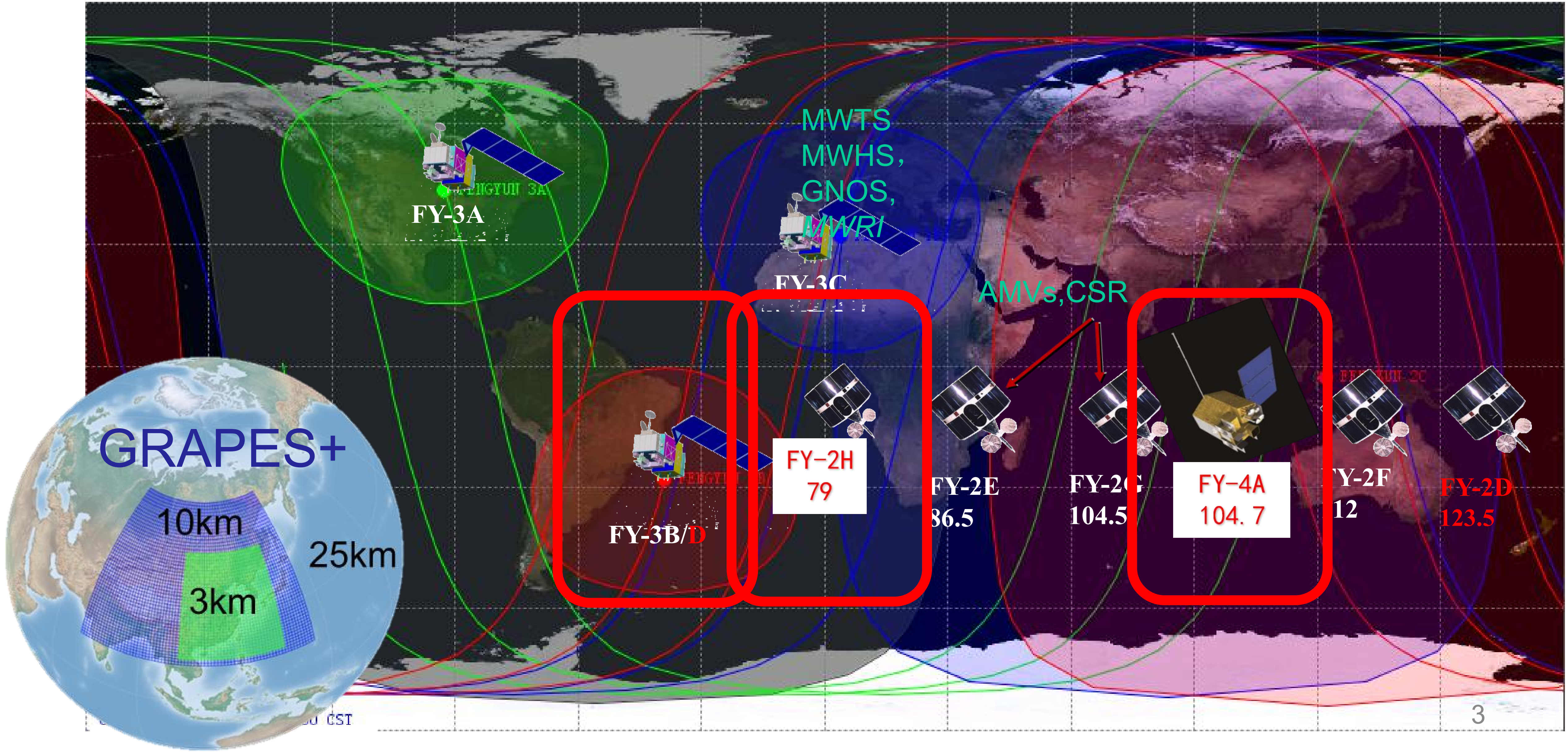

Radiance data used in GRAPES global 4D-Var

- **AMSU-A**
  - NOAA-15: channels 5,7-10;
  - NOAA-18: channels 6,7,10,11;
  - NOAA-19: channels 5,6,9-11;
  - METOP-A: channels 5,6,9-11;
  - METOP-B: channels 5-11;
  - NPP: channels 6-12,18-22;
  - **FY-3D:** channels 5,6,7
- **MHS**
  - NOAA-19: channels 3,4,5;
  - METOP-A: channels 5,6,9-11;
  - METOP-B: channels 5,6,9-11;
  - FY-3C: channels 5,6,11,12
  - **FY-3D:** channels 2,3,4,5,6
- **FY-4A GIIRS:** channels 3-6,9-13,16,19,22,24,26,27,29,32-34,38,63,65,70-75,77-90,84-92,109,112-113,121-125,135-137,154,155,158,159166,184,225,245
- **FY-3D HIRAS:** channels 33-49,51-79,81,83,85-87,91,93,94,97,99,100,102,103,105
- METOP-A and METOP-B IASI: channels 2-11,15-18,25-44,46-51,53-70,72,85,86
- AQUA AIRS: channels 12-14,18-21,26,28-31,44-47,49,50-53,55-80,82
- **FY-3D MWRI:** channels 3,5,7
- **FY2H VISSR:** channels 3
- **FY4A AGRI:** channels 8,9
- Himawari-8 AHI: channels 8,9,10

Data assimilation of FY-4 satellite series

- observation operator, quality control, channel selection, assimilation application
- The operational assimilation has been realized in December 2018, and the 5-day forecast accuracy in East Asia improved by about 2%
- The intelligent satellite observation based on forecast demand is realized, and improved typhoon forecasts.

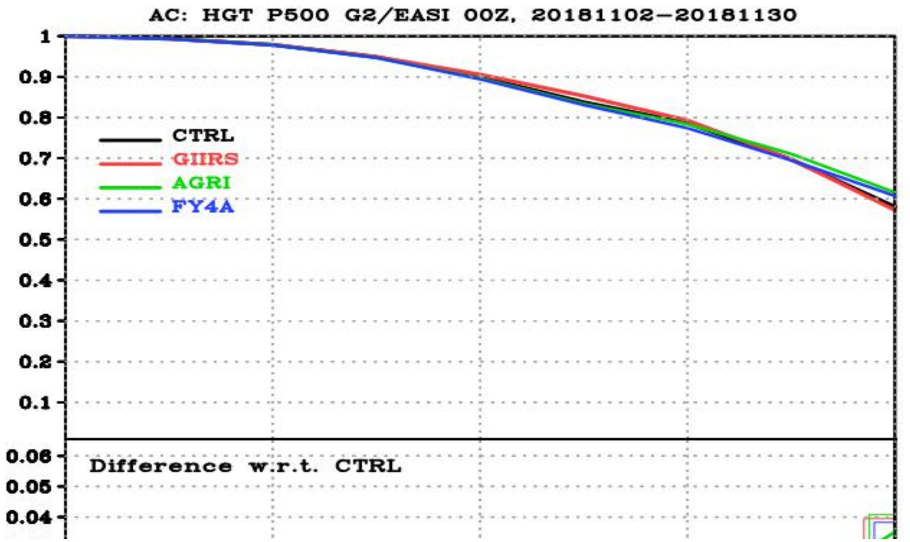

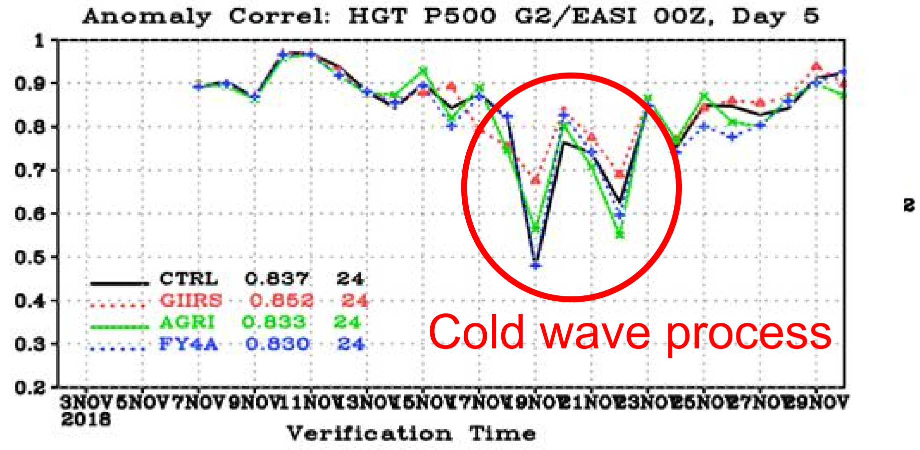

Di di, et al, 2018；Ruoying Yin, et al, 2019;Han W. et al，2019; Fan S. , Han W. 2019 ;Yin R., Han W. et al ,2020

Data assimilation of FY-4 satellite series

Targeted observetion for **Typhoon** Maria (2018)

with a temporal resolution of 15 minutes

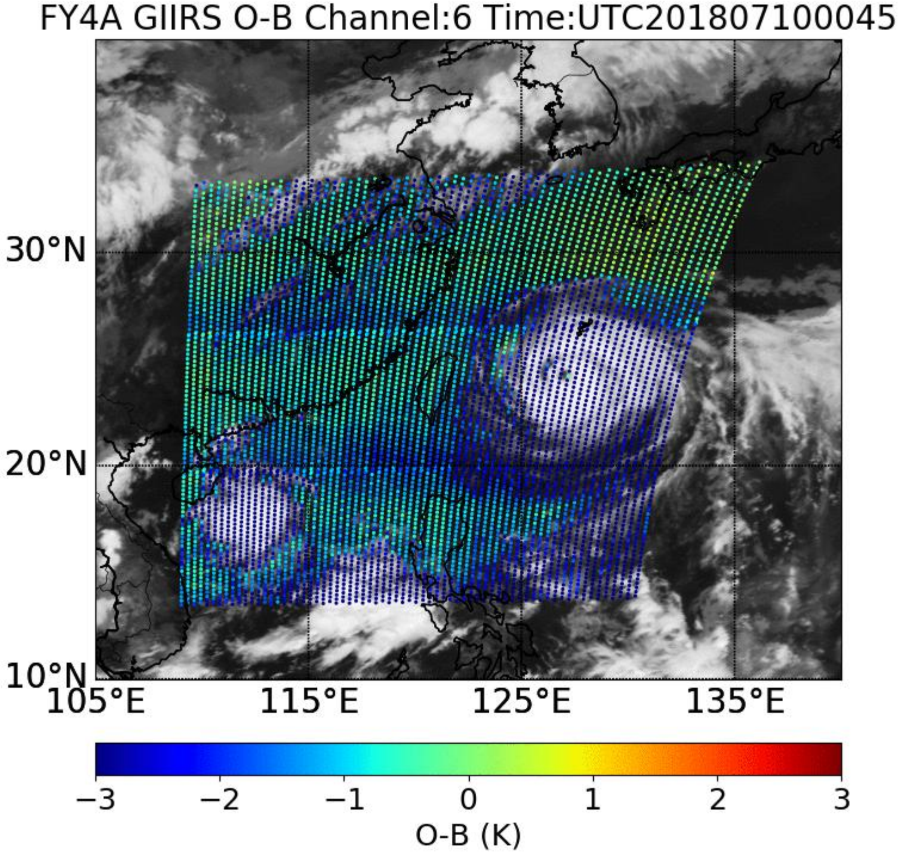

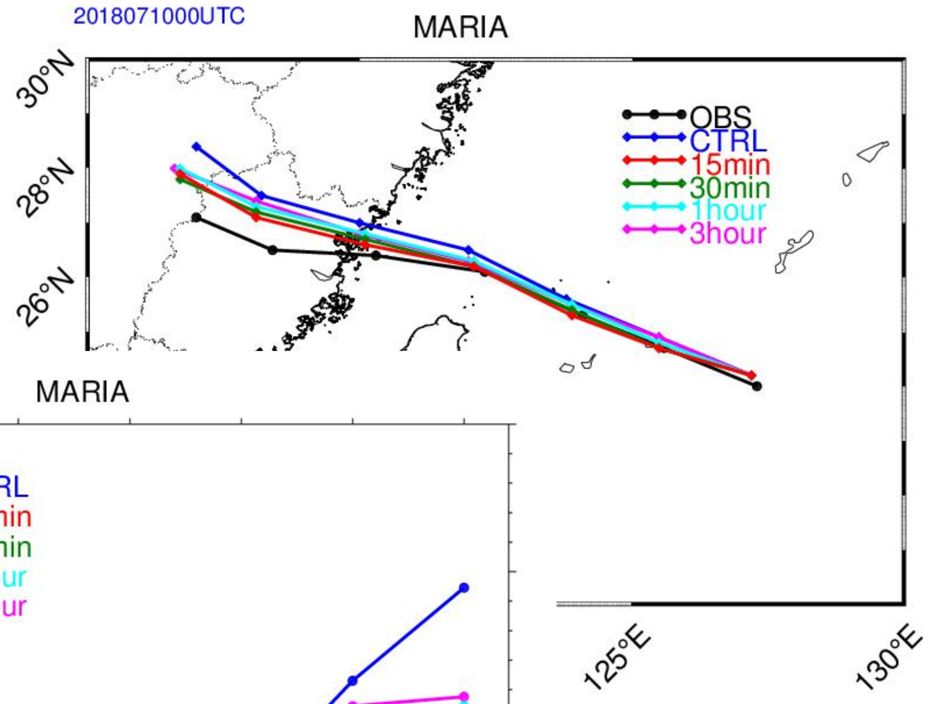

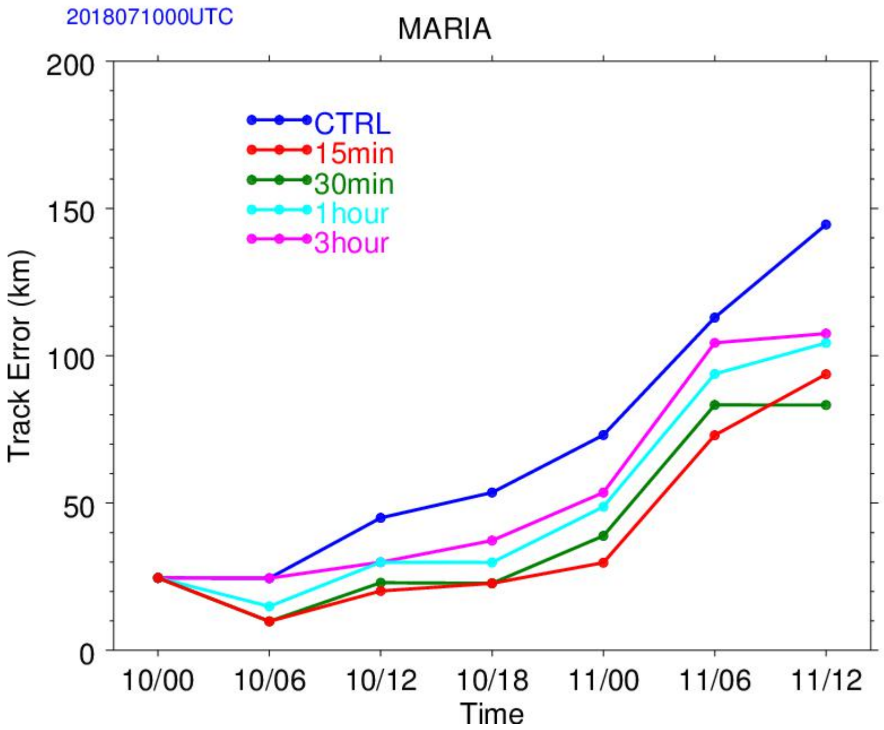

Ruoying Yin. et al ,2021, Impact of high temporal resolution FY-4A Geostationary Interferometric Infrared Sounder (GIIRS) radiance measurements on Typhoon forecasts: Maria (2018) case with GRAPES global 4D-Var assimilation system, submitted to *GRL*.

The evaluation of FY4A GIIRS L1 data calibration（V3, 20191107）

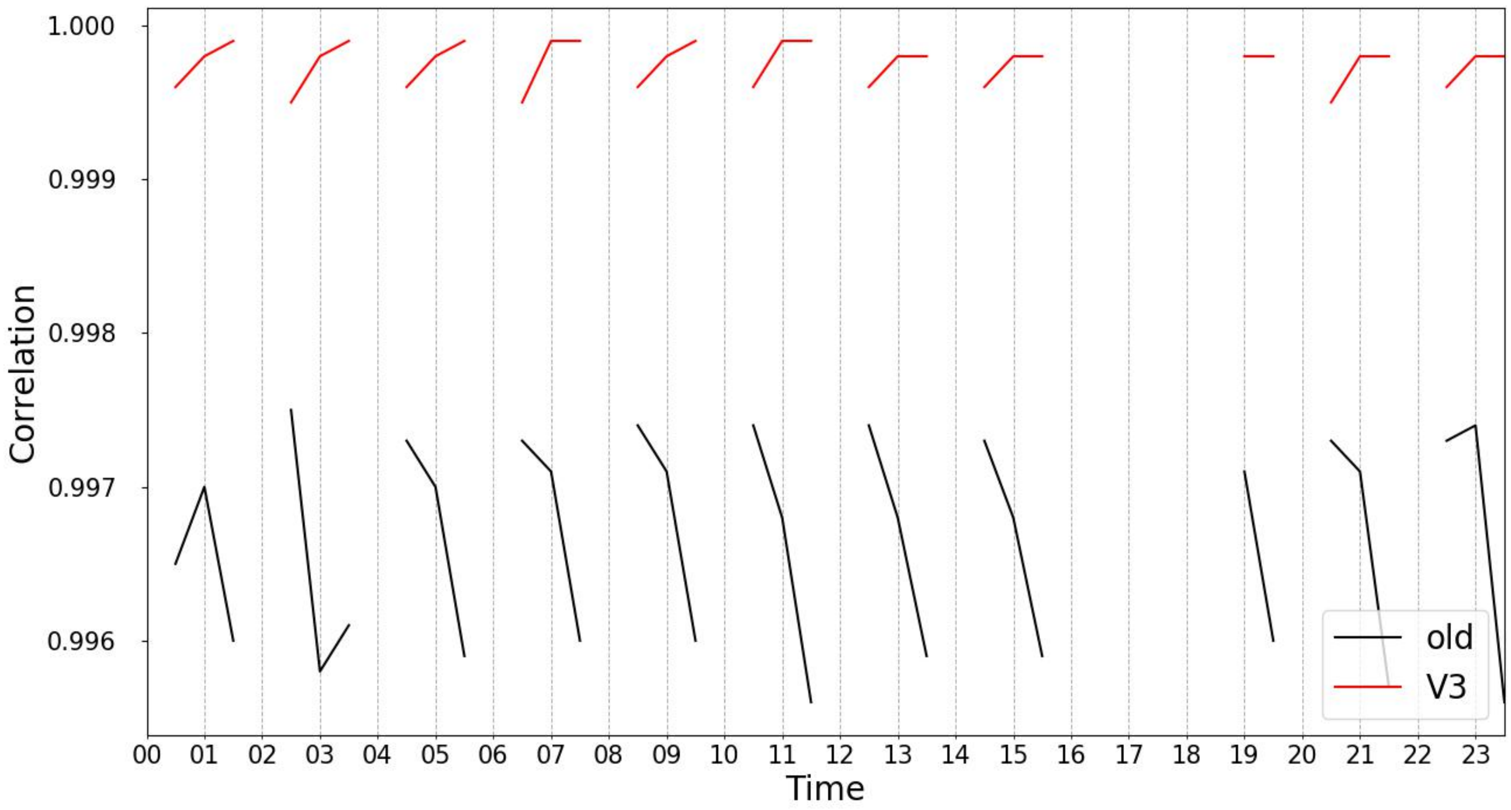

spectral correlation coefficient between observation and simulated brightness temperature over clear-sky ocean on December,12,2018

$$R = \frac{Cov(BT_{obs}, BT_{bkg})}{\sqrt{D(BT_{obs})}\sqrt{D(BT_{bkg})}}$$

On average, R increased from **0.9964** to **0.9998**.

Improvement in Calibration

Biases and standard deviations of two versions for GIIRS channels 1-300.

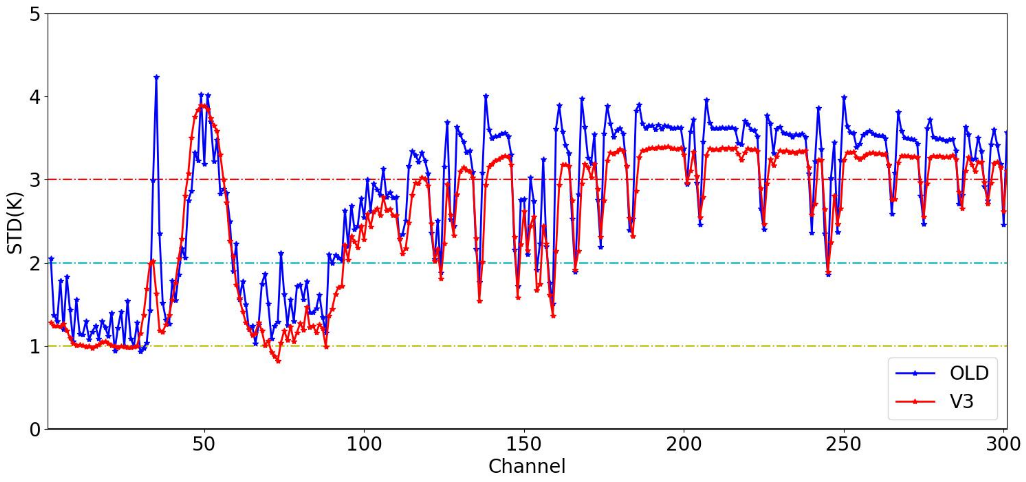

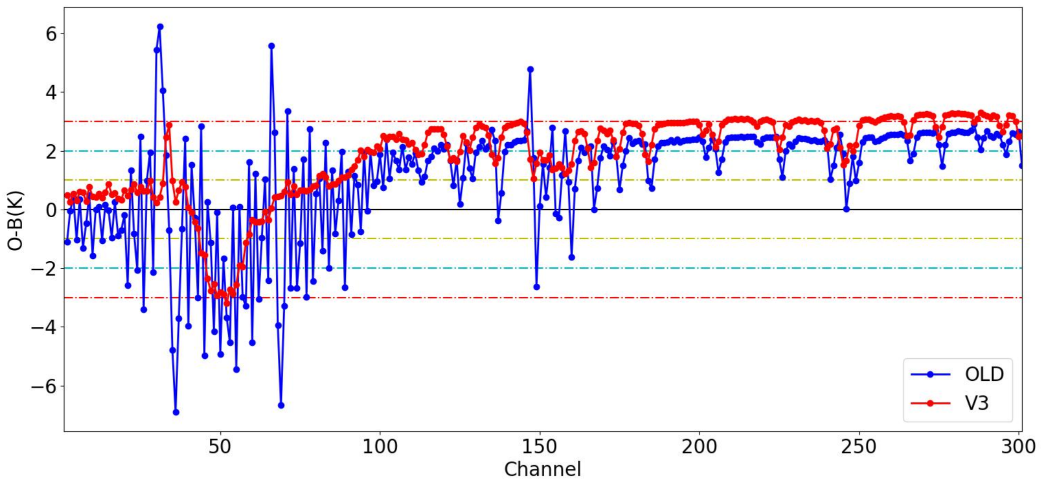

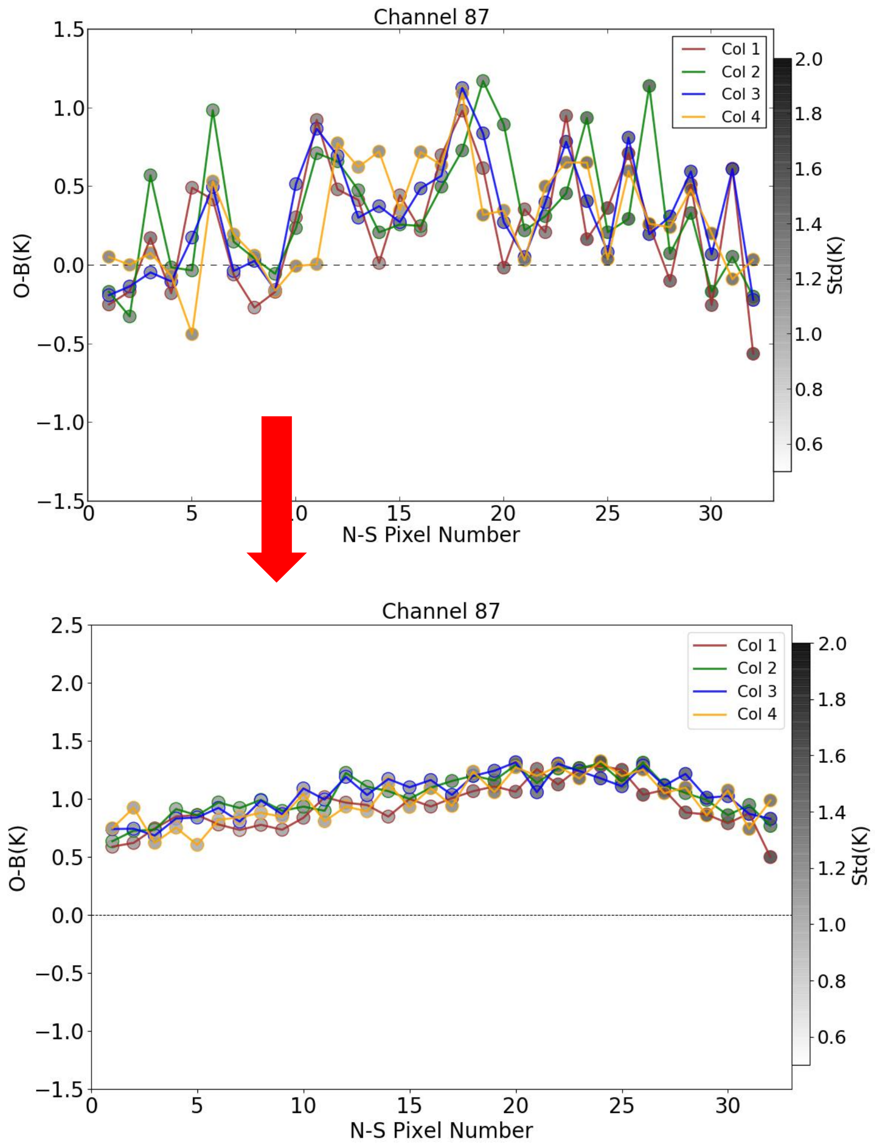

The **uniformity and stability** of bias depending on detection array (**FOVs**) of V3 version data is significantly improved

FOVs dependences of biases (lines) and standard deviations (circles) of GIIRS channel 87

Impact of GIIRS (V3) assimilation over East Asia (2020)

Neutral to positive impact

temperature field

moisture field

wind field

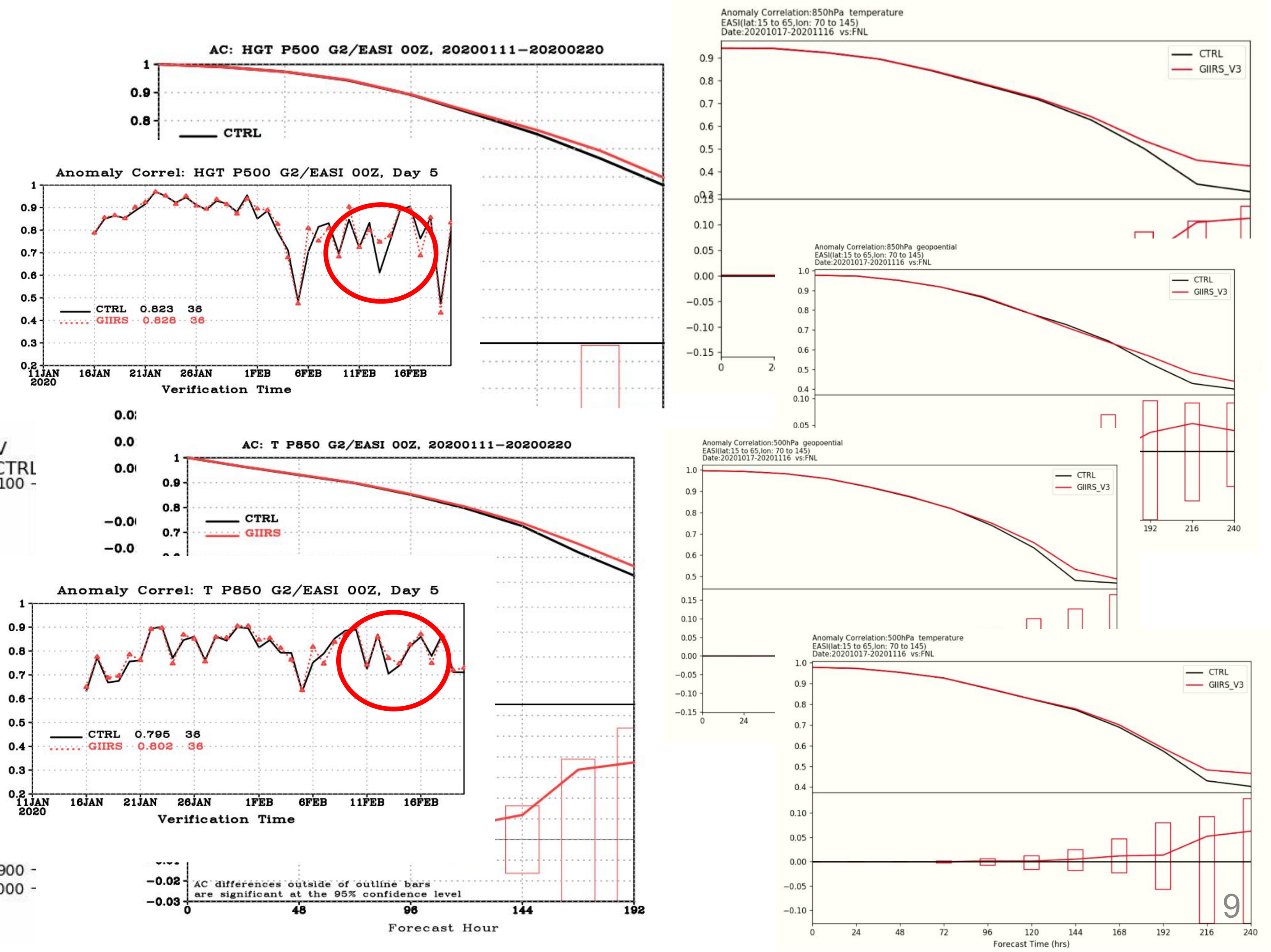

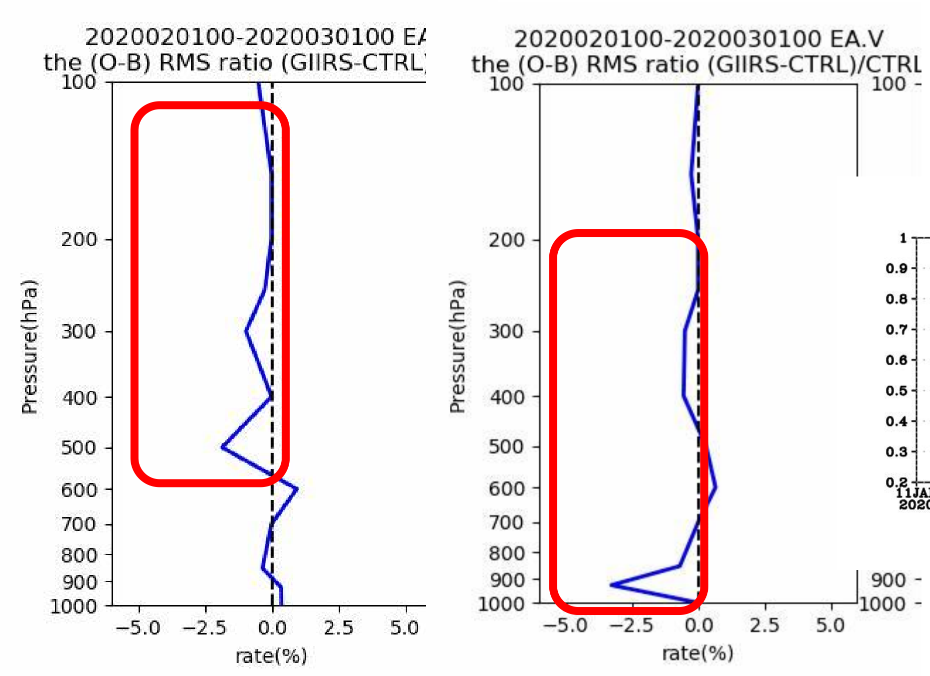

The preliminary evaluation of FY4A GIIRS MW assimilation

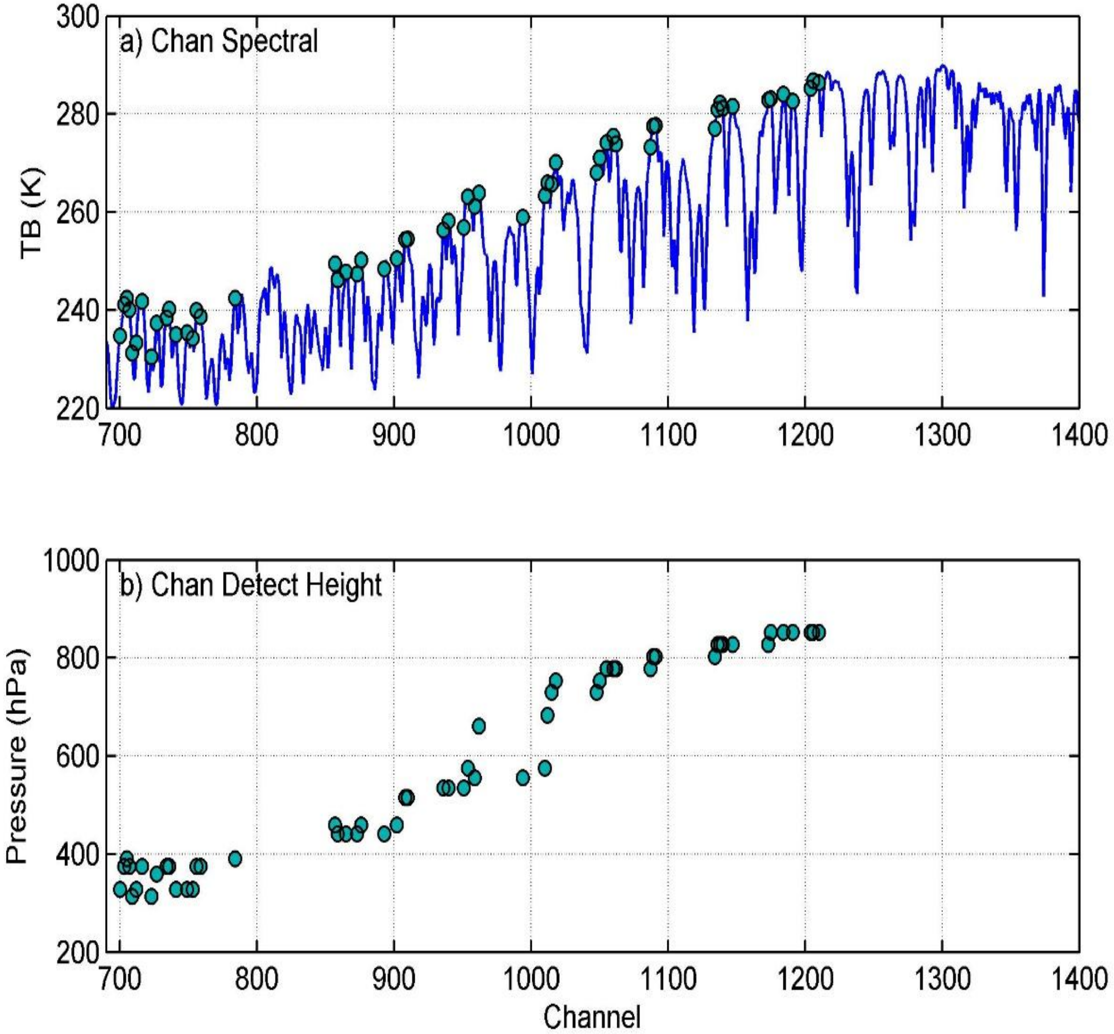

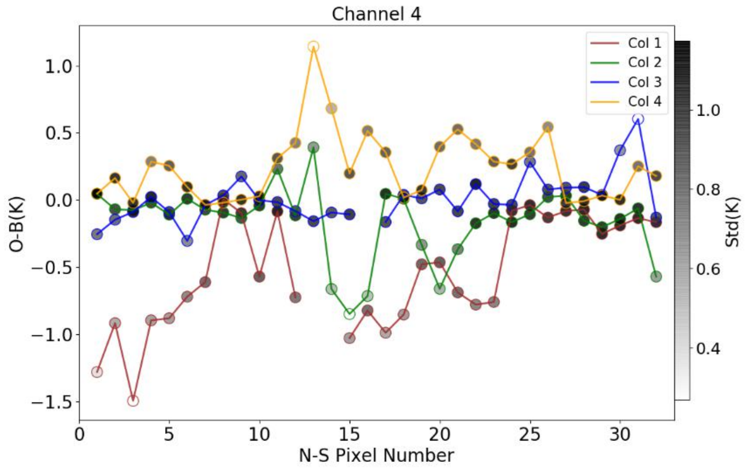

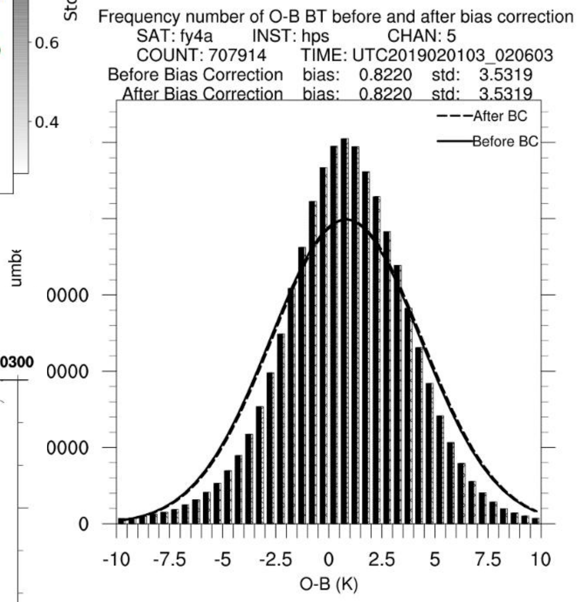

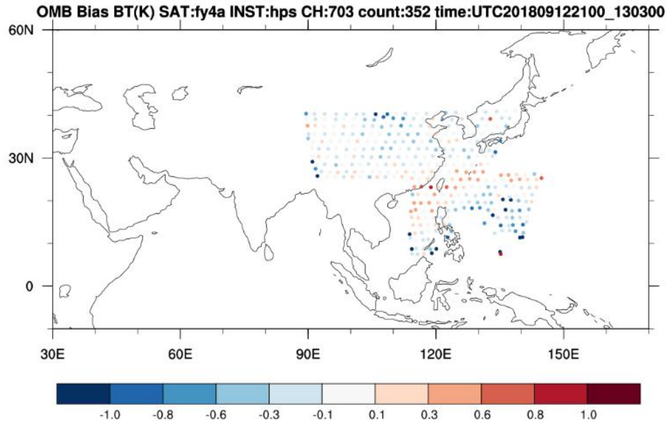

Di, D., et.al., 2021. Geostationary Hyperspectral Infrared Sounder Channel Selection for Capturing Fast-Changing Atmospheric Information. IEEE Transactions on Geoscience and Remote Sensing 1–10. https://doi.org/10.1109/TGRS.2021.3078829

Impact on Typhoon Mangkhut (2018)

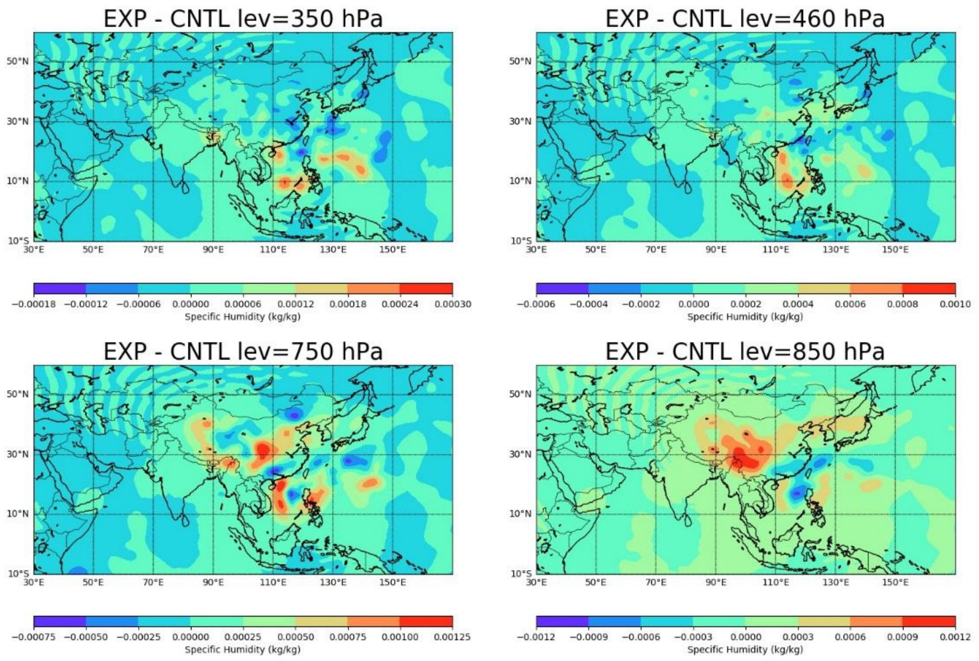

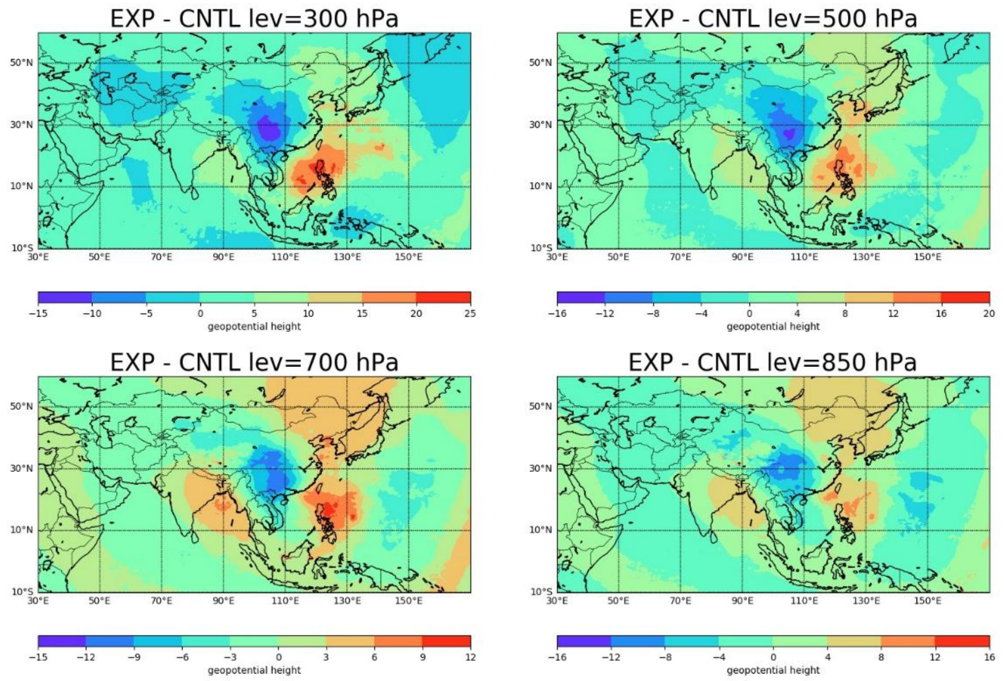

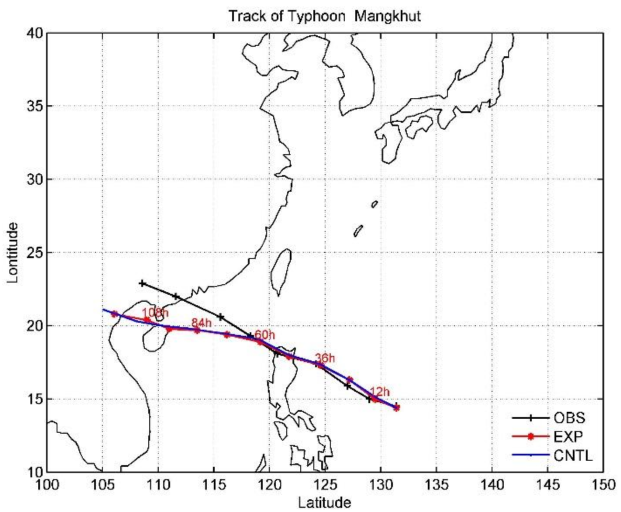

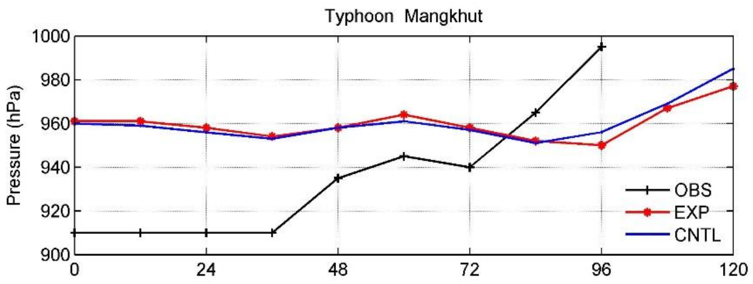

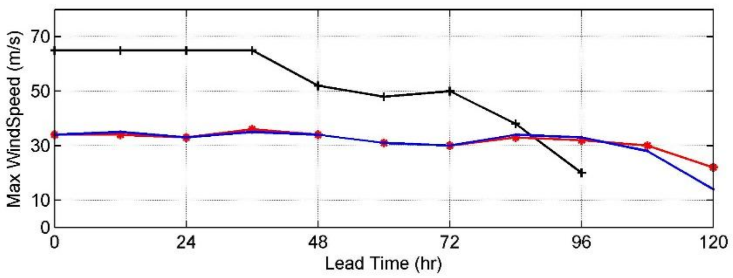

Neutral impact

FY-4A AGRI data Assimilated in GRAPES

Quality Control Scheme	Specific content of the scheme
1. Abnormal brightness temperature test	Eliminate pixels with brightness temperature less than 50K and higher than 550K
2. Surface type inspection	Eliminate mixed pixels
3. Zenith Angle Quality Control	Eliminate pixels with a zenith angle greater than 60°
4. Observation error test	Eliminate pixels with O-B greater than 3 times the observation error
5. Cloud detection	（1） Match L2 cloud detection products （2） 10.8μm window zone channel threshold control
6. Observation residual test	Eliminate pixels with observation residuals greater than 1.5K

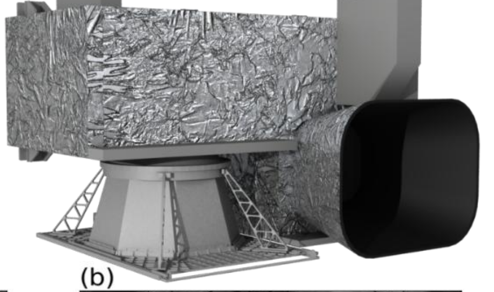

Typhoon Jongdari (2018)

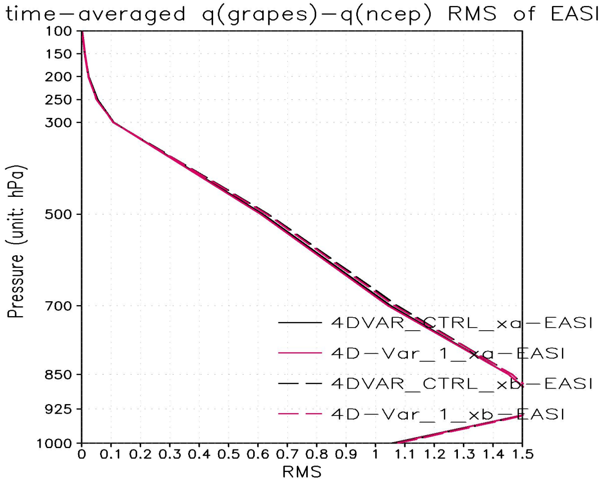

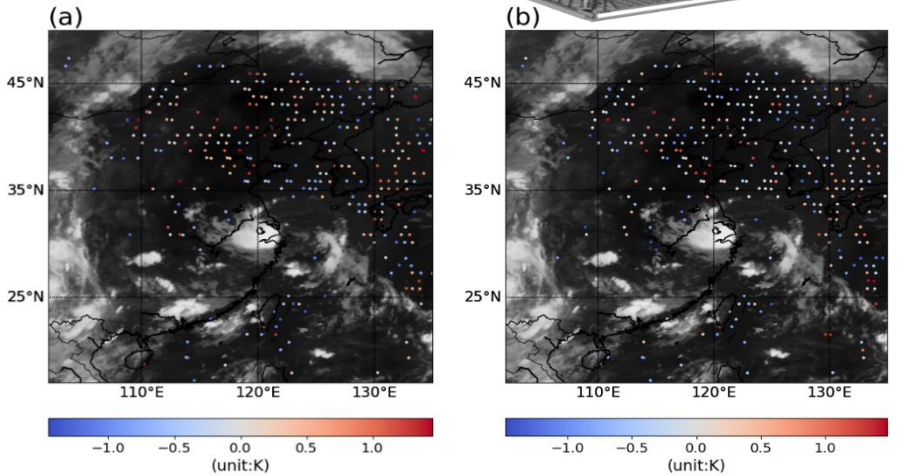

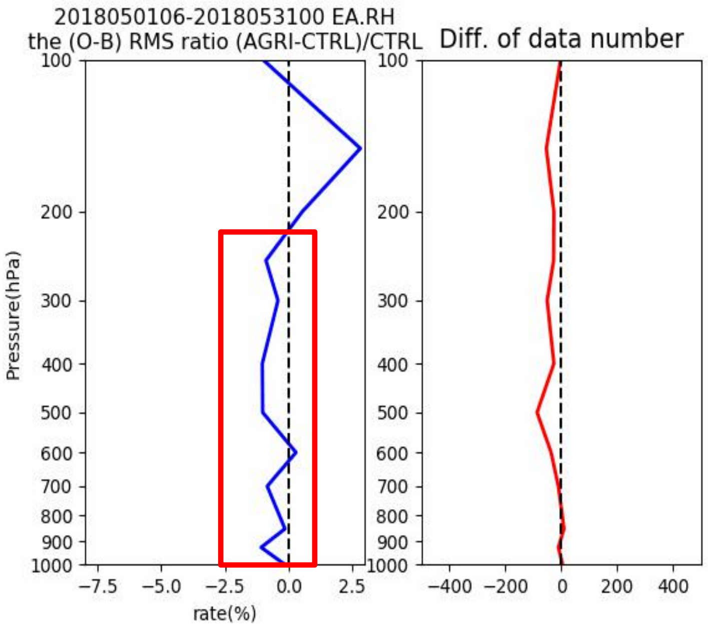

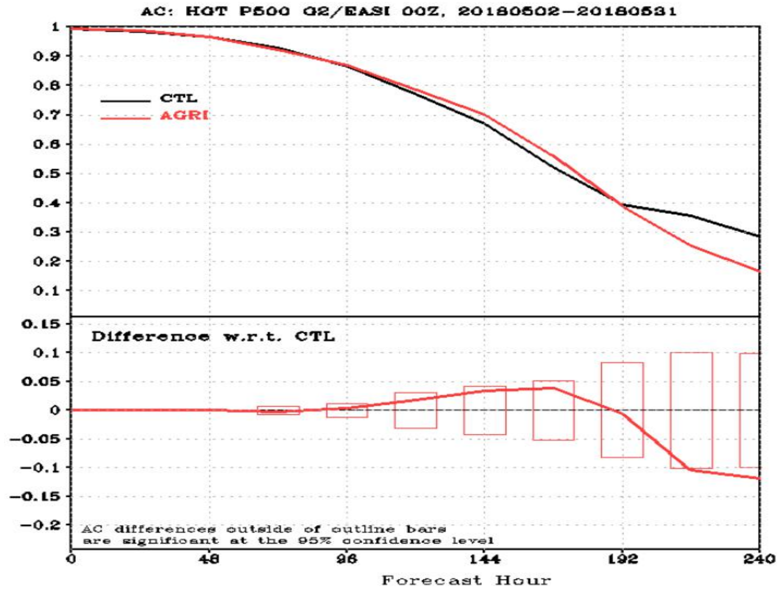

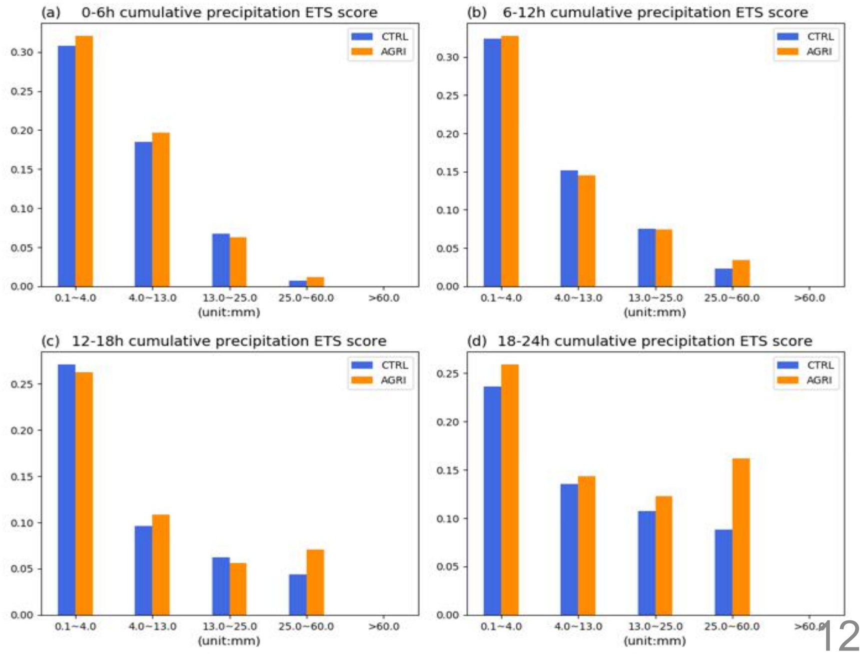

FY-2H VISSR data Quality Control and Assimilation effect

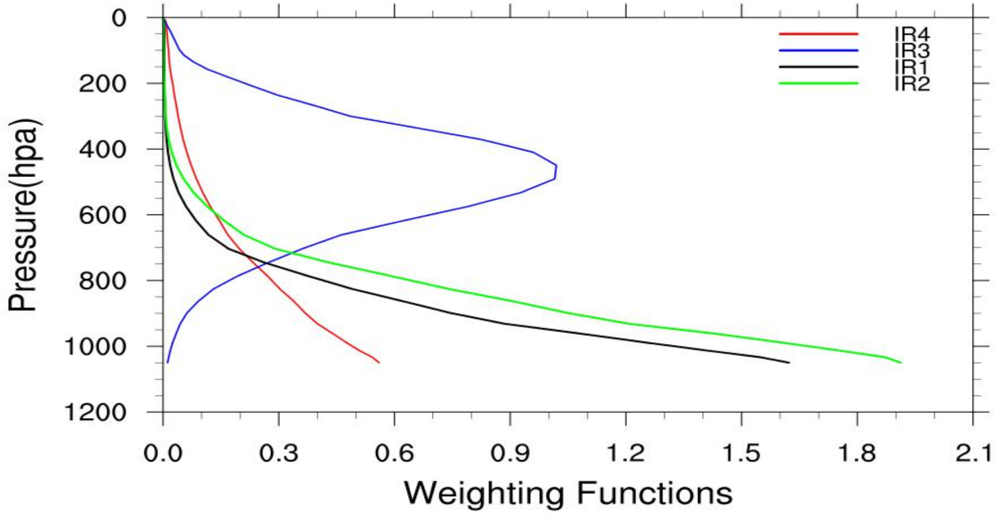

Quality Control Scheme	Specific content of the scheme
1. Abnormal brightness temperature test	Eliminate pixels with brightness temperature less than 50K and higher than 550K
2. Surface type inspection	Eliminate mixed pixels
3. Zenith Angle Quality Control	Eliminate pixels with a zenith angle greater than 60°
4. Observation error test	Eliminate pixels with O-B greater than 3 times the observation error
5. Cloud detection	（1）Match L2 cloud detection products （2）10.8μm window zone channel threshold control
6. Observation residual test	Eliminate pixels with observation residuals greater than 1.5K

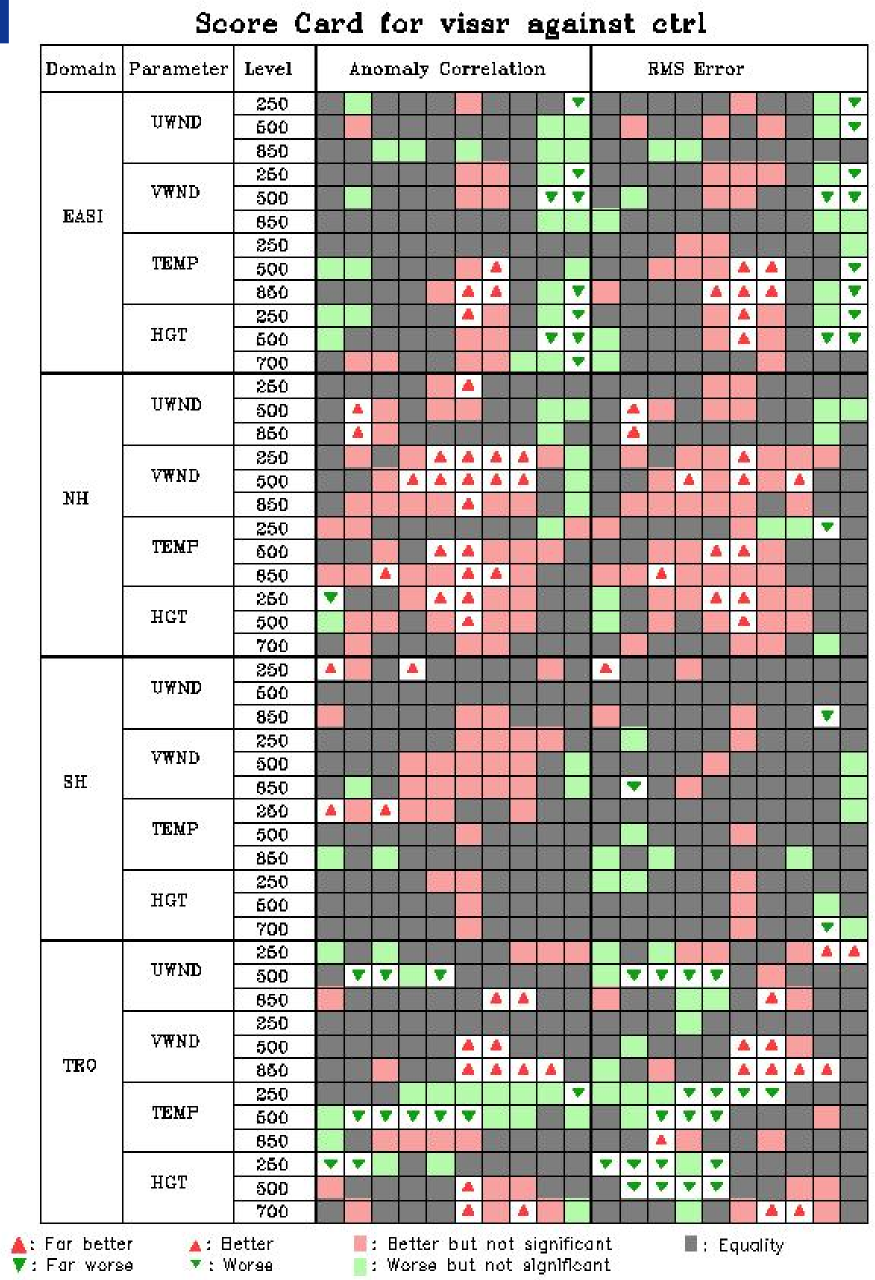

Assimilation of FY3D-MWRI: Introduction

(Hongyi Xiao, Han Wei)

Frequency (GHz)	10.65	18.7	23.8	36.5	89
Bandwidth (MHz)	180	200	400	400	3000
Polarisations	V H	V H	V H	V H	V H
NEΔT	0.5 K	0.5 K	0.5 K	0.5 K	0.8 K
IFOV (km*km)	51 x 85	30 x 50	27 x45	18 x30	9 x15
Pixel(km)	40 x11.2	40 x11.2	20 x11.2	20 x11.2	10 x11.2
Zenith Angle	45±0.1°				
Sensibility	Surface Emissivi -ty	Ice/Snow	Water Vapour	Cloud Liquid	Precipitat ion

L1-data： Brightness Temperature

L2-data： CLW (Cloud Liquid Water)、SWS (Surface Wind Speed)、SST (Sea Surface Temperature)、SIC (Sea Ice)、TPW (Total Precipitation Water)、Rain Rate (MRR)

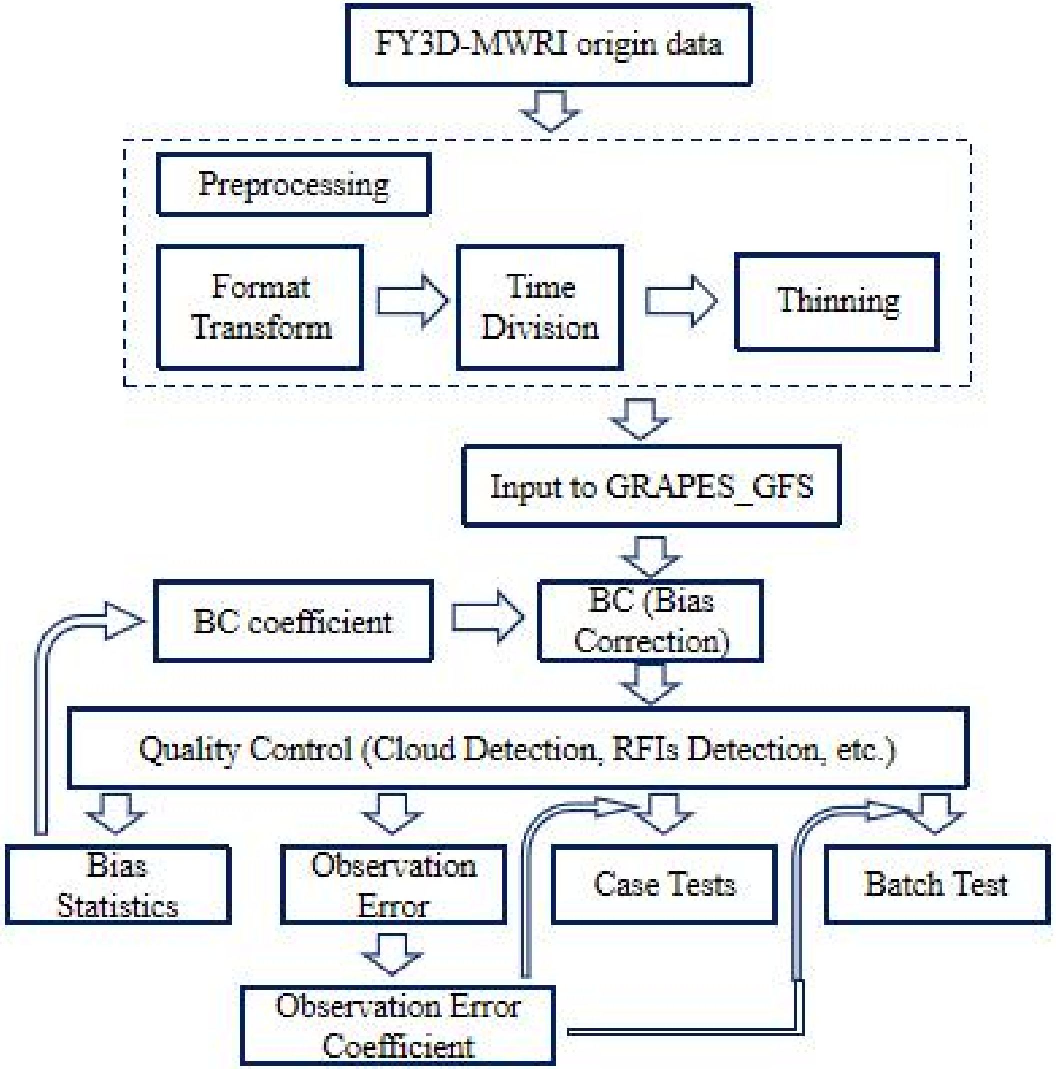

DA of FY3D-MWRI: Quality Control

(Hongyi Xiao, Han Wei)

	QC scheme	Details
Abnormal Factor	1. Gross value	T_b<70K or T_b>320K (Huang et al., 2013).
	2. Absolute departure	Absolute departure>3K (Yang et al., 2016).
	3. Relative departure	Relative departure>$3\sigma_0$ (Yang et al., 2016).
Surface Factor	4. Surface type	1， SIC$\neq 0$ (Huang et al., 2013). 2， SST<274K (Xiao et al., 2020). 3， ASI algorithm (Speen et al., 2008): $P = T_V^{89} - T_H^{89} < P_0 = 47K$; $GR(37/19) = (T_V^{37} - T_V^{19})/(T_V^{37} + T_V^{19}) < 0.045$; $GR(23/19) = (T_V^{23} - T_V^{19})/(T_V^{23} + T_V^{19}) < 0.04$。
	5. Land-sea contamination	$T_v^{10} > 175K$ or $T_H^{10} > 95K$ (Huang et al., 2013).
Weather Factor	6. Abnormal TPW	TPW<0 (Yang et al., 2017).
	7. Abnormal wind speed	SWS>30m/s (Nielsen-Englyst et al., 2018).
	8. Rain region	1， MRR$\neq 0$ (Liu et al., 2012). 2， if anyone is satisfied (Betthenhausen et al., 2006): $T_V^{37} - 0.979T_H^{37} < 55$; $1.175T_V^{18.7} - 30 > T_V^{37}$; $T_V^{18.7} > 170$; $T_V^{37} > 210$.
	9. Cloud detection	LWP $> \begin{cases} 0.3\text{mm}, & \text{CH3} \\ 0.25\text{mm}, & \text{CH5} \\ 0.1\text{ mm}, & \text{CH7} \end{cases}$ LWP is calculated by Zou and Tang (2017).
Anthropic factor	10.RFIs detection	$T_H^{19} - T_H^{23} > 5K$, $T_V^{19} - T_V^{23} > 5K$ (Zou et al., 2013).

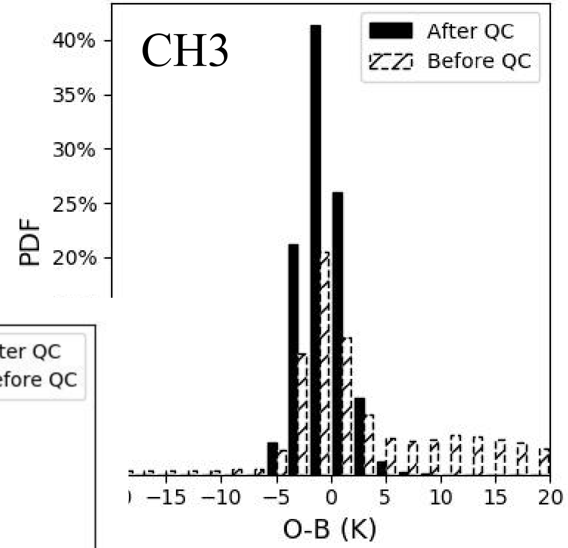

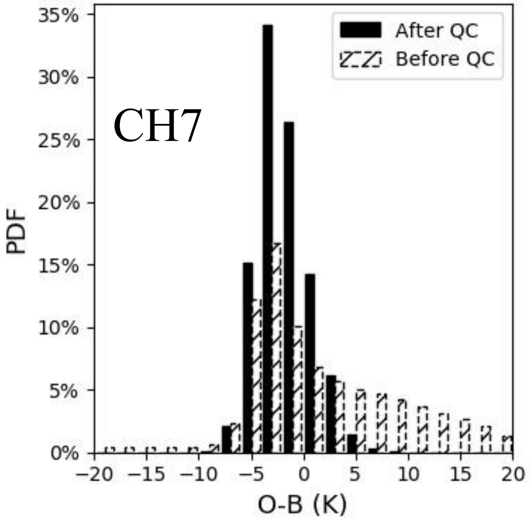

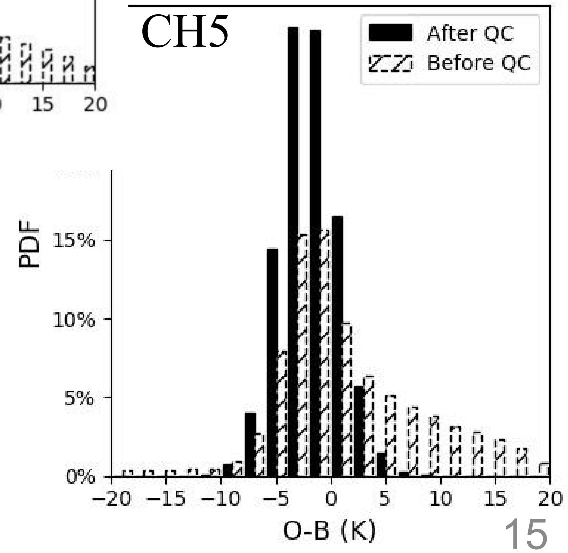

DA of FY3D-MWRI: Bias Correction and Observation Error

(Hongyi Xiao, Han Wei)

Bias Correction

Scan bias Correction
+
Airmass Bias correction

1. Thickness（1000-300hPa） 2. Thickness（200-50hPa）
3. Surface Temperature
4. Total Column Water Vapour

The statistics of bias correction coefficient of FY3C/D-MWRI is made by radiances data during 20180713-0725 in GRAPES_GFS2.4.

FY3D

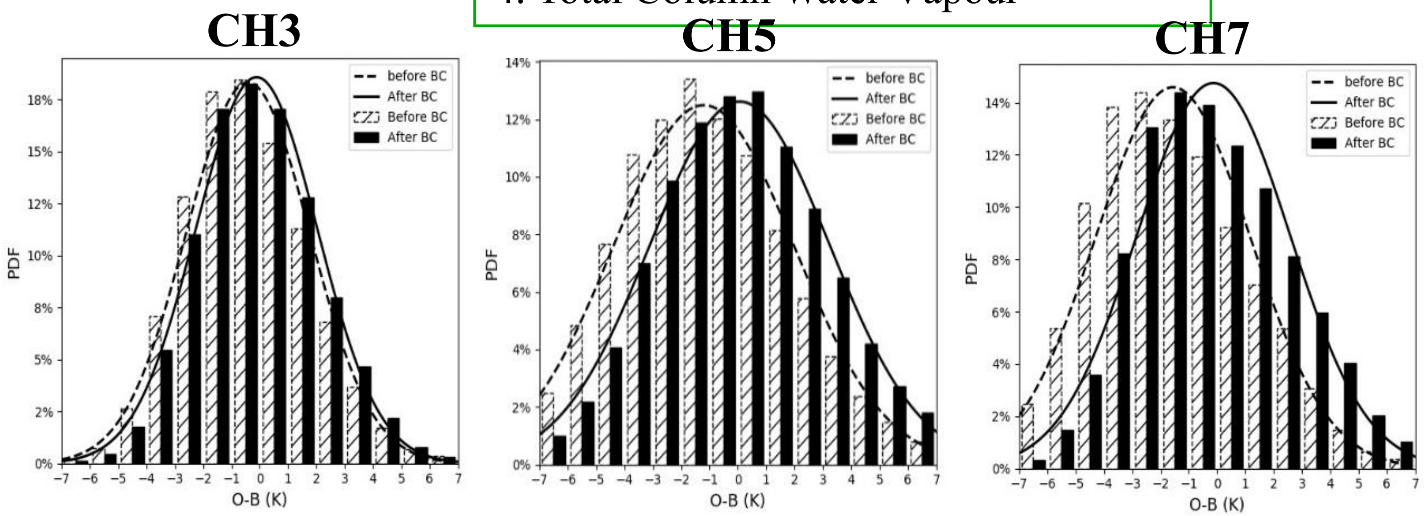

Observation error

The statistics of observation error of FY3C/D-MWRI is made by radiances data during 20180713-0725 in GRAPES_GFS2.4.。

$$\sqrt{(O-B)(O-A)} = (O-T)$$

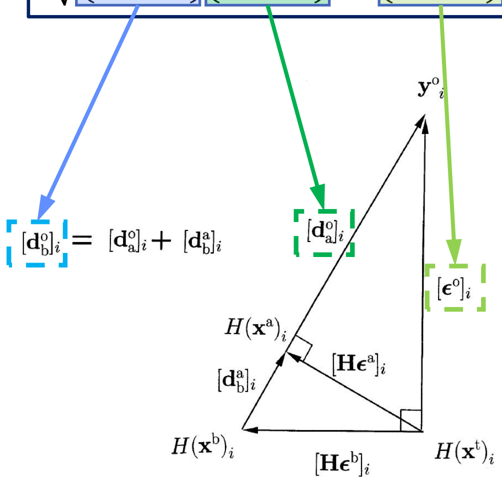

FY3D-MWRI	
CH3	1.21 K
CH5	1.39 K
CH7	1.69 K

DA of FY3D-MWRI: Case Experiments

(Hongyi Xiao, Han Wei)

Typhoon Shanshan（1813）

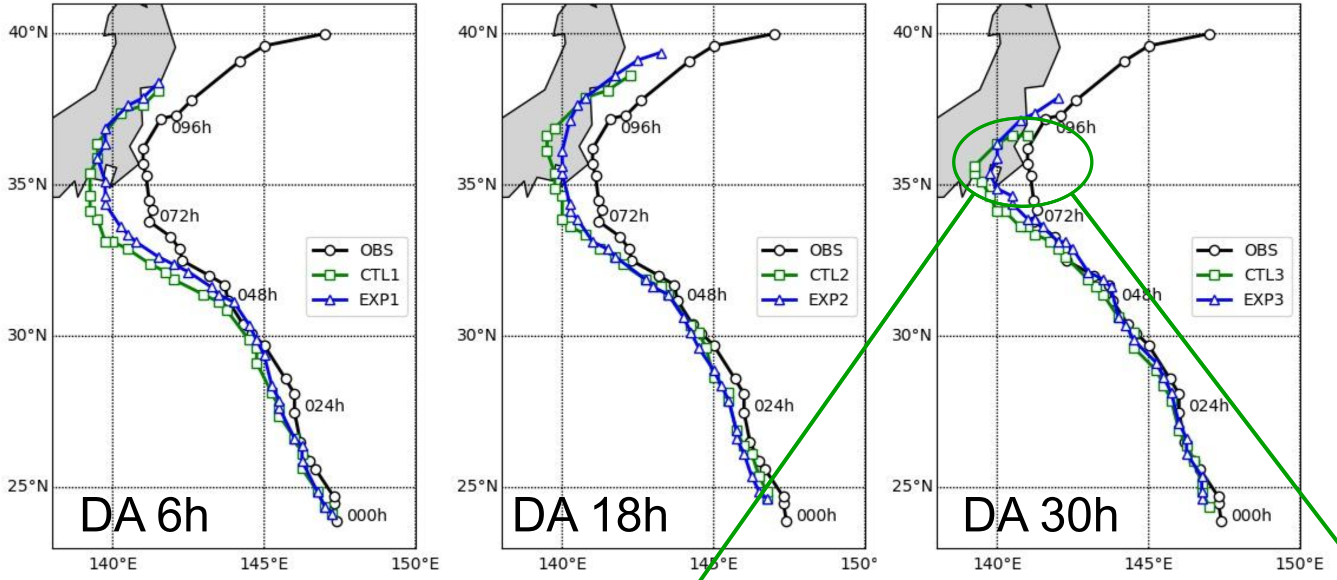

After assimilating the MWRI radiance data into GRAPES, there was a positive impact on the location of the subtropical high, which led to improvements in forecasts of the track of Typhoon Shanshan.

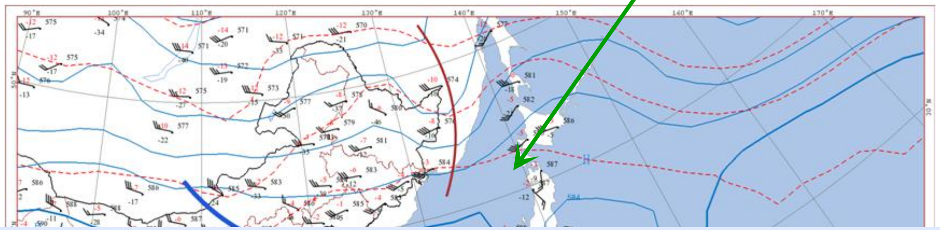

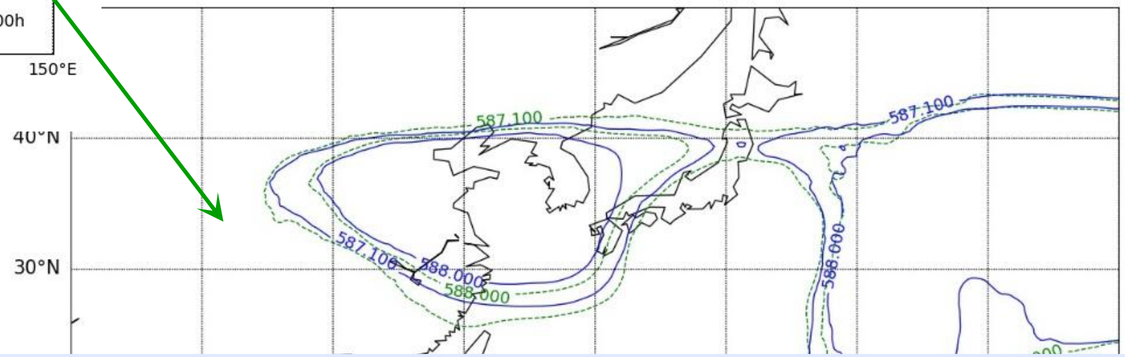

Hongyi Xiao' oral presentation (8.03), Impact of FY-3D MWRI Radiance Assimilation in GRAPES 4D-Var on Typhoon Shanshan Forecasts

Assimilation of FY3D-MWRI: Batch Experiments

(Hongyi Xiao, Han Wei)

Version： GRAPES_GFS2.4
Data Segment： One month（20180725~20180825）

CTRL： Default Satellite Data
EXP： CTRL+fy3dmwi (**19V/24V/37V**)

Specific humidity of Northern Hemisphere

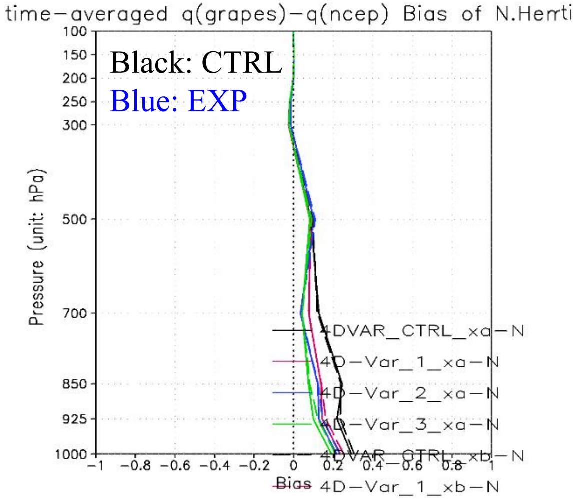

Specific humidity of Southern Hemisphere

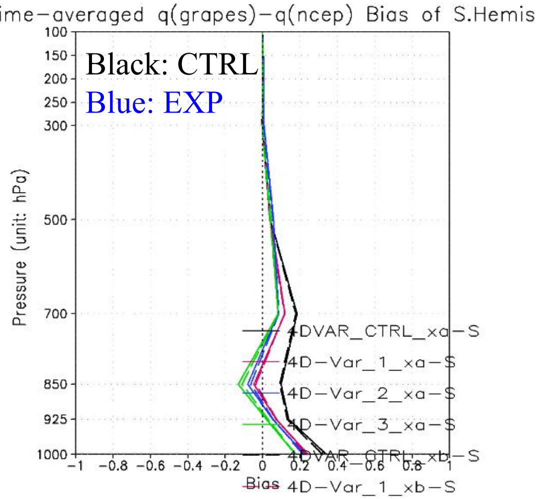

Bias of Geopotential Height on 850 hPa

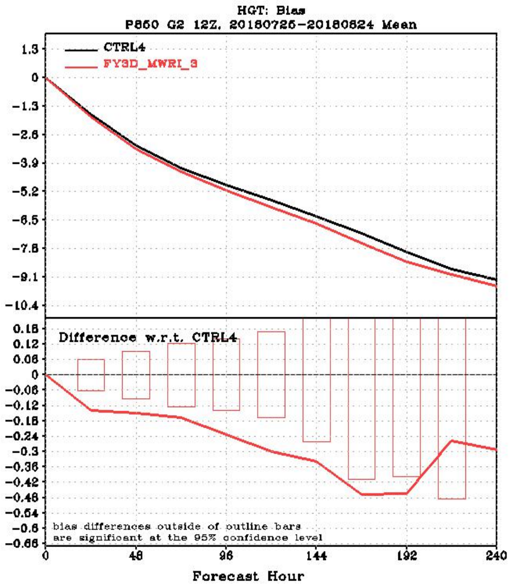

ACC of Geopotential Height on 850 hPa

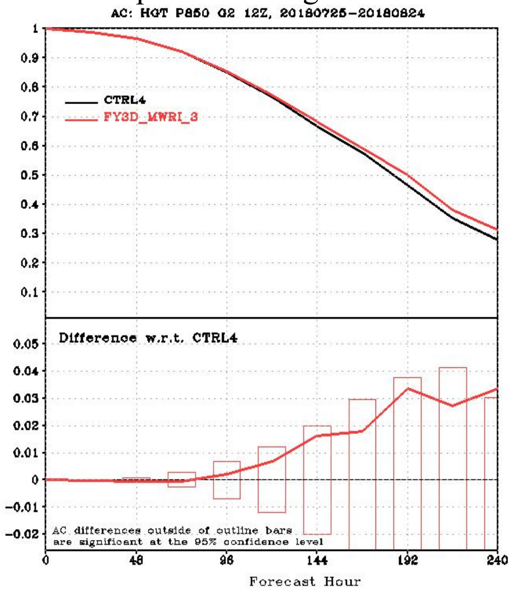

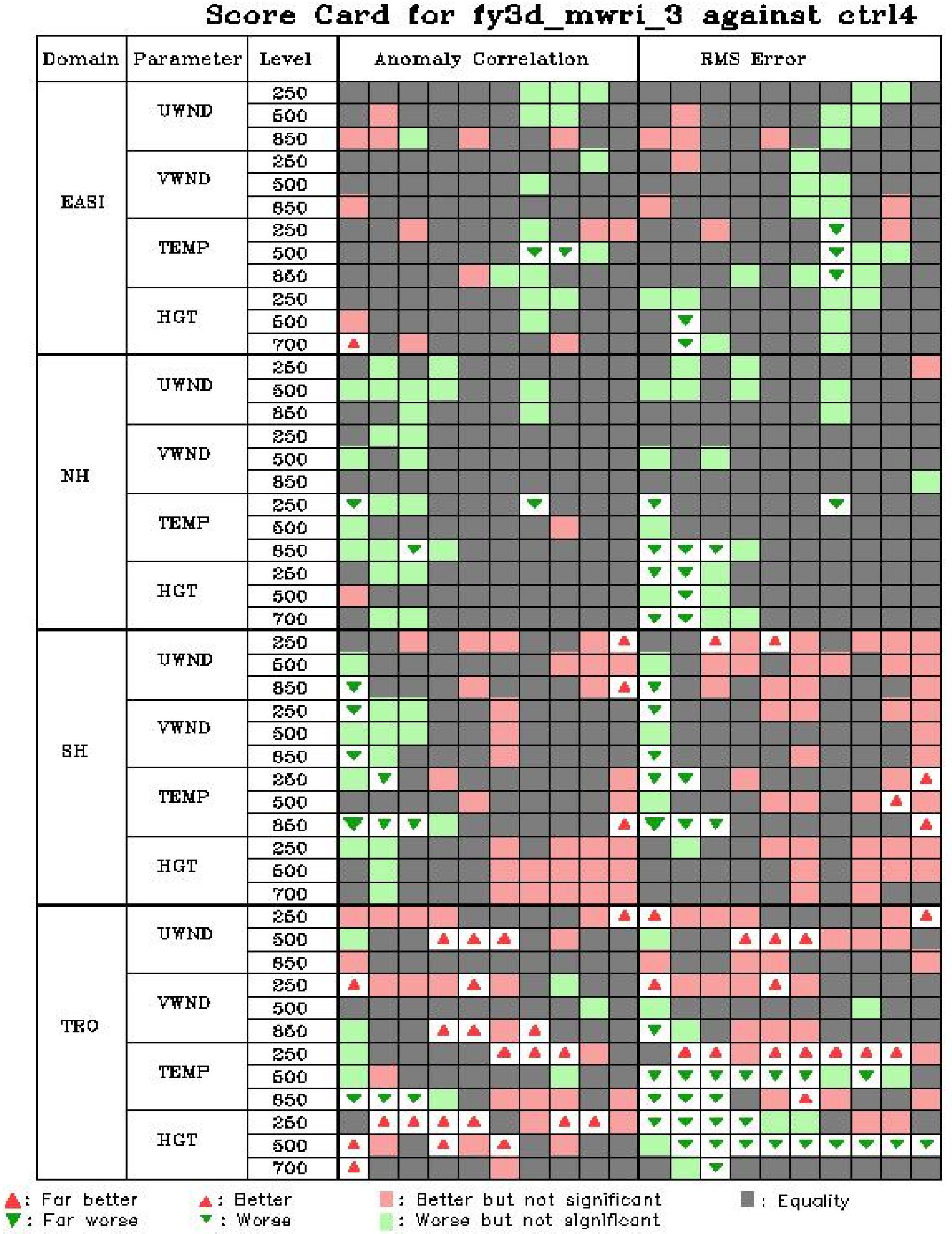

Adaptive Channel Selection for FY-3D HIRAS

Local integrated channel selection scheme for assimilation: different channel subsets according to different atmospheric profile characteristics, background errors and channels sensitivity characteristics of different levels of different regions.

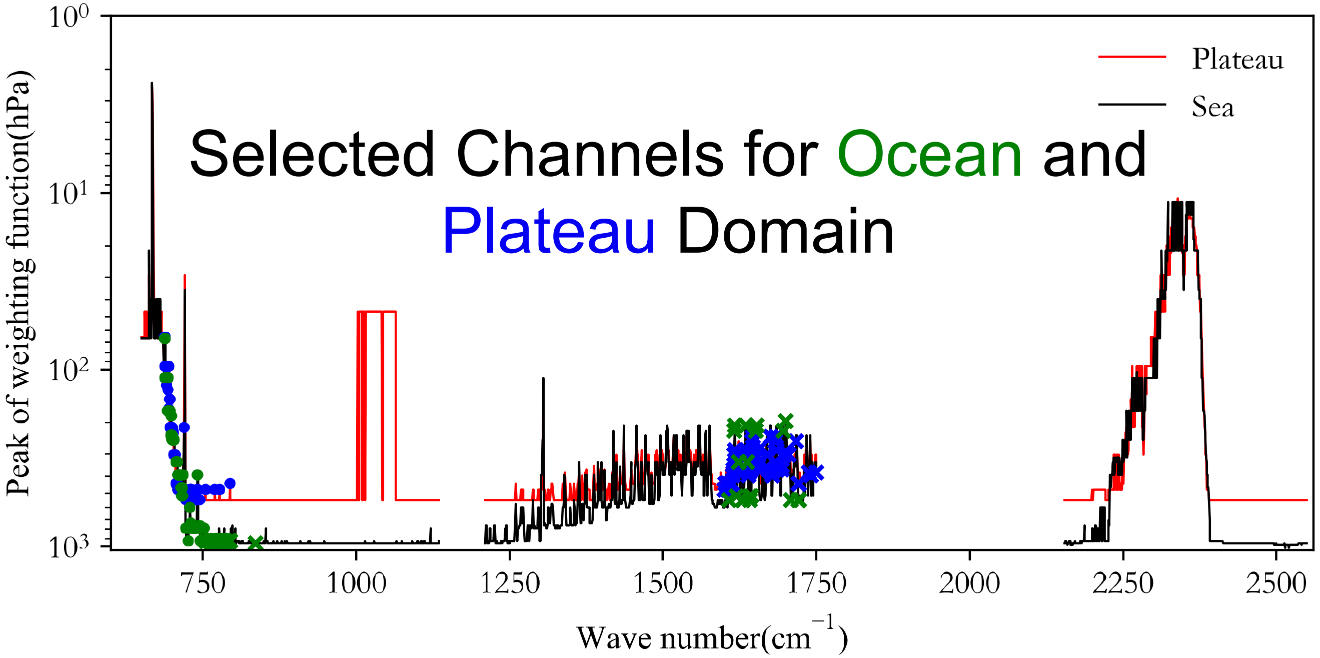

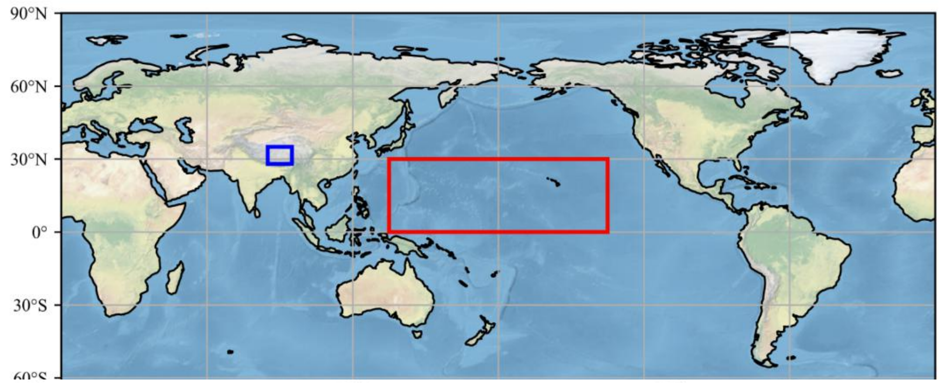

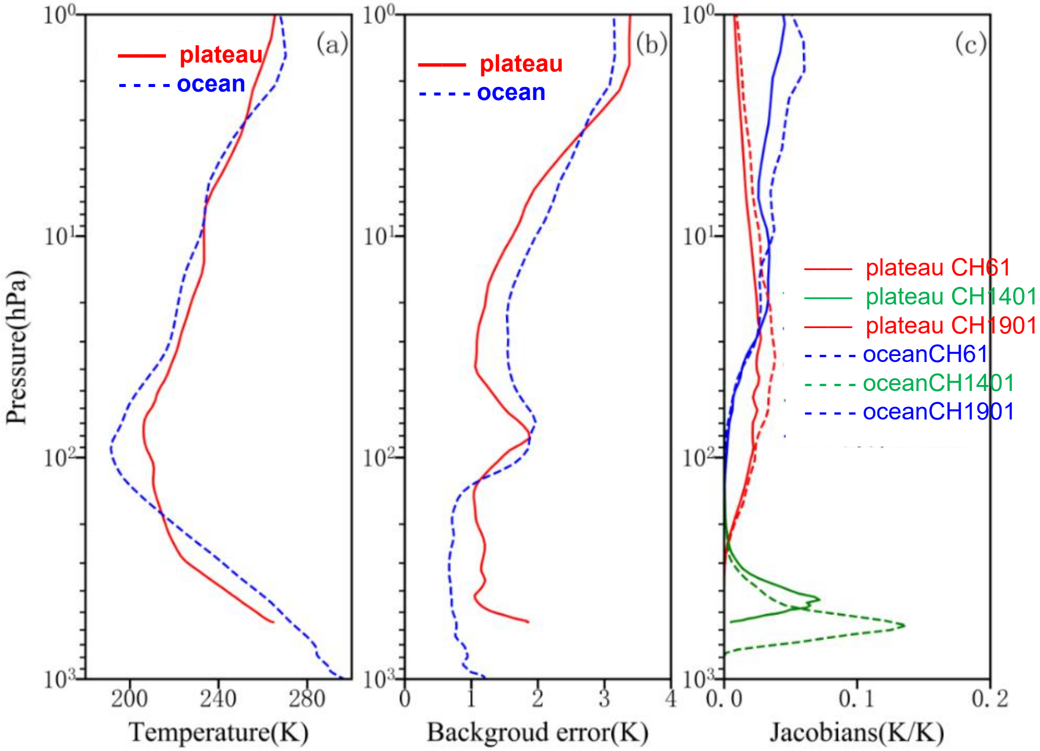

Fan, H., W. Wang, J. Wang, W. Han, 2021.

1DVAR experiment

Ocean Background

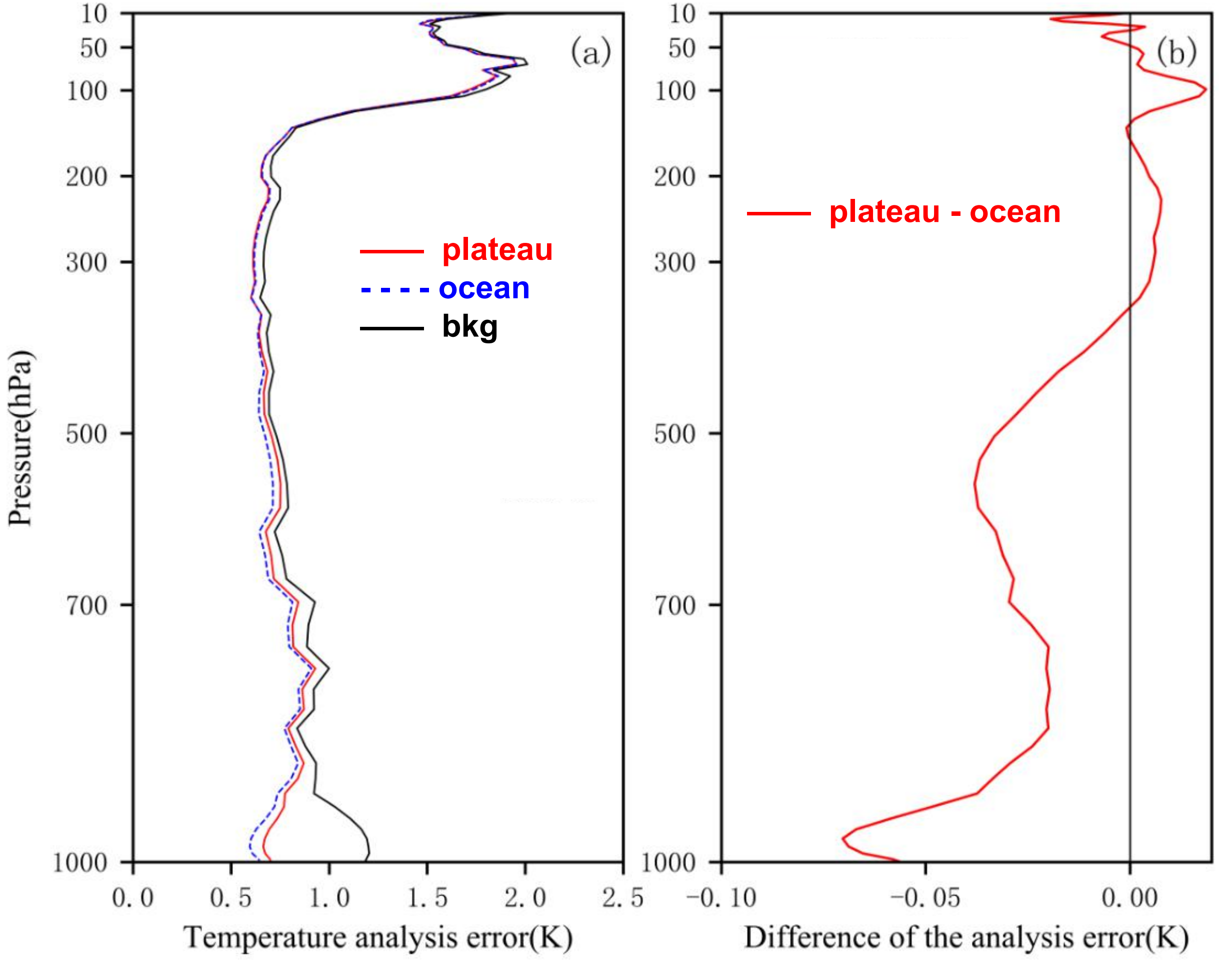

Plateau Background

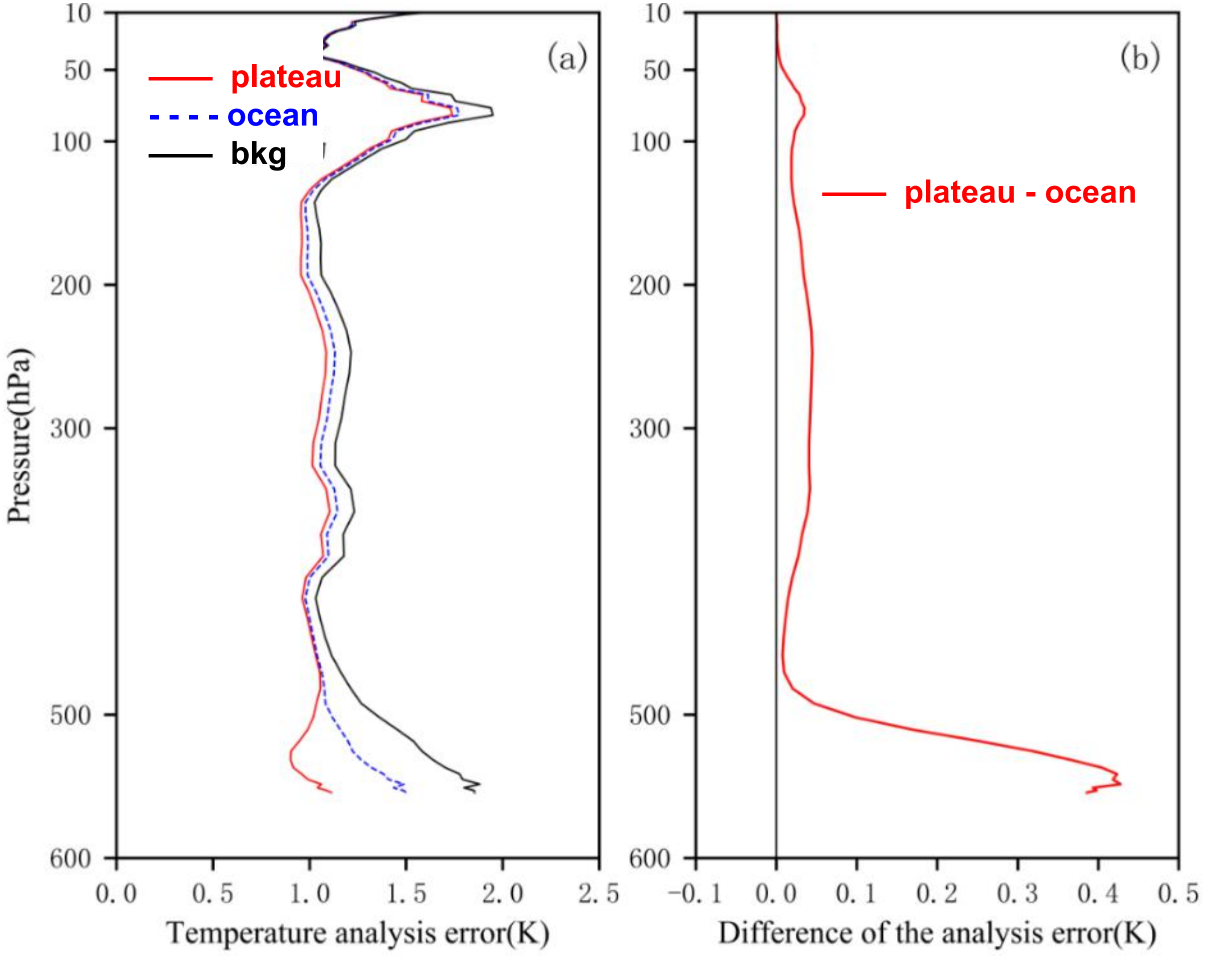

Background Error
Analysis Error assimilated “Ocean Channels”
Analysis Error assimilated “Plateau Channels”

Local integrated channel selection scheme can significantly reduce the analysis error.

Assimilation of NOAA19 AMSU-A over land

(Hongyi Xiao, Han Wei)

LSE .vs. frequency

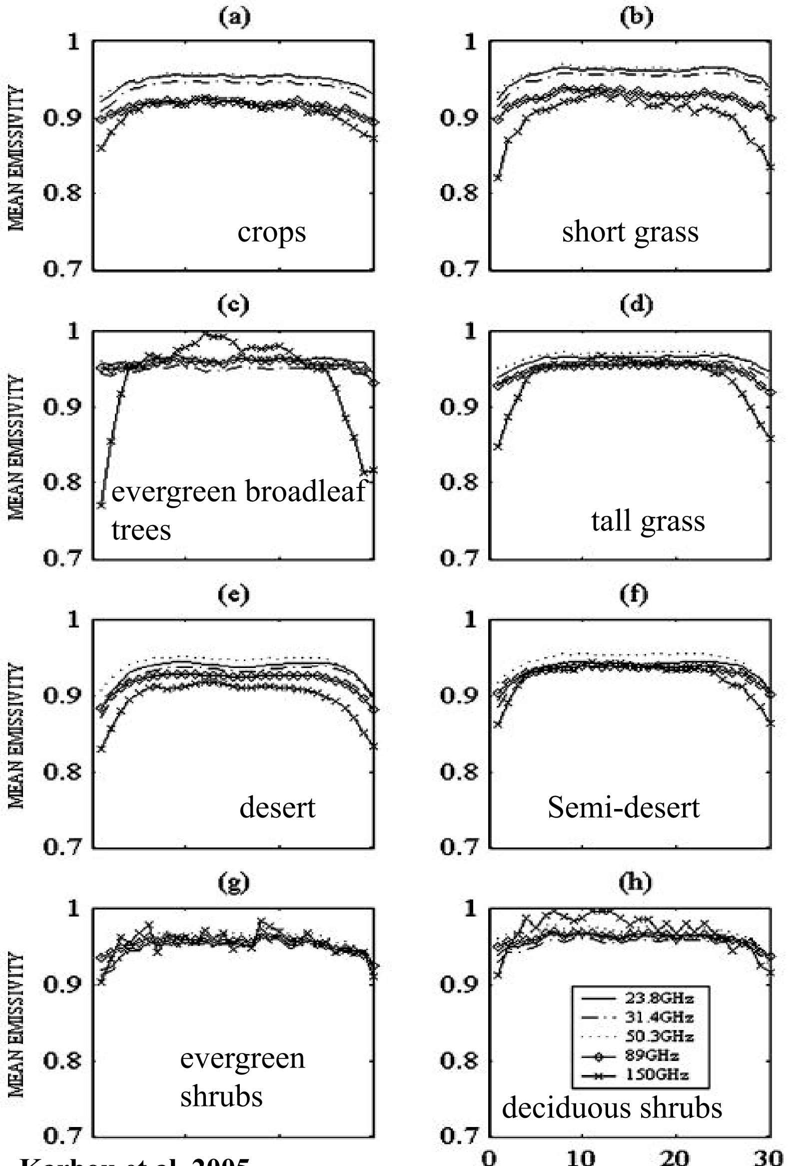

Karbou et al, 2005.

LSE retrieval by window channel

AMSU-A (NOAA-15/16/17/18/19, MetOp-A/B, AQUA)		
Ch#	Frequency(GHz)	Sensitivity
1	23.8	Surface
2	31.4	Surface
3	50.3	Surface
4	52.8	Temperature
5	53.596±0.115	Temperature
6	54.4	Temperature
7	54.9	Temperature
8	55.5	Temperature
9	57.290(=ν_9)	Temperature
10	ν_9±0.217	Temperature
11	ν_9±0.322±0.048	Temperature
12	ν_9±0.322±0.022	Temperature
13	ν_9±0.322±0.010	Temperature
14	ν_9±0.322±0.0045	Temperature
15	89	Surface

window channel — to-be-assimilated channels

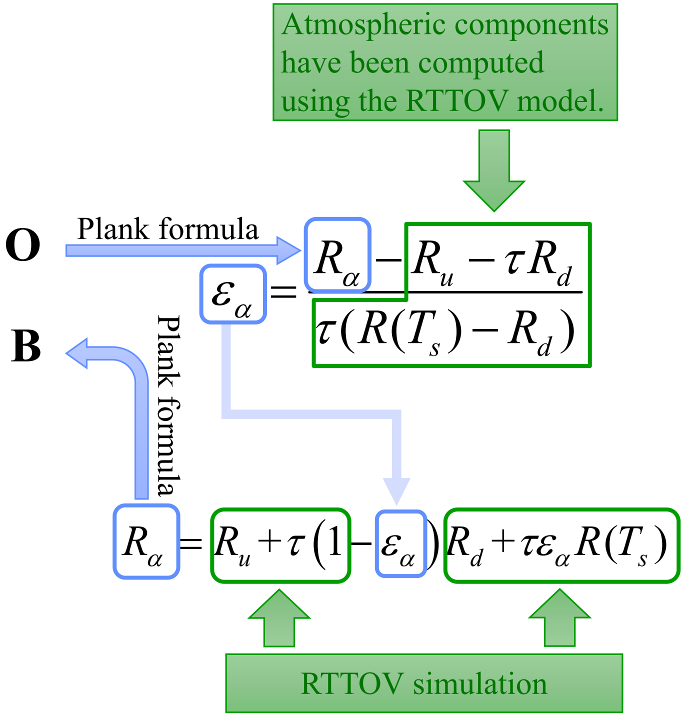

Previous analyses have revealed that, for most surfaces, AMSU emissivities vary smoothly with frequency and that it is possible to use window frequency emissivities for sounding ones. Thus, emissivity estimates obtained at window channels can be allocated to higher frequency channels without extrapolation.

DA of NOAA19 AMSU-A over land: LSE calculation

(Hongyi Xiao, Han Wei)

LSE

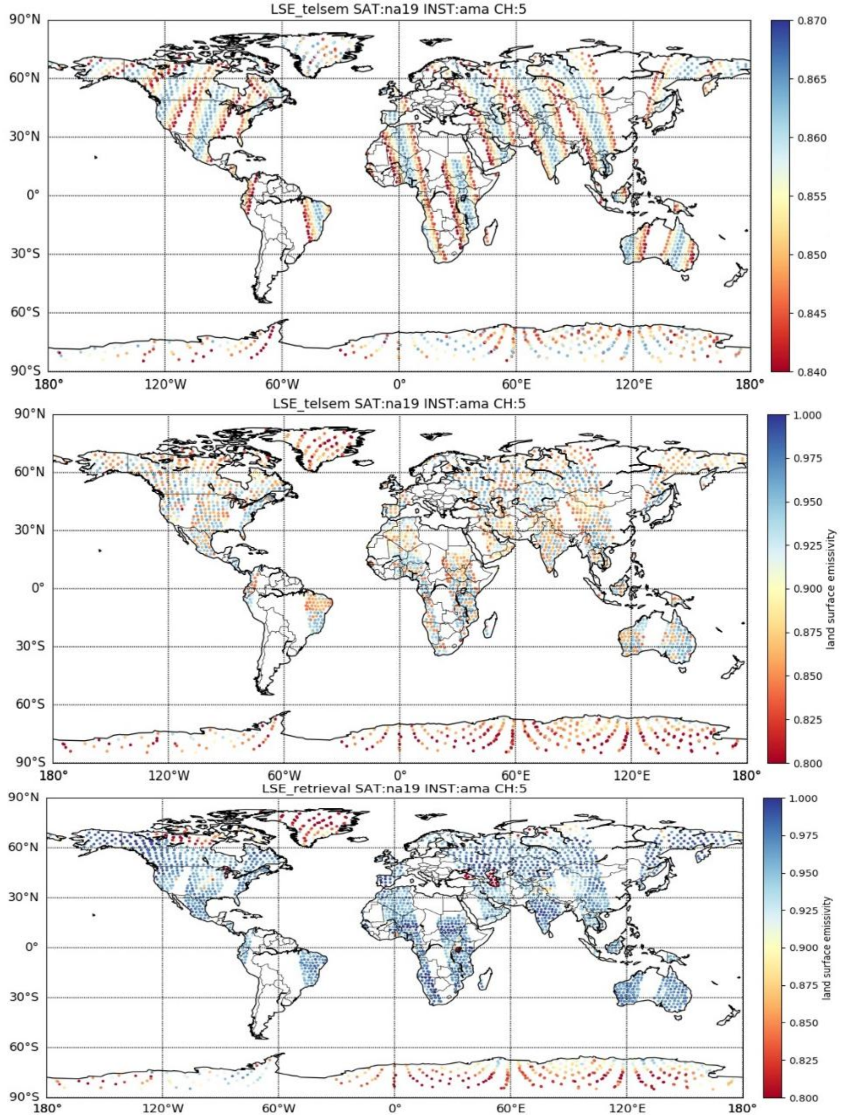

FASTEM

Bias=0.32K
Std=1.33K

TELSEM2

Bias=0.17K
Std=1.22K

Retrieval

Bias=0.01K
Std=1.30K

OMB

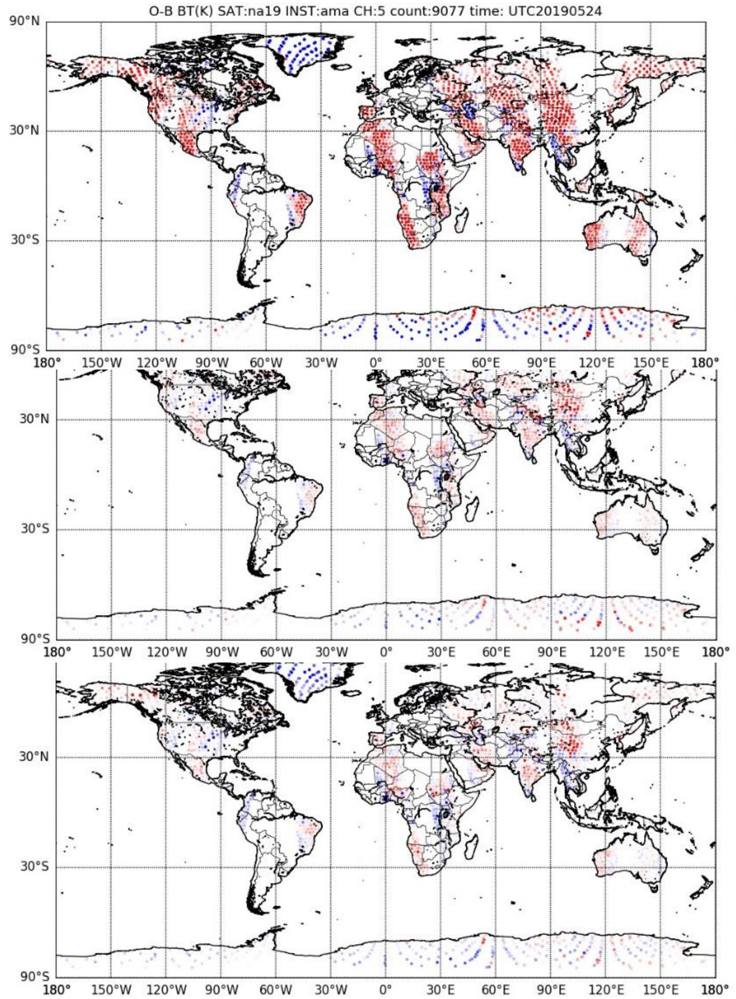

OMB PDF

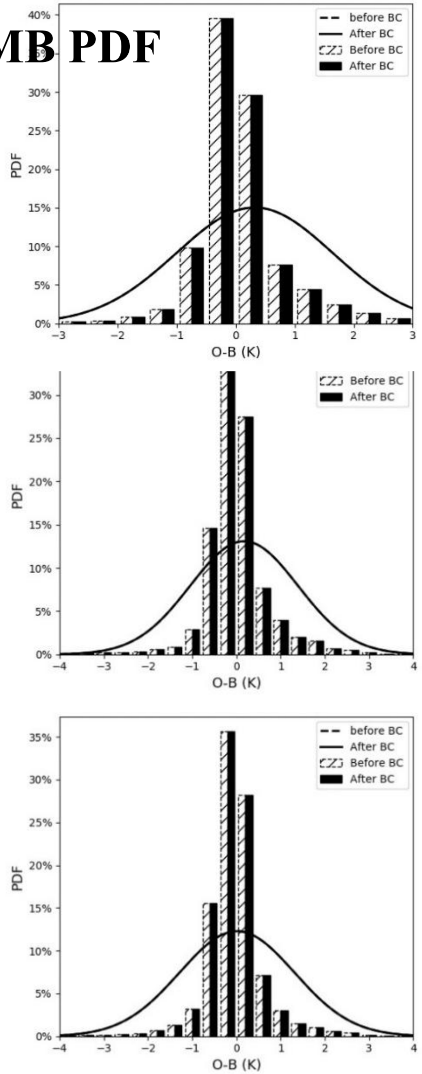

The results given by TELSEM2 are better than FASTEM, while worse than LSE retrieval by window channel.

AMSU-A	CH#	Std of (LSE_retrieval – LSE_TELSEM2)	threshold
NOAA19	5	0.053	0.11
	6	0.053	0.11

DA of NOAA19 AMSU-A over land: Quality Control

(Hongyi Xiao, Han Wei)

AMSU-A质量控制			
No.	Algorithms	Targets	References
1	latitude ＞ 60°	ice/snow	Baordo and Geer, 2016: Q. J. R. Meteorol. Soc., 142: 2854-2866.
2	mixed surface type	Land contamination	
3	land surface temperature ＜ 278K	ice/snow	
4	LSE(TELSEM－retrieval)> threshold	abnormal	
5	$C = 0.8^2 + \left[w_4 \Delta T_b(6)\right]^2 \geq 1$	precipitating cloud	Zhu, Liu, Kleist, et al., 2016: Mon. Wea. Rev., 144:4709-4735.
6	$C = (w_1 \times 0.6)^2 + \left[w_2 \Delta T_b(4)\right]^2 > 0.5$	thick-cloud	
7	Ch5 (>500m); Ch6 (>1500m)	land contamination	Yang, Han, Dong, 2011: Meteorol. Mon., 37(11): 1395-1401.

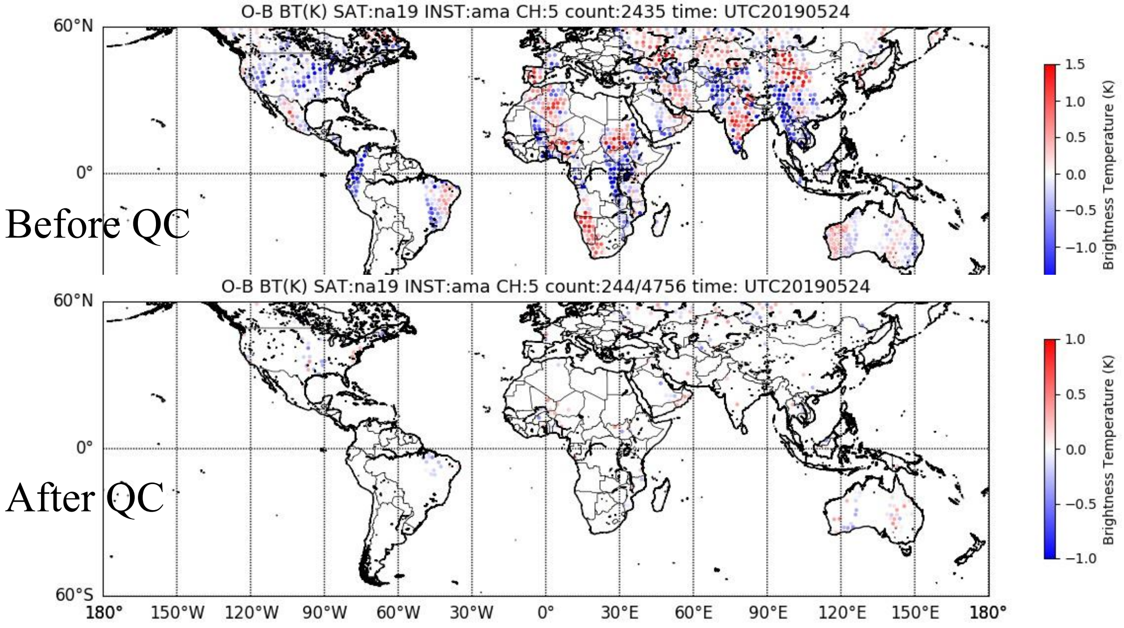

Before QC
Bias=-0.16 Std=0.91

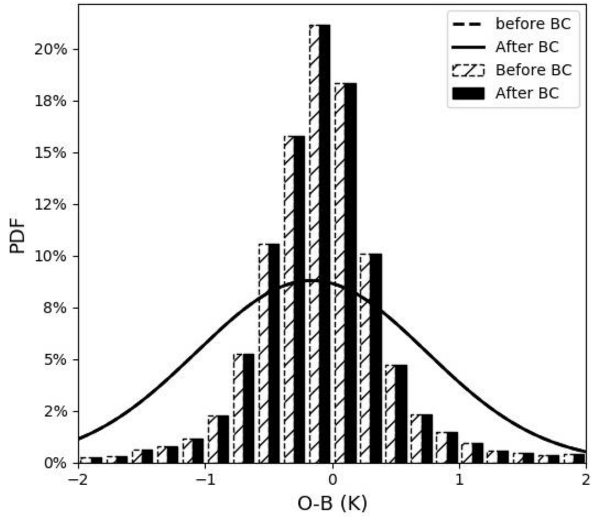

After QC
Bias=-5E-4 Std=0.24

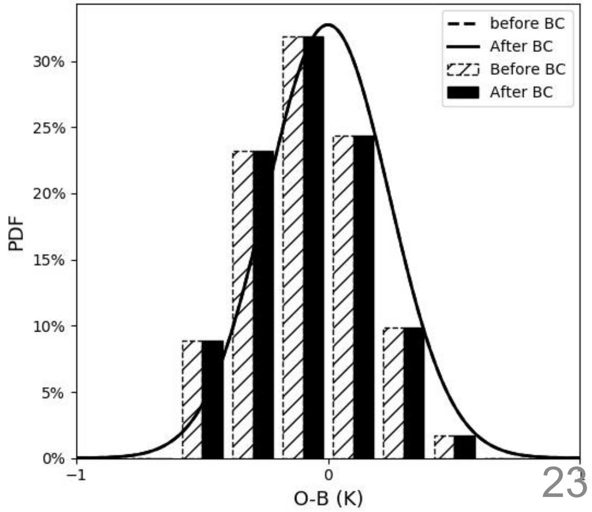

HSCAT-B Wind Assimilation in GRAPES_GFS 4DVAR

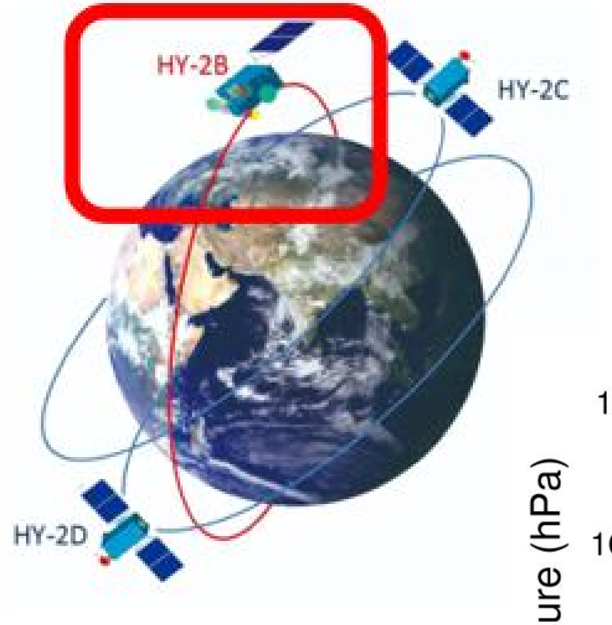

Impact on

Typhoon

NOUL(202011)

Analysis Sea Level Pressure at 2020091600

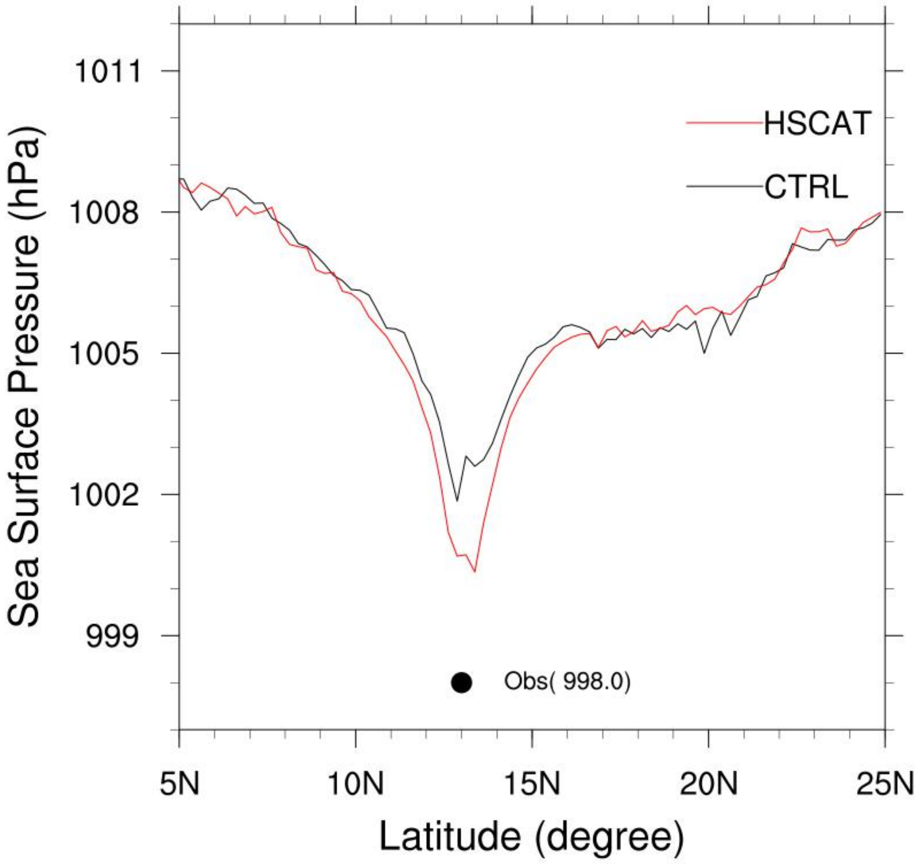

Forecast Minimum Sea Level Pressure of NOUL

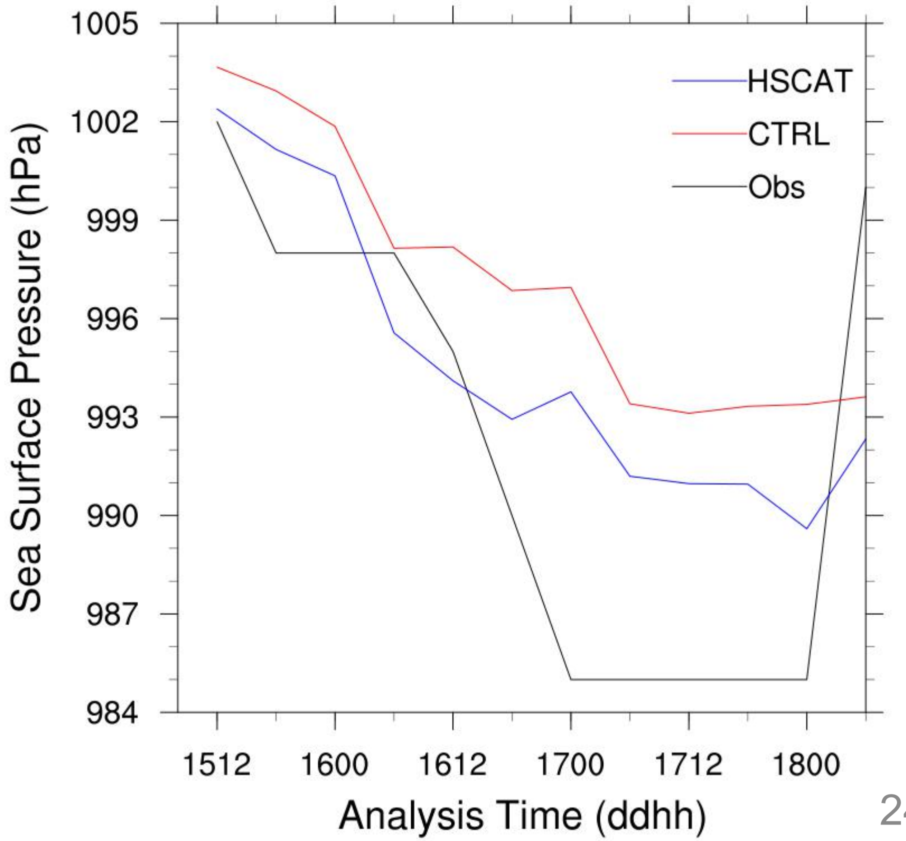

Impact on GRAPES-GFS analyses and forecasts

Experiments: 20200901-20200930

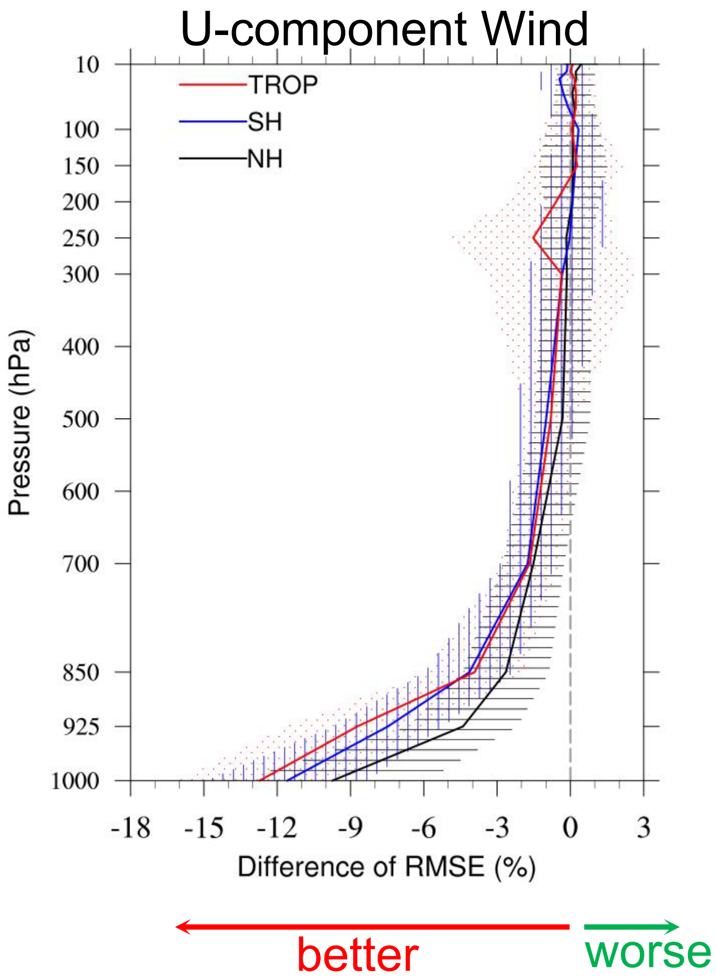

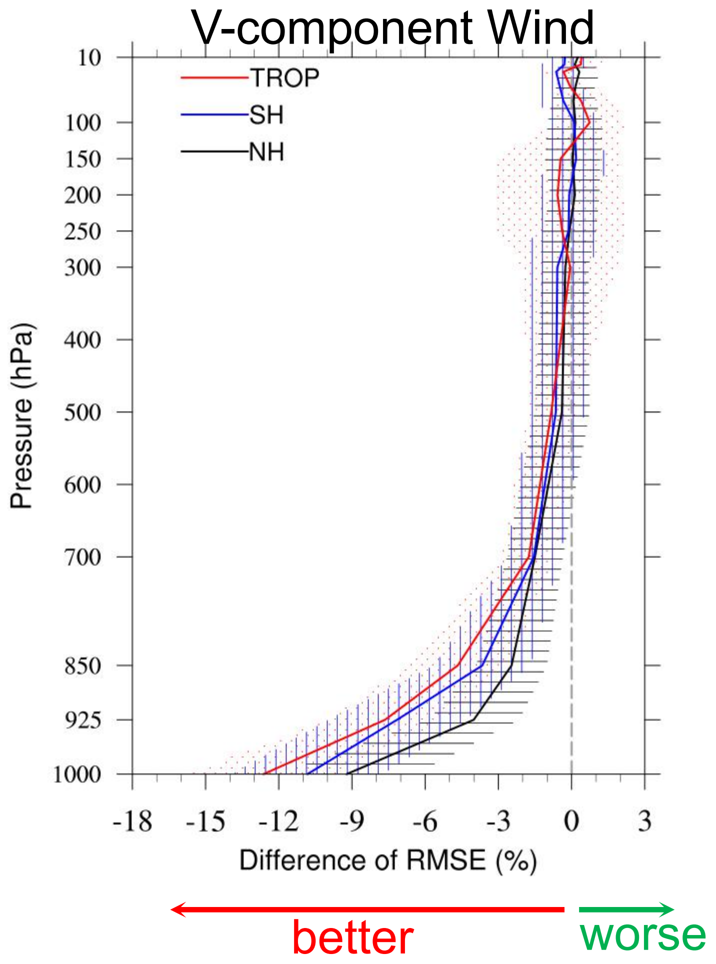

Root Mean Squared Error Reduction Rate of U and V analyses by HSCAT-B Wind Assimilation

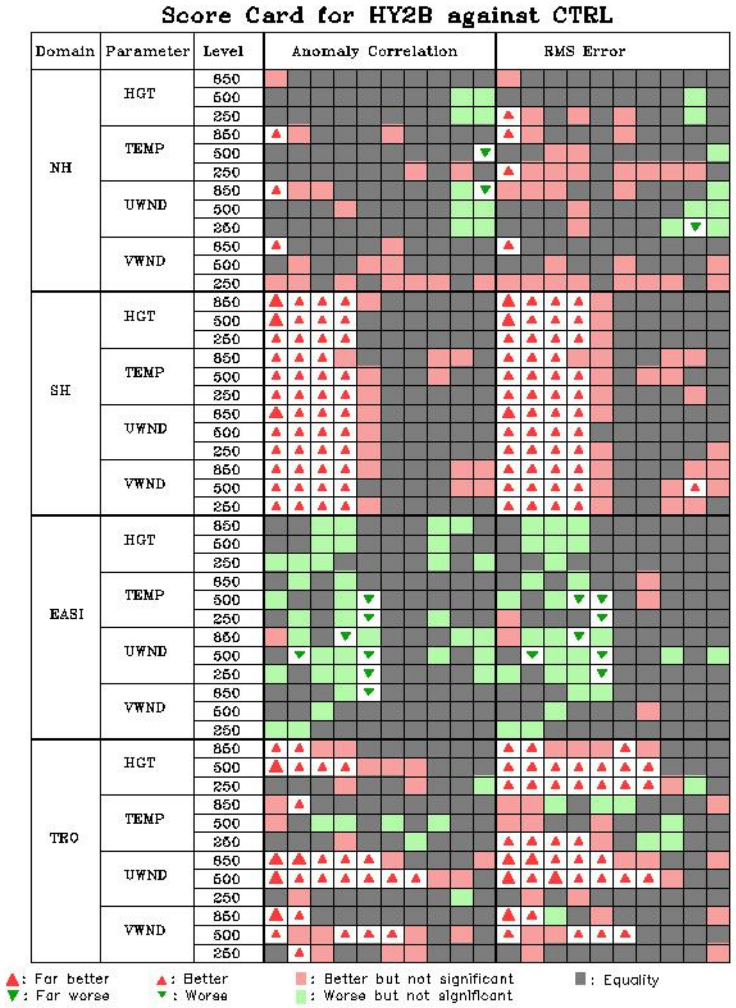

The forecast skills are **improved significant** for Southern Hemisphere and Tropics.

The impact of considering actual spectral response of FY-3D MWTS in radiance assimilation

Comparing with ideal Spectral Response Function(SRF),

1. Dose actual SRF affect the microwave radiance simulation(MRS)?
2. How much dose actual SRF affect the simulation?
3. How dose actual SRF affect the simulation?

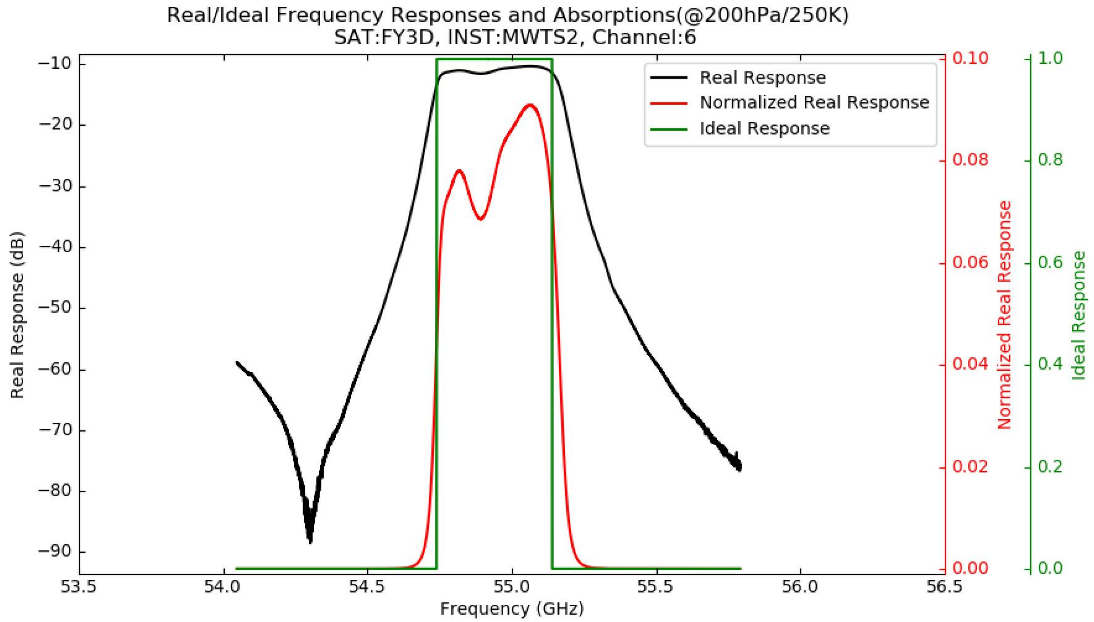

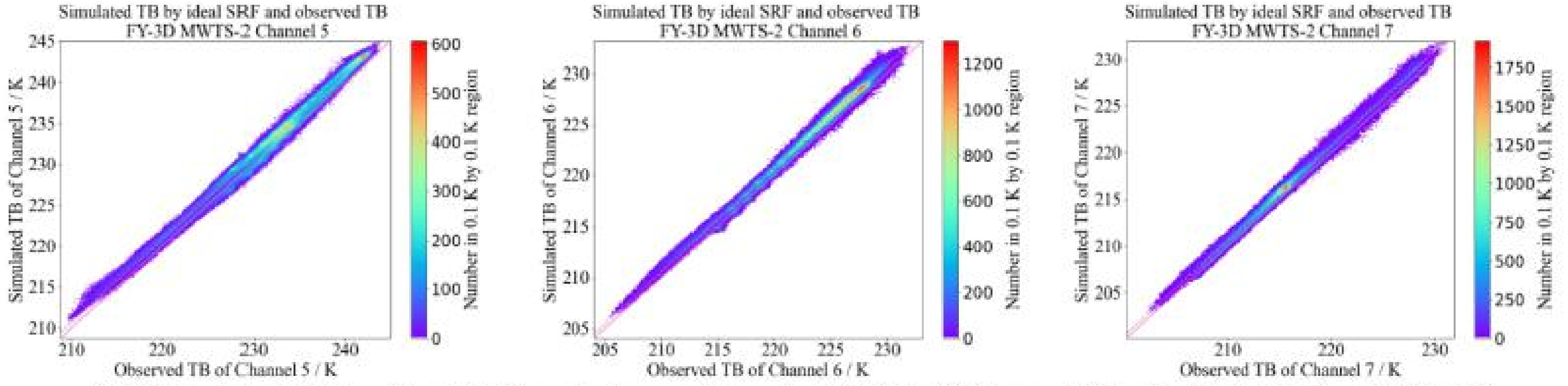

(b) Simulated TB by ideal SRF and observation of MWTS-2 Channel 5(left), 6(middle) and 7(right)

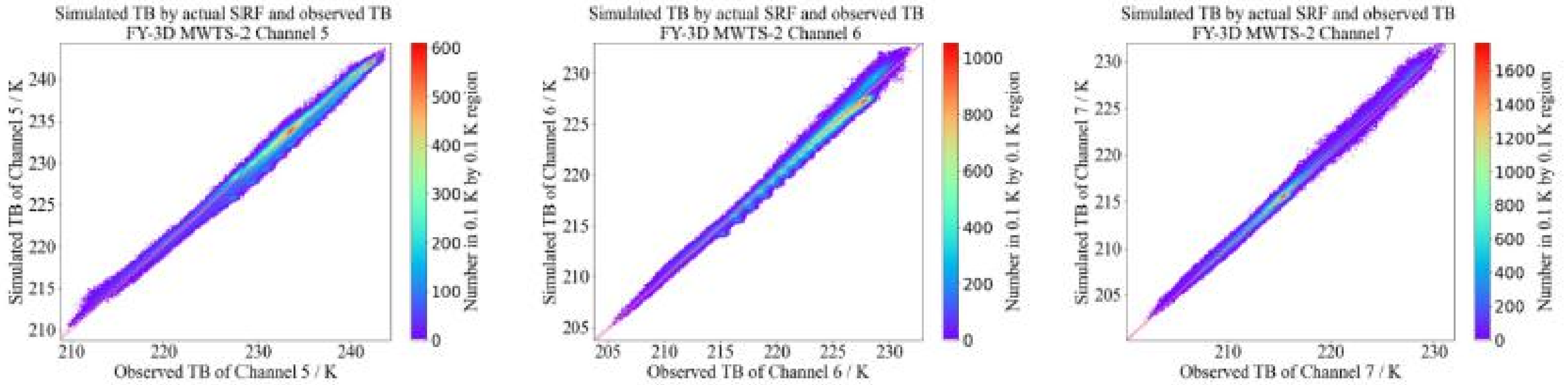

(c) Simulated TB by actual SRF and observation of MWTS-2 Channel 5 (left), 6 (middle) and 7 (right)

Actual SRF does affect the MRS.

Chen, H.*, Han, W.*, Wang, H., Pan, C., An, D., Gu, S., & Zhang, P. (2021). Why and how does the actual spectral response matter for microwave radiance assimilation?. *Geophysical Research Letters*, *48*, e2020GL092306. https://doi.org/10.1029/2020GL092306

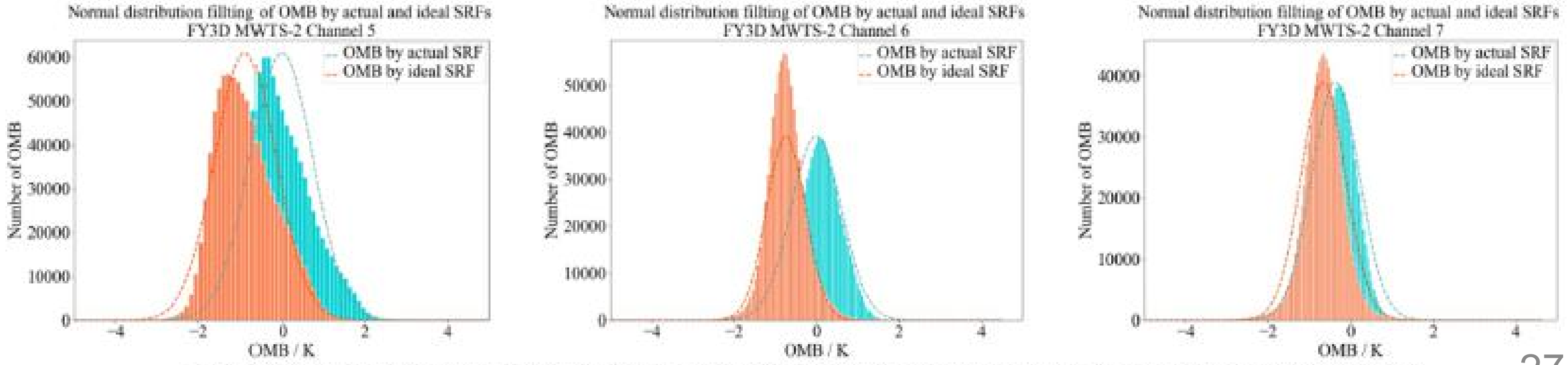

(d) OMB by actual and ideal SRFs of MWTS-2 Channel 5 (left), 6 (middle) and 7 (right)

Effects of actual SRF on MRS varies according to channel ID and latitude

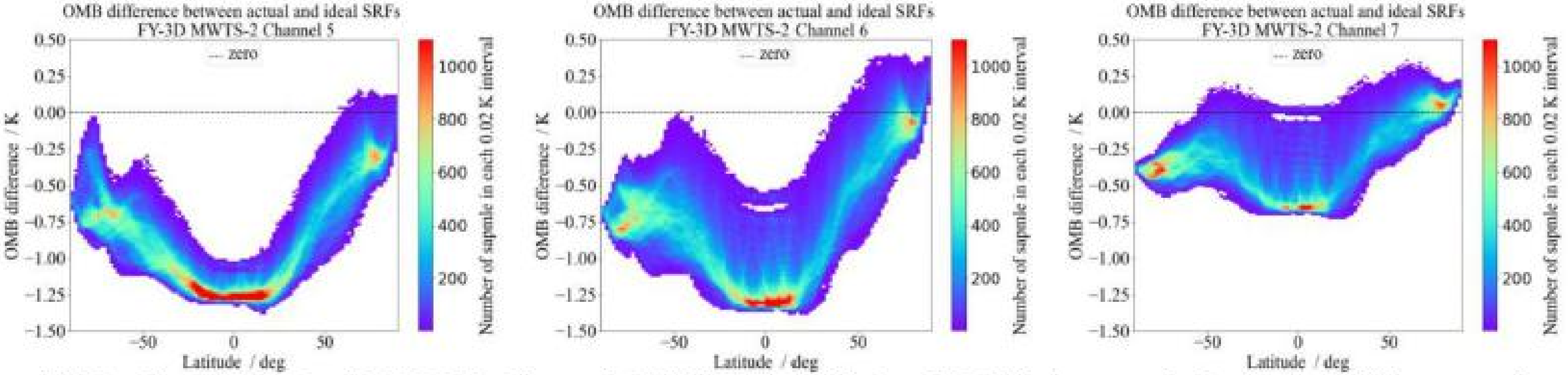

(e) Number of OMB of MWTS-2 Channel 5 (left), 6 (middle) and 7 (right) versus latitude and difference value

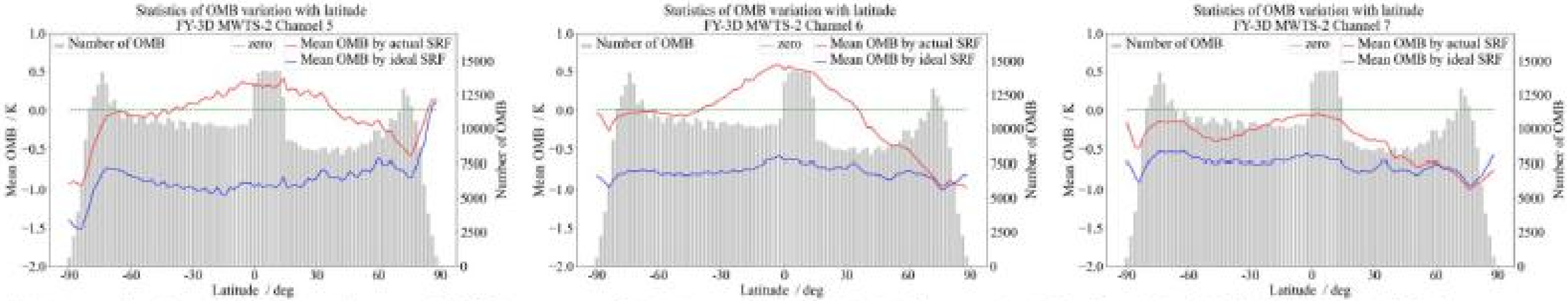

(f) Longitude-mean number and difference of OMB of MWTS-2 Channel 5 (left), 6 (middle) and 7 (right) versus latitude

Table 1
RMSE of OMB, Bias of Simulated TB, and STDV of OMB by Actual and Ideal SRFs

	Channel 5	Channel 6	Channel 7	Mean	Relative difference between means by actual SRFs and by ideal SRFs
RMSE (K)					
Ideal SRF	1.14	0.88	0.85	0.96	
Actual SRF	0.75	0.61	0.66	0.67	−30.2%
Bias (K)					
Ideal SRF	0.99	0.78	0.72	0.83	
Actual SRF	0.60	0.47	0.48	0.52	−37.3%
STDV (K)					
Ideal SRF	0.75	0.47	0.58	0.6	
Actual SRF	0.73	0.61	0.54	0.63	5%

Abbreviations: OMB, Observation minus Background; RMSE, Root Mean Squared Error; SRF, Spectral Response Function; STDV, STandard DeViation; TB, Brightness Temperature.

Five typical deformation types were formed to demonstrate the mechanism of the effects of actual SRF on MRS.

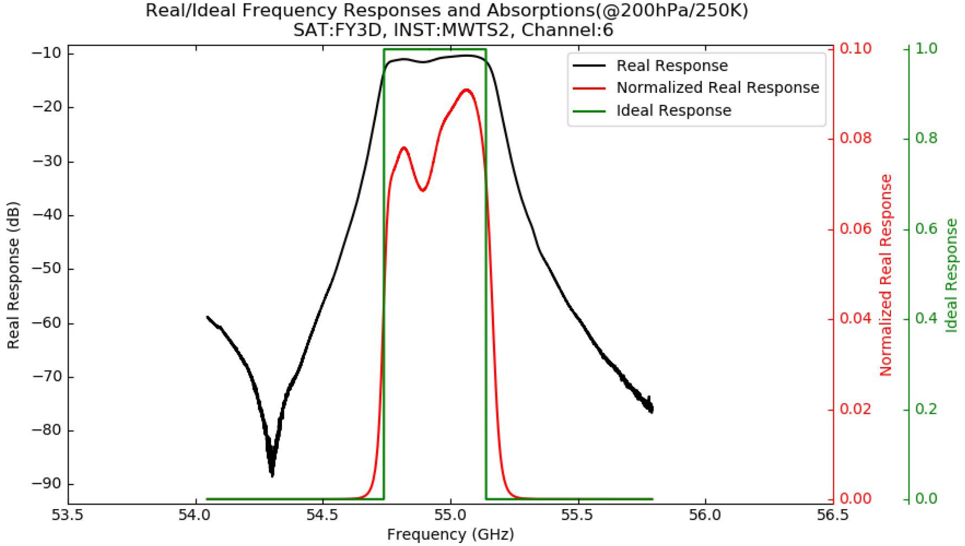

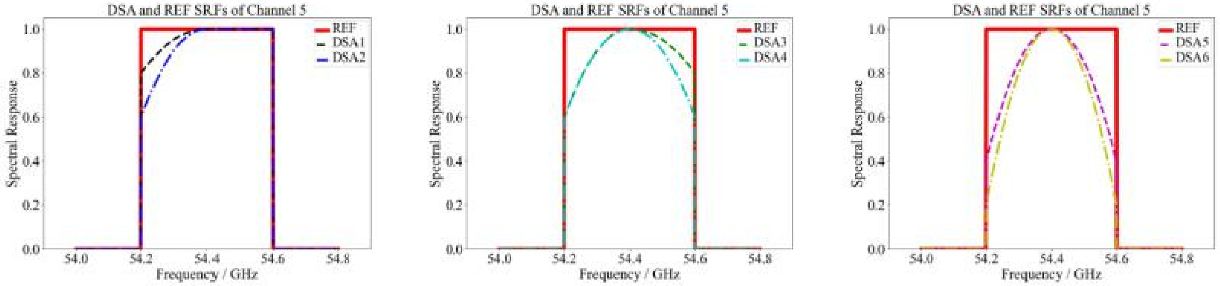

(a) Simulated DSA and REF SRFs of Channel 5

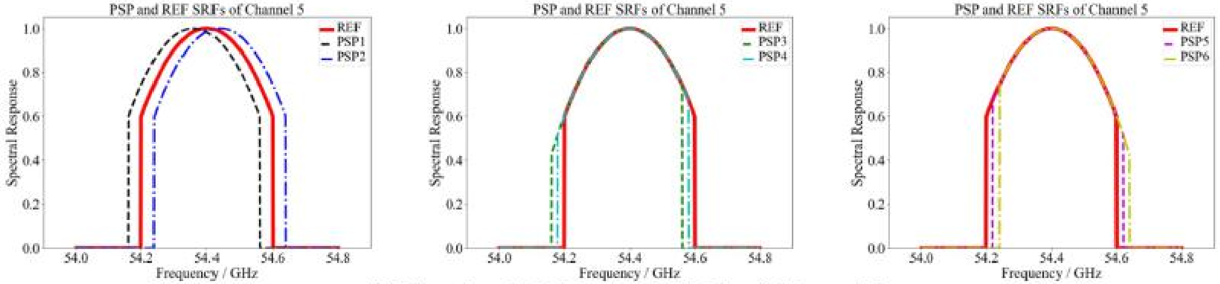

(b) Simulated PSP and REF SRFs of Channel 5

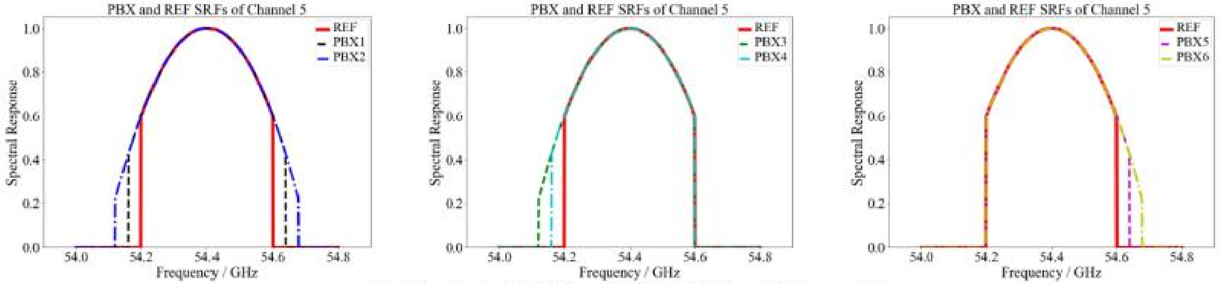

(c) Simulated PBX and REF SRFs of Channel 5

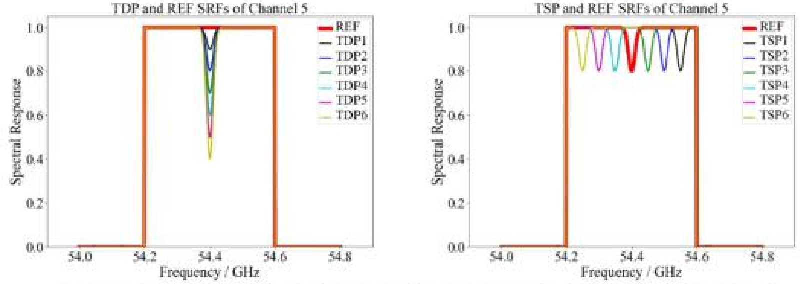

(d) Simulated TDP(left), TSP(right) and REF SRFs of Channel 5

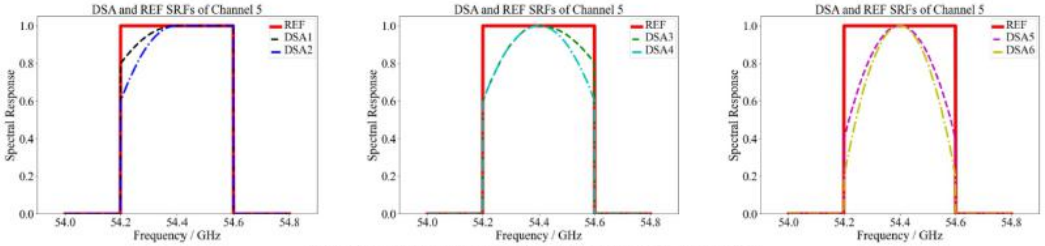

(a) Simulated DSA and REF SRFs of Channel 5

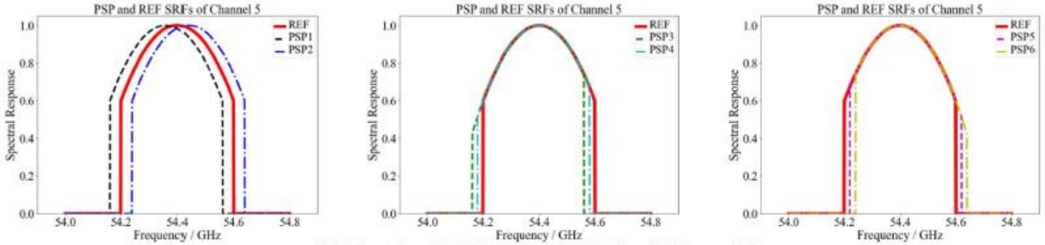

(b) Simulated PSP and REF SRFs of Channel 5

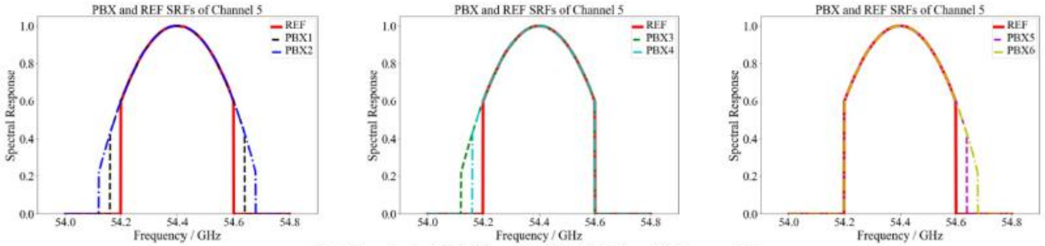

(c) Simulated PBX and REF SRFs of Channel 5

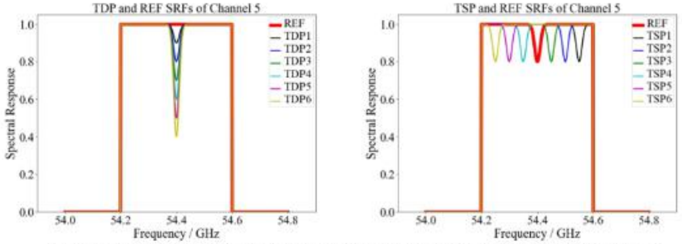

(d) Simulated TDP(left), TSP(right) and REF SRFs of Channel 5

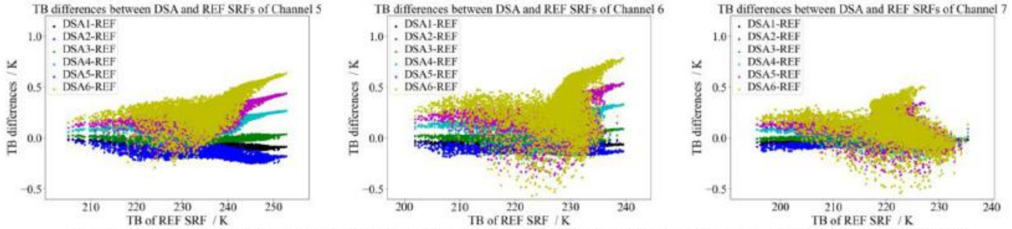

(a) Simulated TB differences between DSA and REF SRFs of Channel 5(left), 6(middle) and 7(right)

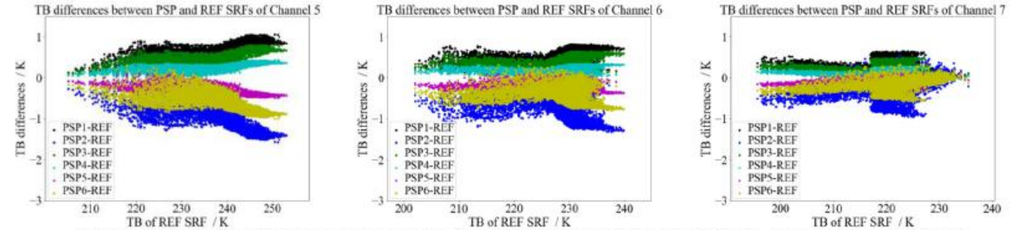

(b) Simulated TB differences between PSP and REF SRFs of Channel 5(left), 6(middle) and 7(right)

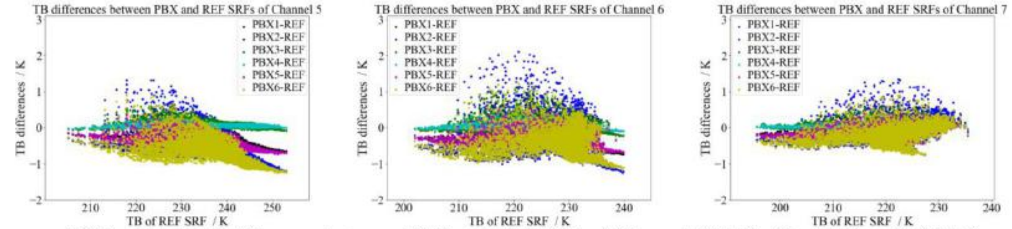

(c) Simulated TB differences between PBX and REF SRFs of Channel 5 (left), 6 (middle) and 7 (right)

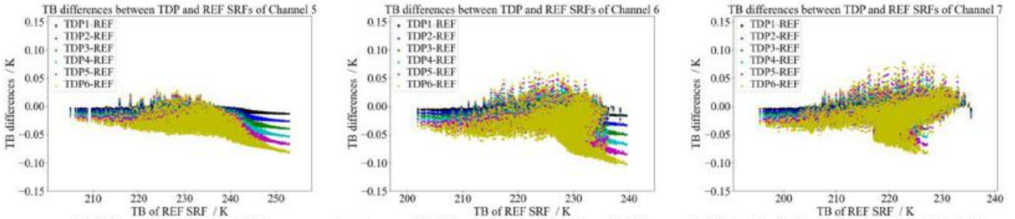

(d) Simulated TB differences between TDP and REF SRFs of Channel 5 (left), 6 (middle) and 7 (right)

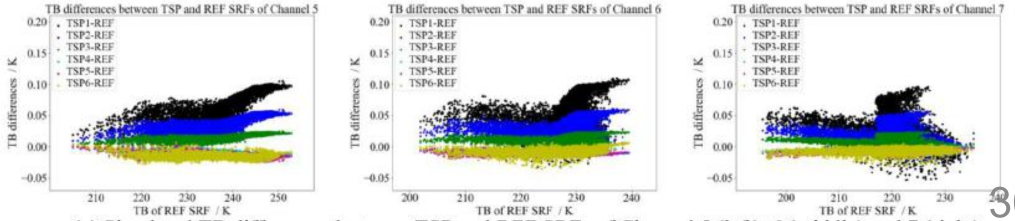

(e) Simulated TB differences between TSP and REF SRFs of Channel 5 (left), 6 (middle) and 7 (right)

Differences of effects on MRS between typical deformations were simulated and analyzed

Different deformations have different degrees of effects on MRS.

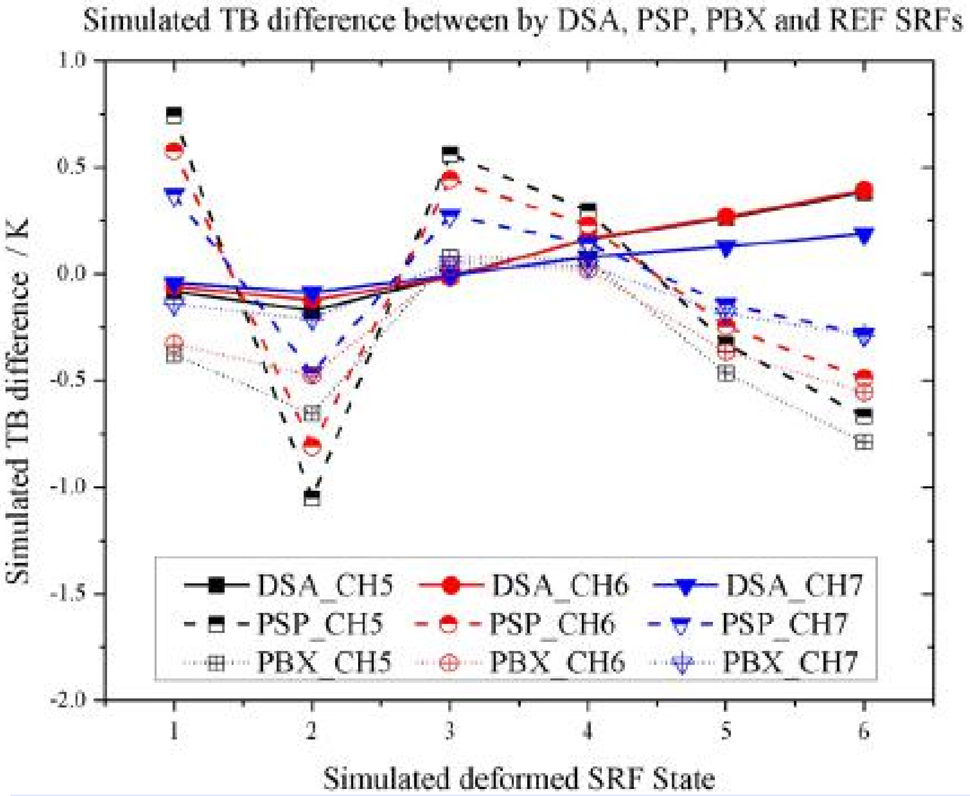

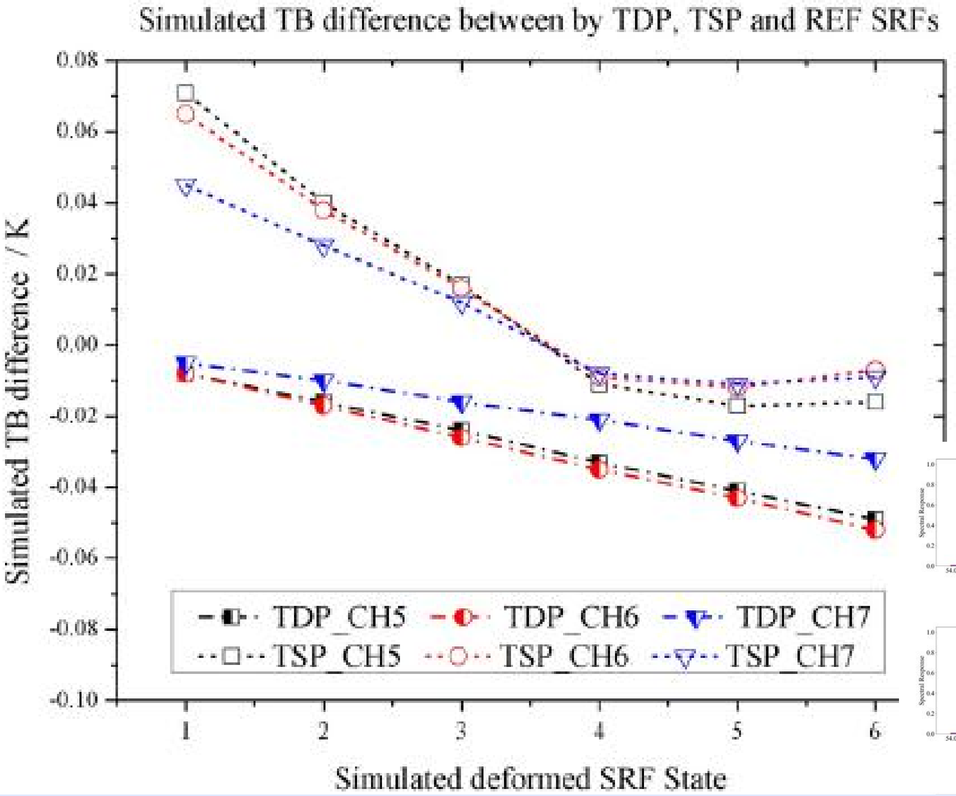

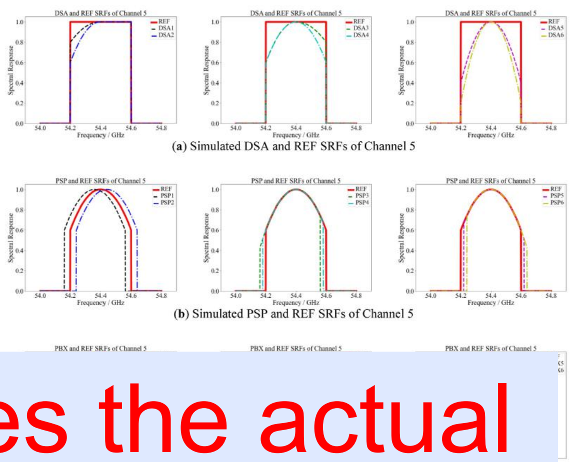

Hao Chen' poster (3p.03), Why and how does the actual spectral response matter for microwave radiance assimilation ?

Progress on Nonspherical Particle Scattering

- Build the original database based on the latest invariant imbedding T-matrix method.

Rigorous and efficient computational technique

(Bi et al., 2014; 2018)

- A new approach to parameterize nonspherical particle shapes

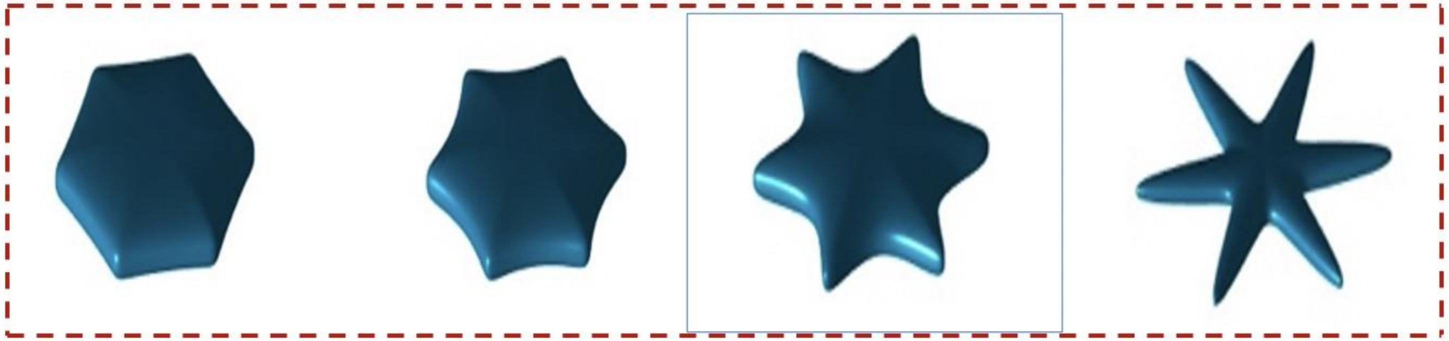

flexible shape control
Continous shape variation

+ A machine learning approach

Progress on Nonspherical Particle Scattering

- Horizontaly oriented ice crystals

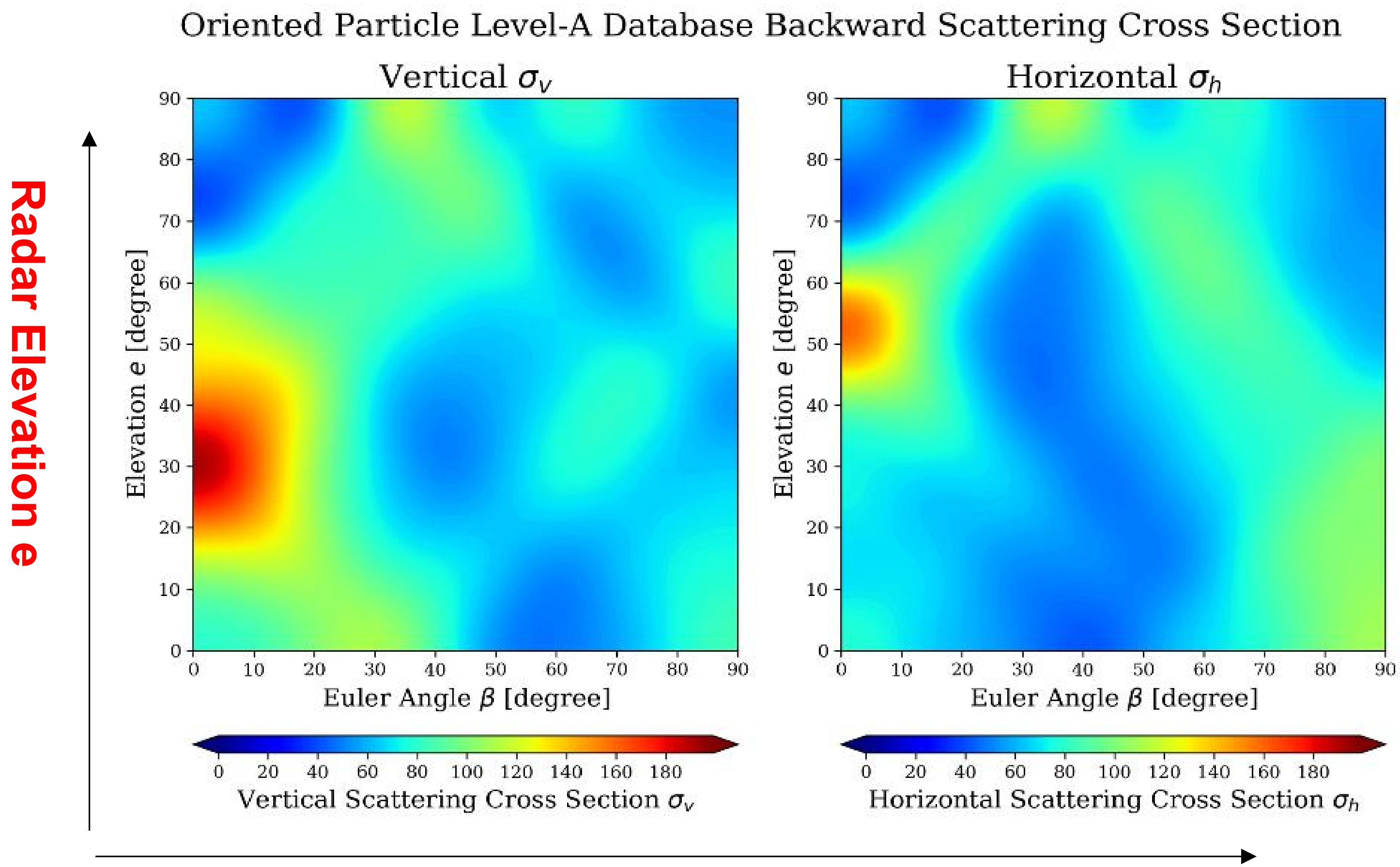

Euler Angle β

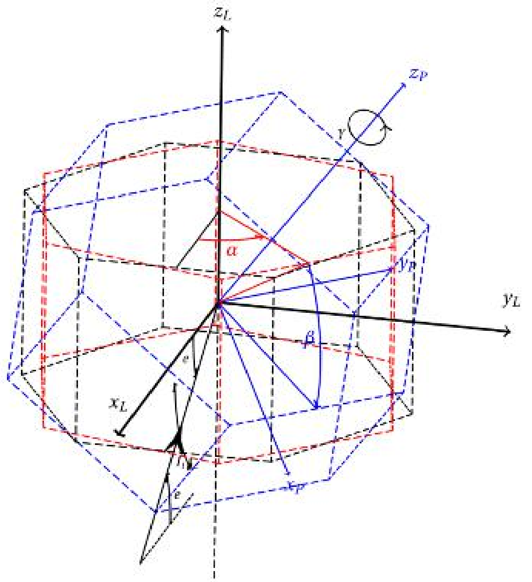

Euler Angle α， β，γ

Progress on Nonspherical Particle Scattering

- Melted ice crystals

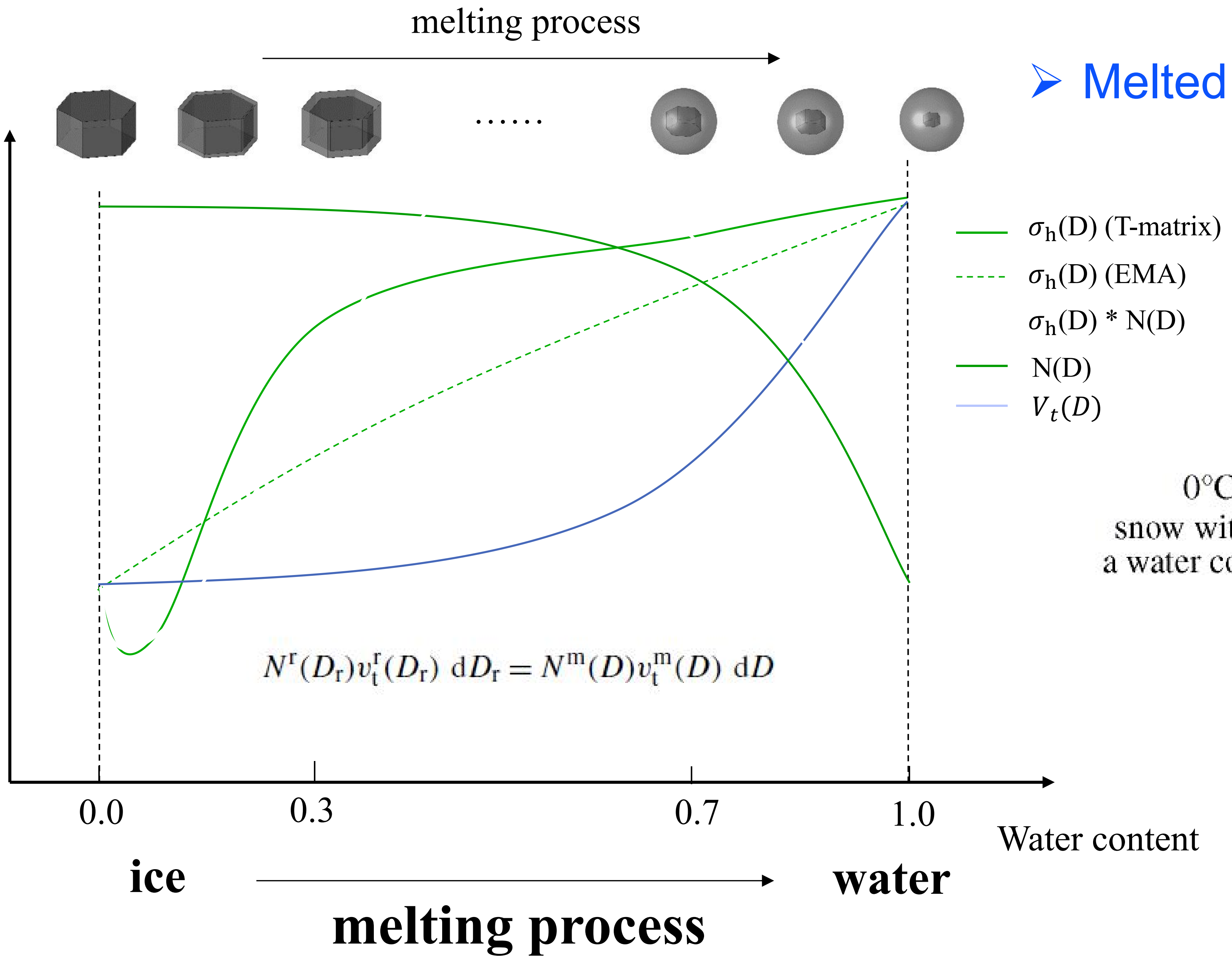

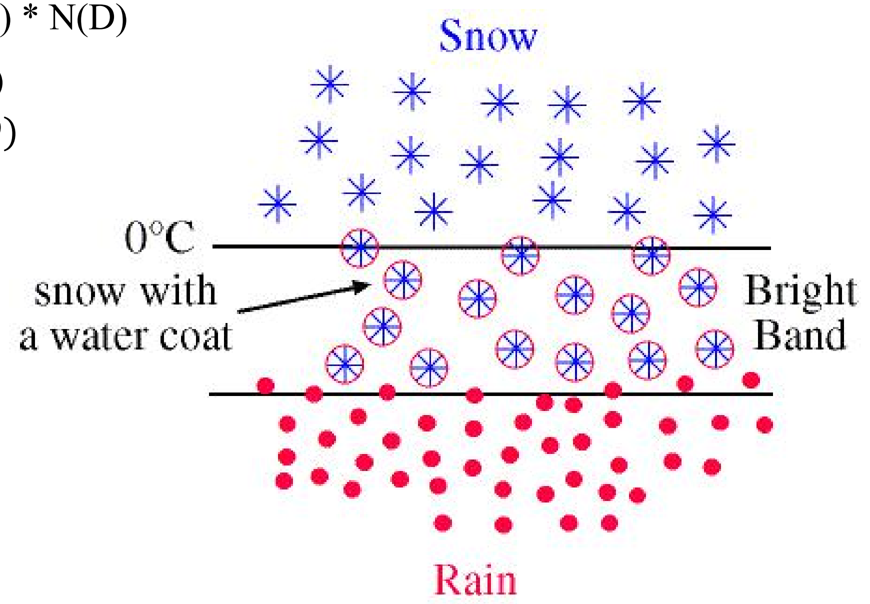

All-sky Passive Microwave Simulations of FY-3D

A vertical distribution of frozen hydrometeors was implemented into the RTTOV radiative transfer model.

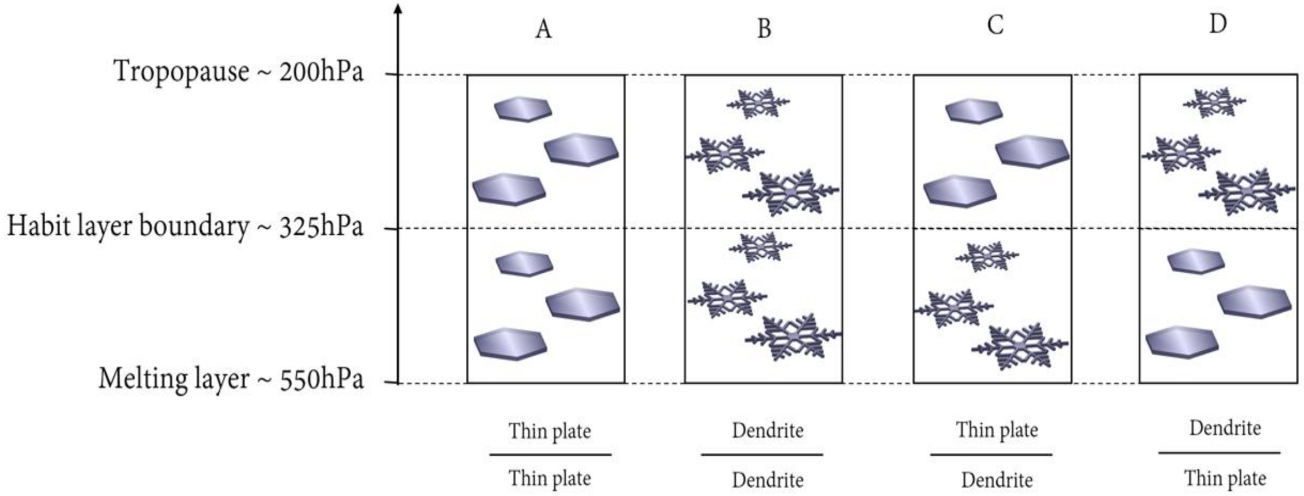

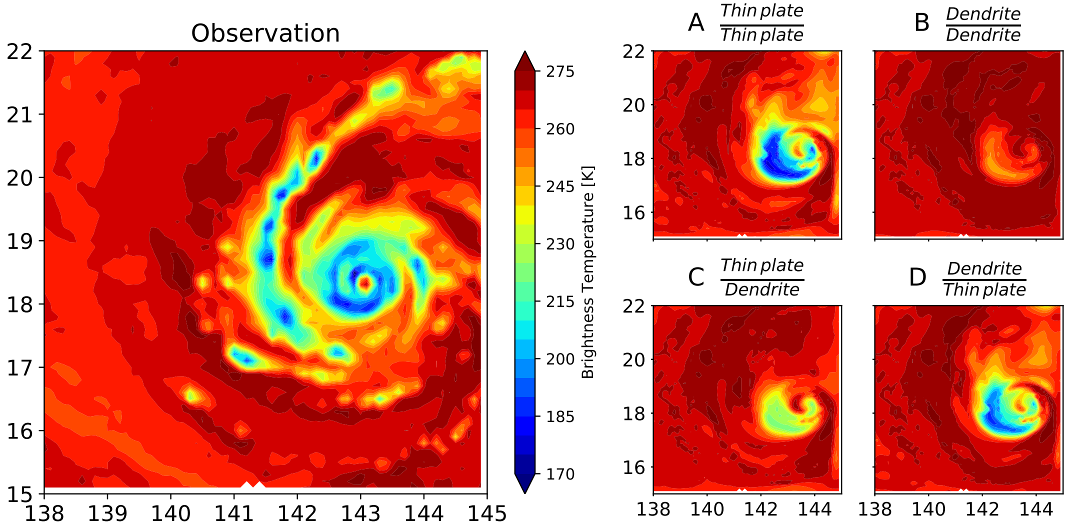

Four vertical inhomogeneity scenarios for sensitivity test

Observation vs Simulation @ 89.0GHz

- ➢ Vertical ice habit variation has significant impact on the TOA bright temperature simulations.

Xie, H., Lei Bi, Wei Han, Jincheng Wang, 2020. *Journal of Geophysical Research: Atmospheres,* 125(21): e2020JD032817.

All-sky Passive Microwave Simulations of FY-3D

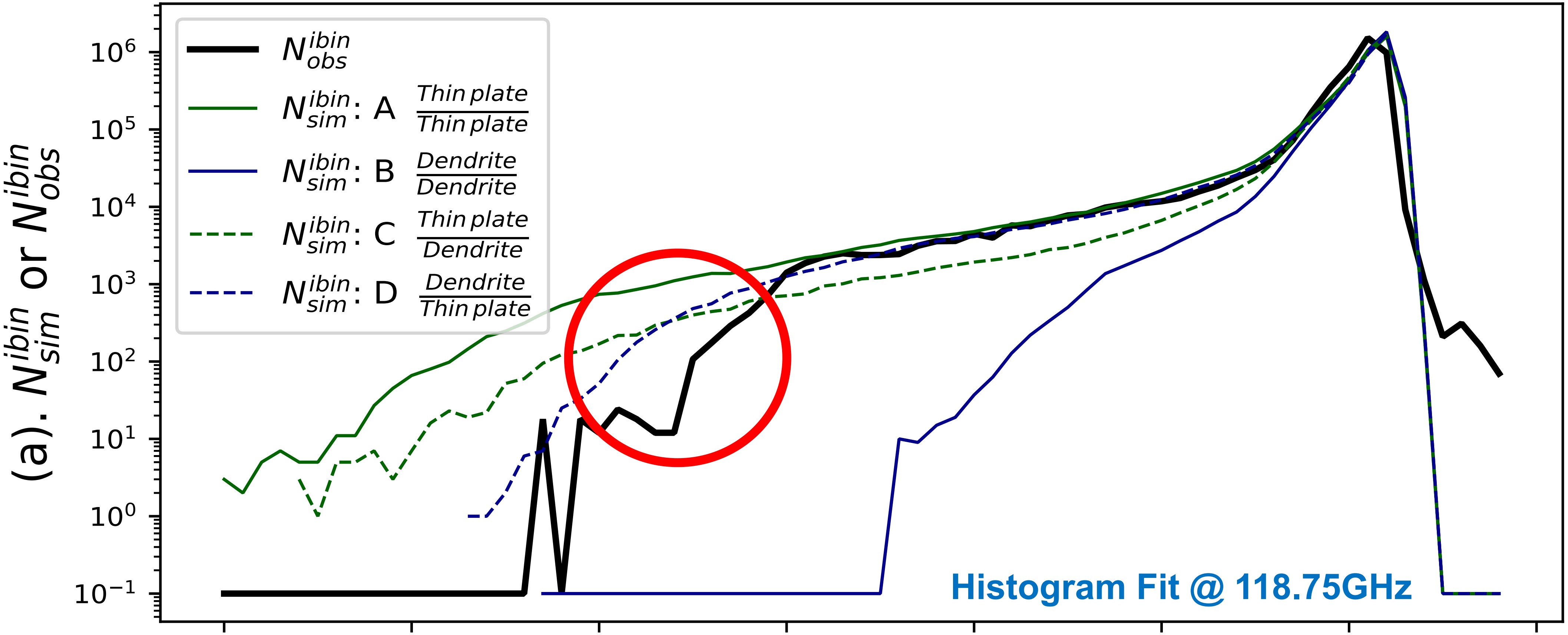

- ➢ An incorporation of vertical habit variation could bring simulations closer to observations.

Xie, H., Lei Bi, Wei Han, Jincheng Wang, 2020. ***Journal of Geophysical Research: Atmospheres,*** **125(21): e2020JD032817.**

Geostationary microwave sounder (GEO-MW)

GEO-MW: Provide high-frequent measurements of 3D atmosphere structure

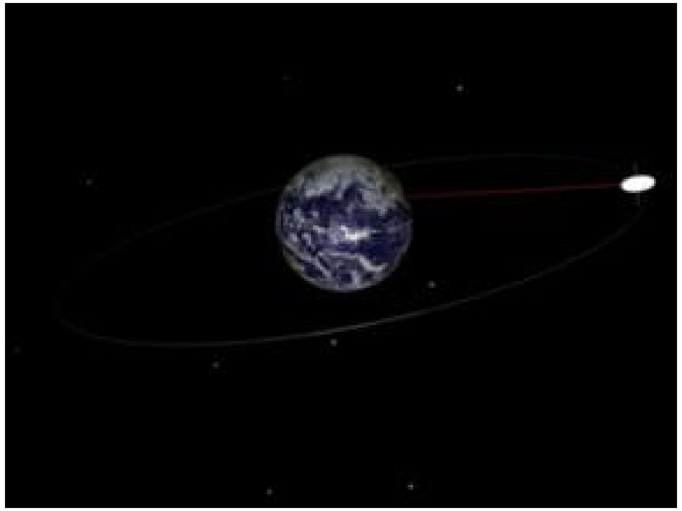

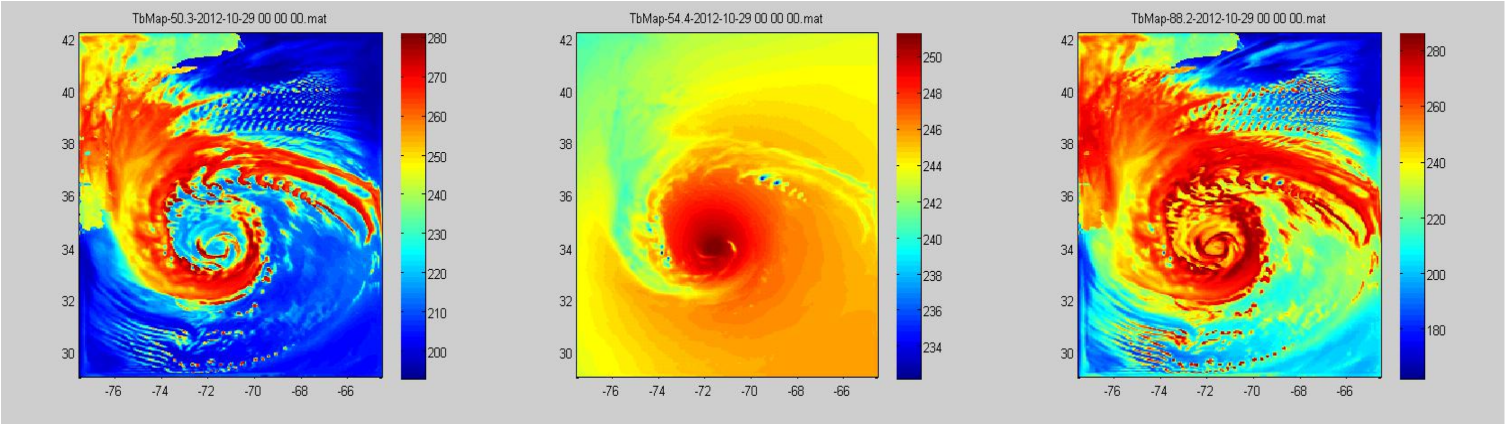

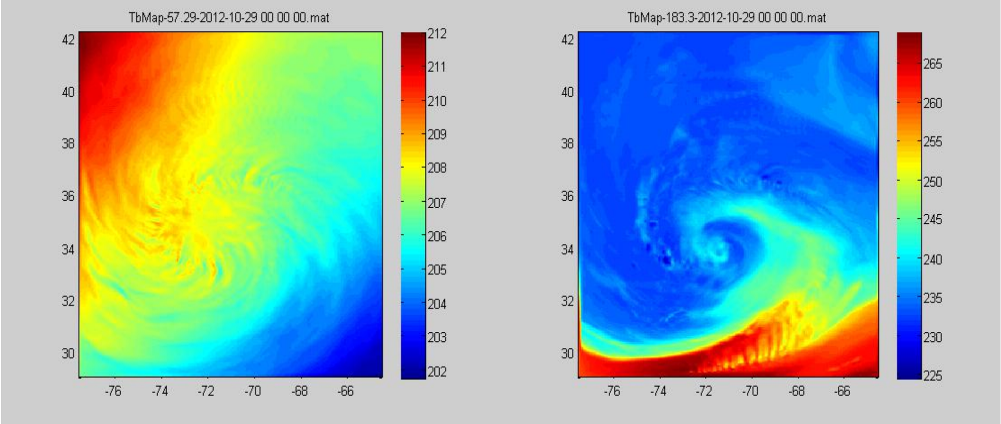

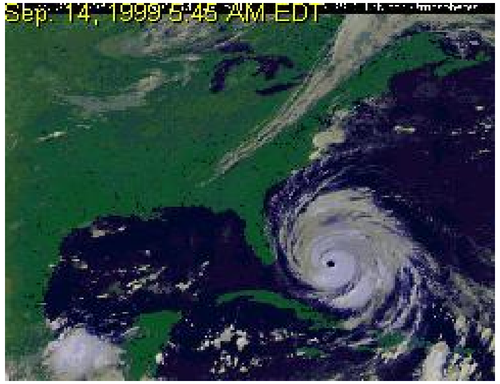

Chen Ke, Hong Pengfei, Han Wei, et al. 2021. Geostationary microwave observation system simulation experiments based on GRAPES 4D-Var. Acta Meteorologica Sinica, accepted. (in Chinese)

Motivation

Problem: As unprecedented satellite observation data, the application effect of GEO- MW observation on numerical weather prediction (NWP) is still unknow.

Goal: Provide an independent assessment of GEO- MW based on Observing System Simulation Experiments (OSSEs) , which examine if these very frequent microwave observations would be beneficial to mesoscale NWP.

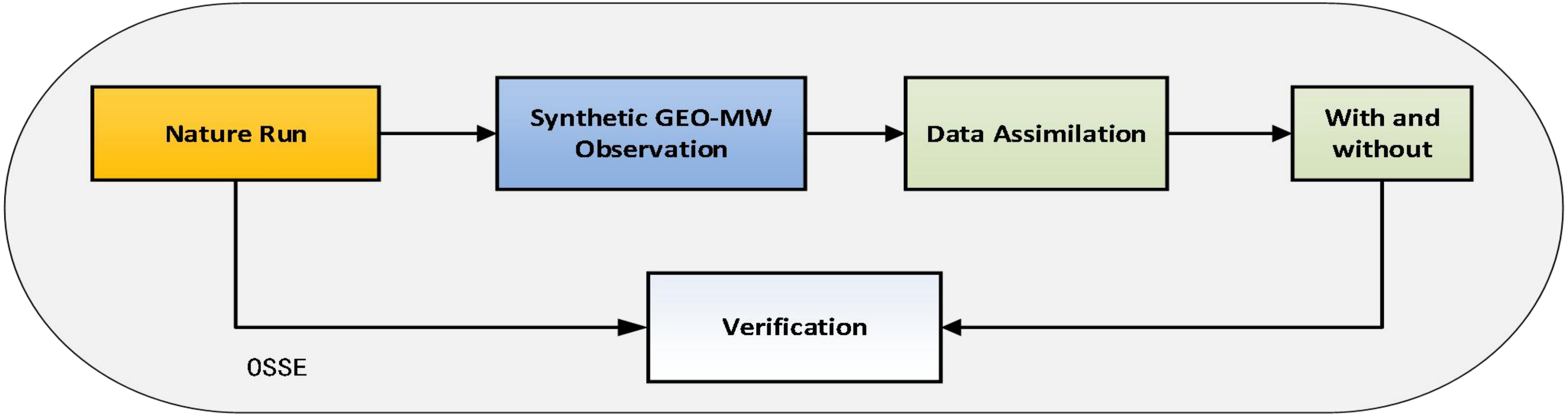

GEO-MW OSSE flow chart based on GRAPES 4D-VAR

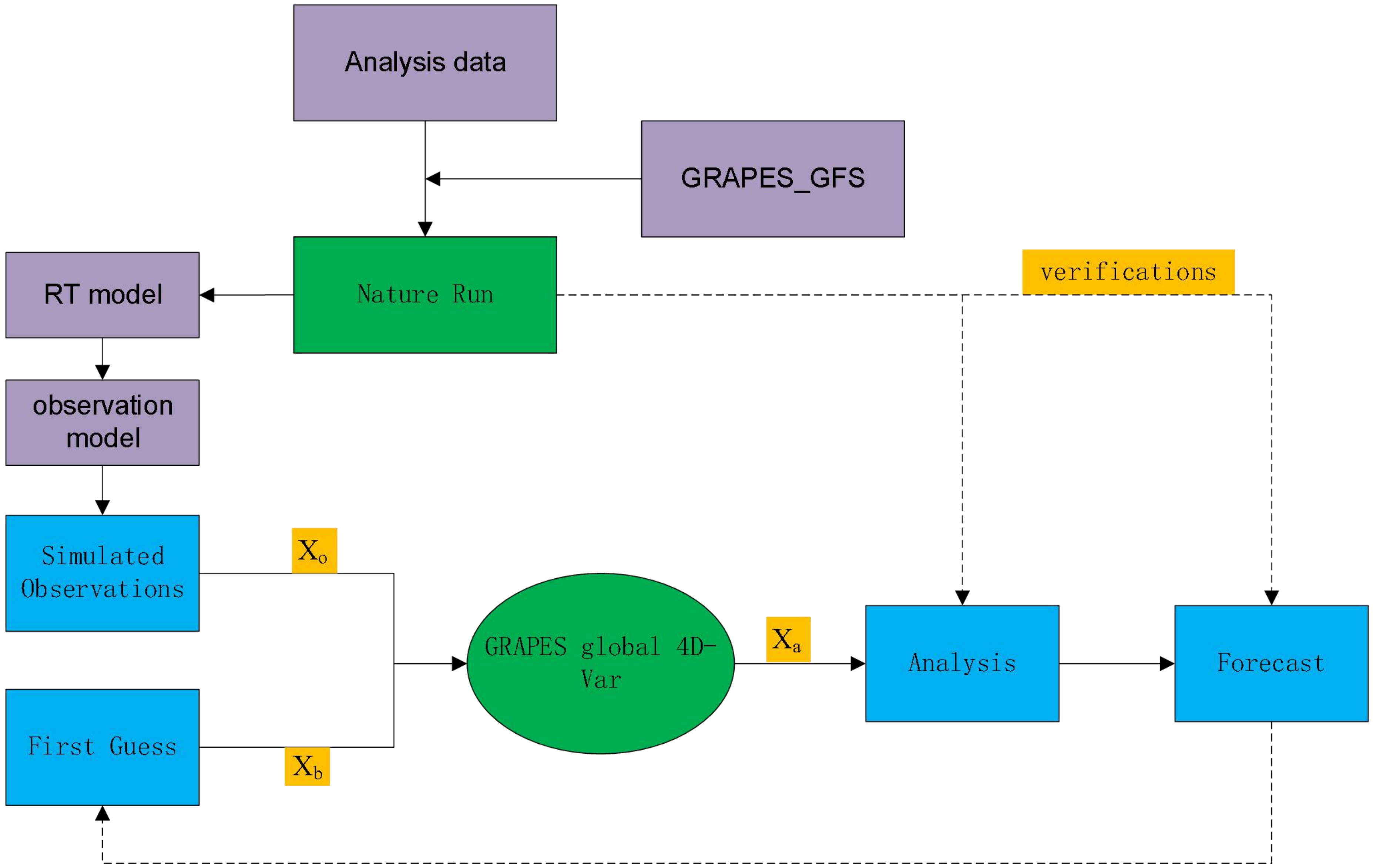

GEO simulated observed brightness temperature

2018 typhoon Maria

Horizontal Polarization	2018-07-08 UTC 12:00:00

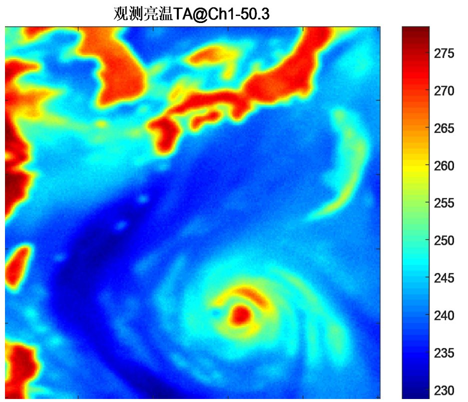

50.3GHz

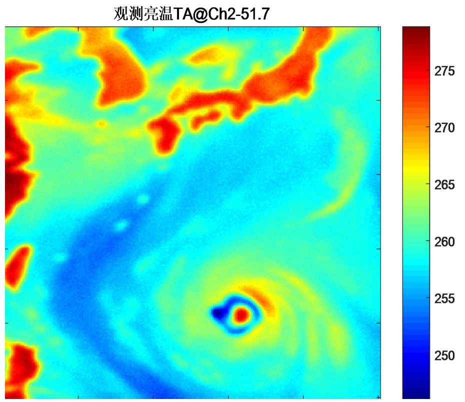

51.76GHz

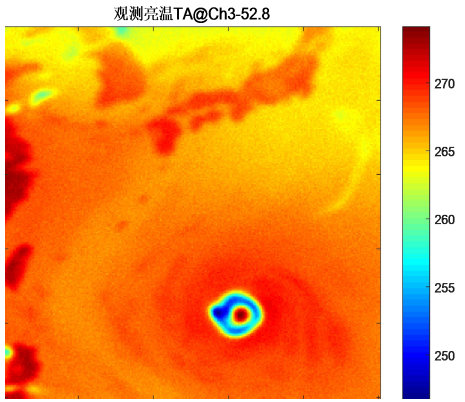

52.8GHz

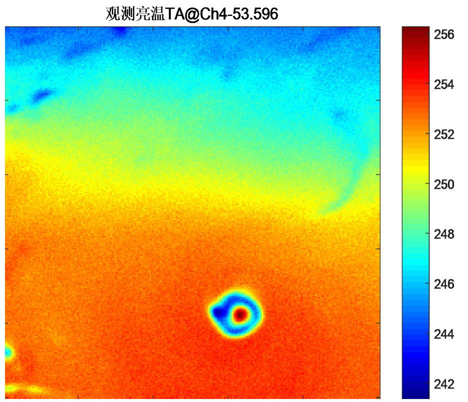

53.596GHz

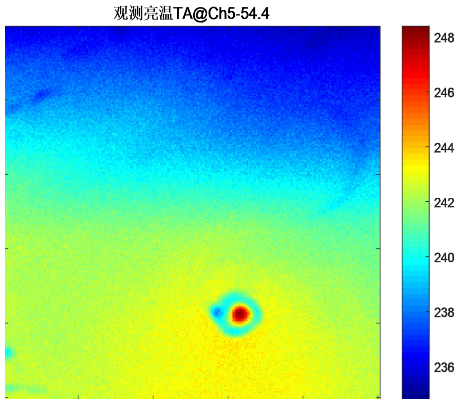

54.4GHz

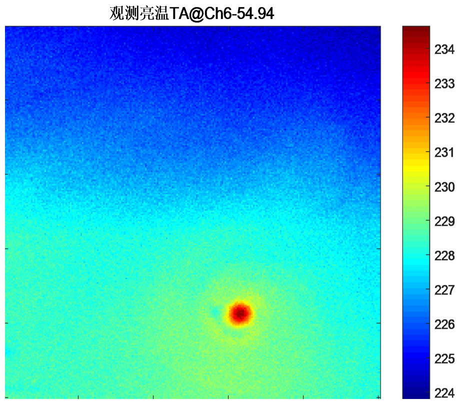

54.94GHz

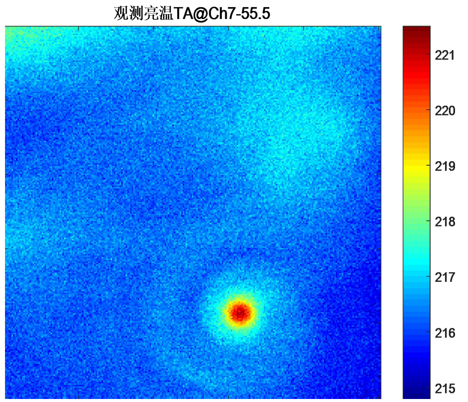

55.5GHz

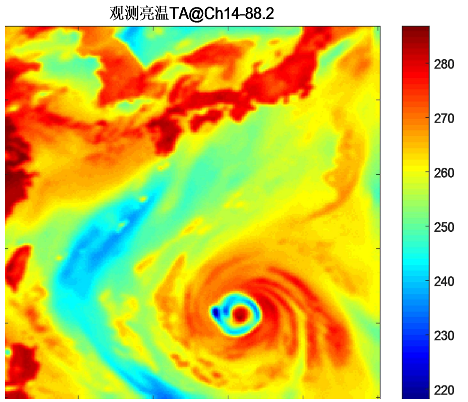

88.2GHz

GEO-MW OSSE – various frequency bands

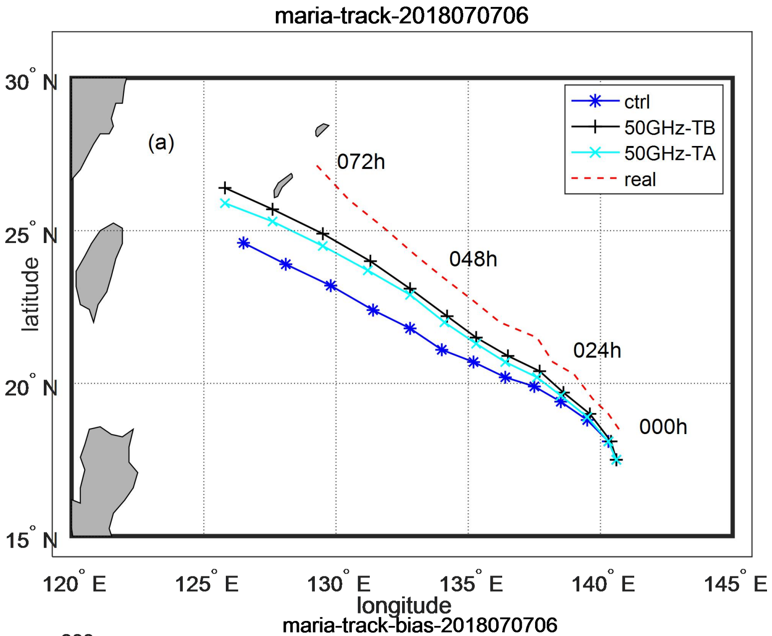

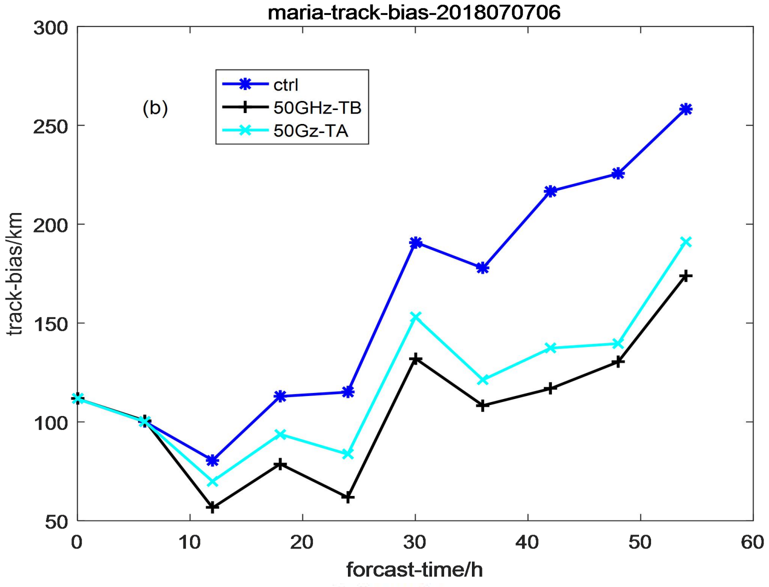

(a) Maria

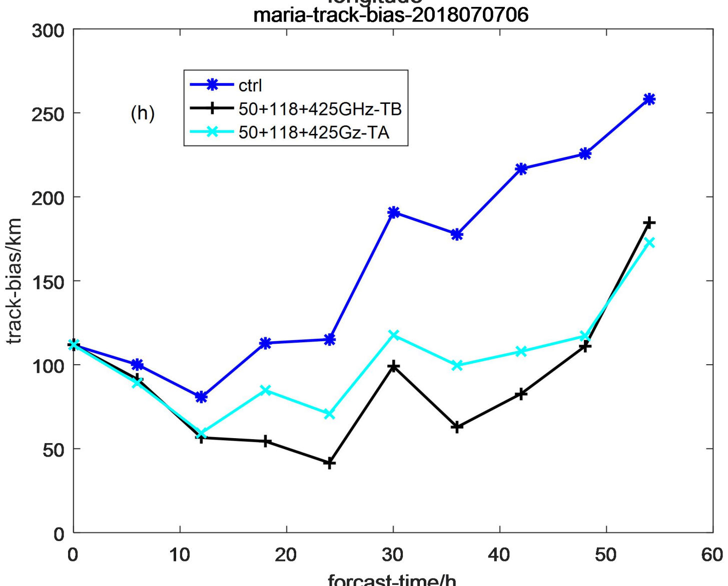

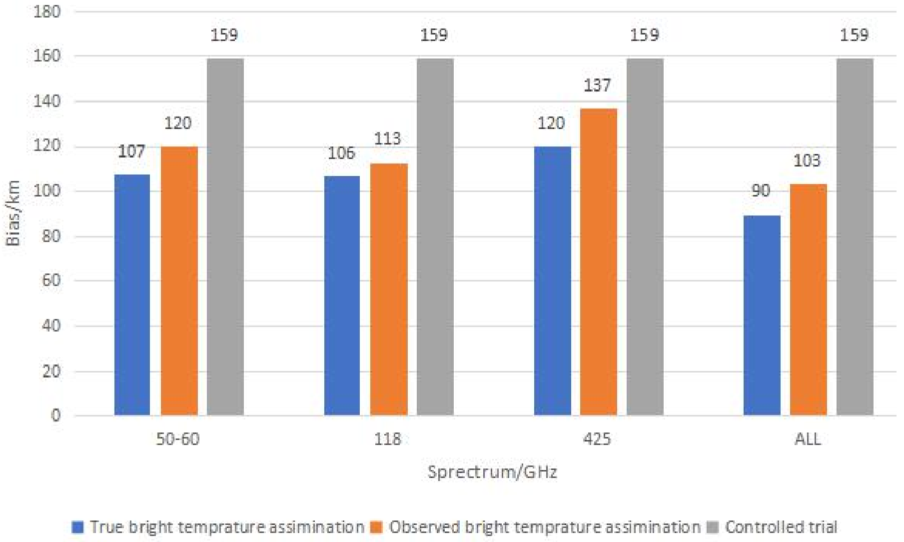

GEO-MW OSSE –various time intervals

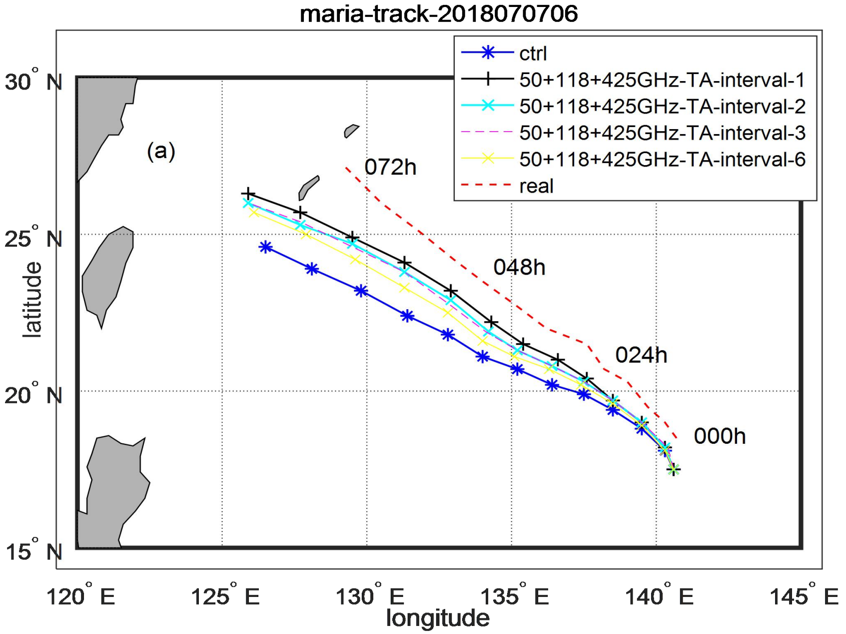

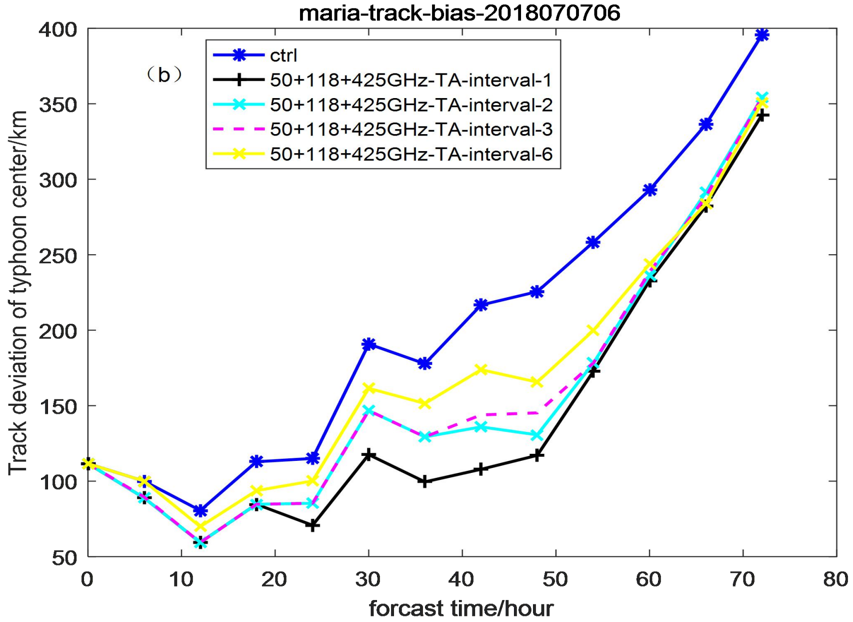

(a) Maria

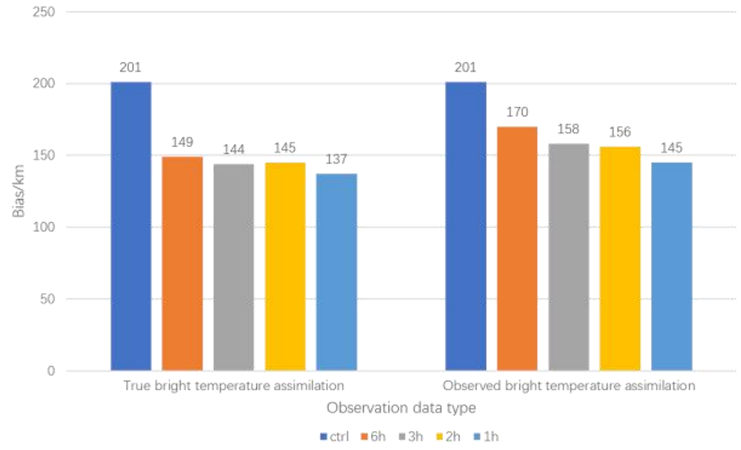

(c) Maria

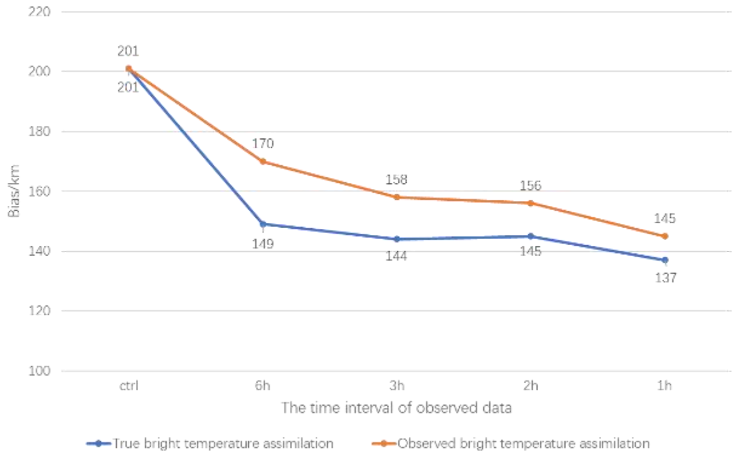

GEO-MW OSSE –various noise level

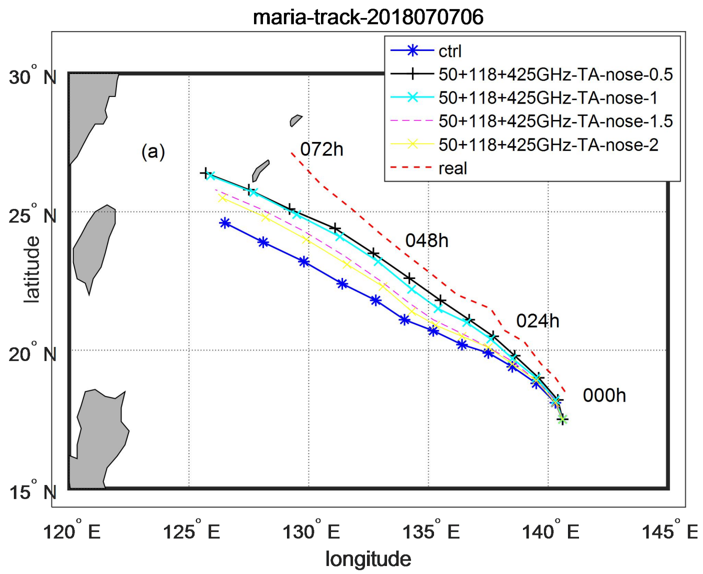

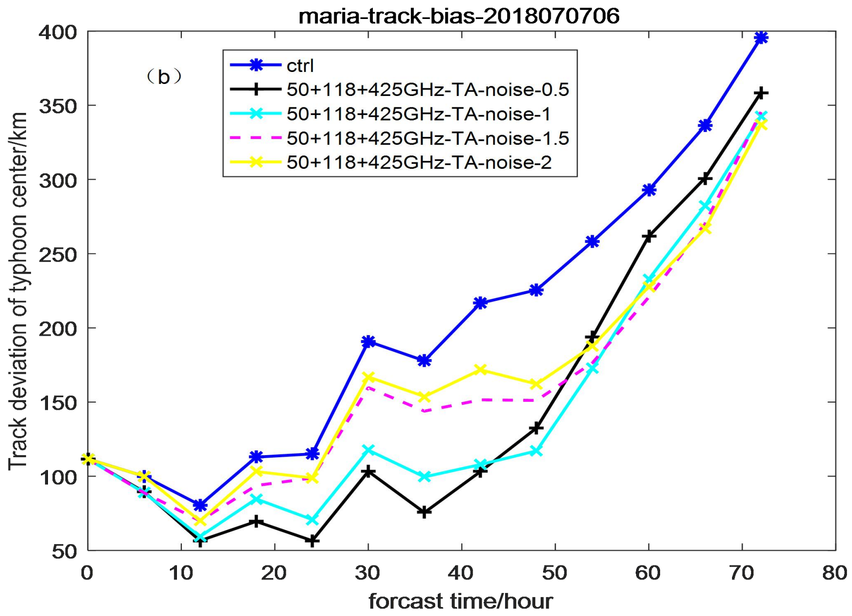

(a) Statistical histogram of mean trajectory deviation in each group

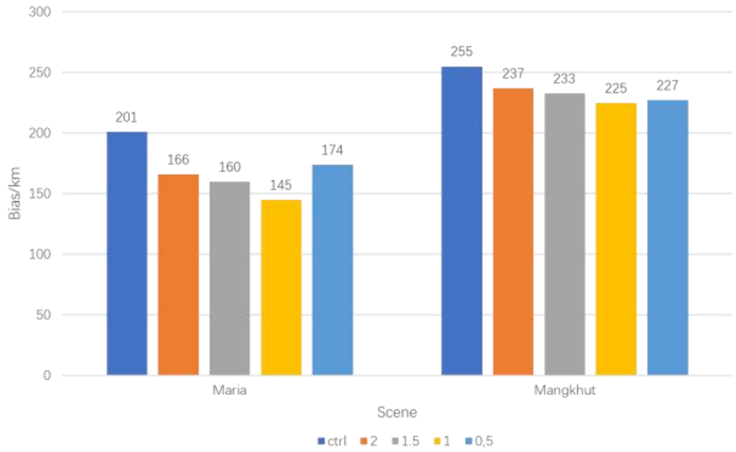

(b) Statistical line graph of mean trajectory deviation in each group

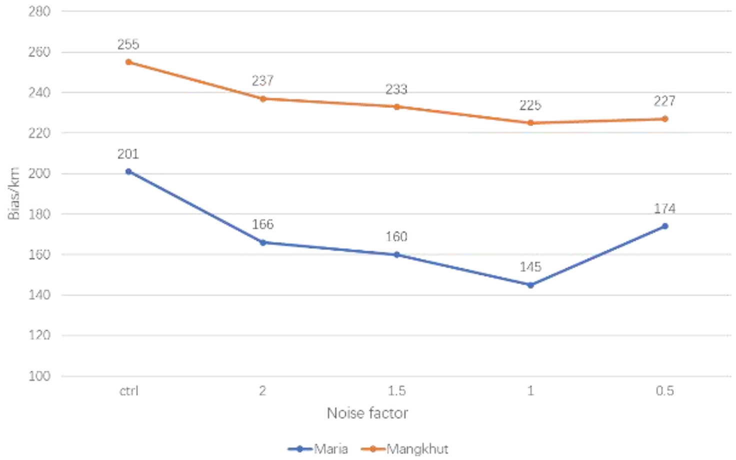

Summary

- **Progresses on Satellite data assimilation in GRAPES**

  FY-4A GIIRS,AGRI

  FY-2H VISSR, FY-3D MWRI, HIRAS

  HY-2B HSCAT-B Winds

- **Ongoing developments on Satellite data assimilation**
  - Use of surface sensitive channels
  - Considering the actual spectral response of microwave sensors in RT models
  - All-sky assimilation: Nonspherical Particle Scattering (shape, size, parameterization,…)
  - OSSE for GEO-MW: Channels, Resolution,NeDT, …

This study has been jointly supported by the National Natural Science Foundation of China (42075155) and National Key Research and Development Programs of the Ministry of Science and Technology of China (2018YFC1506405)

References

- Yin, R.,W. Han, Z.Gao and D.Di. 2020, The evaluation of FY4A's Geostationary Interferometric Infrared Sounder (GIIRS) longwave temperature sounding channels using the GRAPES global 4D‐ Var. *Quarterly Journal of the Royal Meteorological Society*, 146, 1459–1476. https://doi.org/10.1002/qj.3746.
- Yin R., W. Han, Z.Gao , G. Wang, 2019, A study on longwave infrared channel selection based on estimates of background errors and observation errors in the detection area of FY-4A. *Acta Meteorologica Sinica*, 77(5): 898-910, doi:10.11676/qxxb2019.051
- Di, D., J. Li, W. Han, W. Bai, C. Wu, and W. P. Menzel, *2018:* Enhancing the fast radiative transfer model for FengYun-4 GIIRS by using local training profiles, *Journal of Geophysical Research - Atmospheres*,123, doi:10.1029/2018JD029089.
- Xiao, H., Han, W., Wang, H., Wang, J., Liu, G., Xu, C., 2020. Impact of FY-3D MWRI Radiance Assimilation in GRAPES 4DVar on Forecasts of Typhoon Shanshan. *J Meteorol Res* 34, 836–850. https://doi.org/10.1007/s13351-020-9122-x
- Xie, H., Bi, L., Han, W., Wang, J., 2020. Vertical Inhomogeneity Effect of Frozen Hydrometeor Habits in All‐Sky Passive Microwave Simulations. *Journal of Geophysical Research: Atmospheres* 125, e2020JD032817. https://doi.org/10.1029/2020JD032817
- Chen, H., Han, W., Wang, H., Pan, C., An, D., Gu, S., Zhang, P., 2021. Why and How Does the Actual Spectral Response Matter for Microwave Radiance Assimilation? *Geophysical Research Letters* 48, e2020GL092306. https://doi.org/10.1029/2020GL092306
- Di, D., Li, J., Han, W., Yin, R., 2021. Geostationary Hyperspectral Infrared Sounder Channel Selection for Capturing Fast-Changing Atmospheric Information. *IEEE Transactions on Geoscience and Remote Sensing* 1–10. https://doi.org/10.1109/TGRS.2021.3078829
- Chen Ke, Hong Pengfei, Han Wei, Li Zeyu, Wang Hao, Wang Jincheng, Chen Hao, Zhang Zhiqing, Xie Zhenchao. 2021. Geostationary microwave observation system simulation experiments based on GRAPES 4D-Var. *Acta Meteorologica Sinica*, accepted. (in Chinese)